ORNL-4168

Contract No. W-7405-eng-26

HEALTH PHYSICS DIVISION ANNUAL PROGRESS REPORT

For Period Ending July 31, 1967

K. Z. Morgan, Director
W. S. Snyder, Assistant Director
E. G. Struxness, Assistant Director

OCTOBER 1967

OAK RIDGE NATIONAL LABORATORY
Oak Ridge, Tennessee
operated by
UNION CARBIDE CORPORATION
for the
U. S. ATOMIC ENERGY COMMISSION

Contents

PART II. RADIATION ECOLOGY

PART III. RADIATION PHYSICS

PART IV. RADIATION DOSIMETRY

PART V. INTERNAL DOSIMETRY

PART VI. HEALTH PHYSICS TECHNOLOGY

THESES, PAPERS, PUBLICATIONS, AND LECTURES

Summary

PART I. RADIOACTIVE WASTE DISPOSAL

1. Fate of Radionuclides in Terrestrial Environment

Field plots were installed and tagged with ^{137}Cs and ^{134}Cs in a design which allowed locating the source of runoff and erosion losses. These plots also served as replicates of earlier ^{137}Cs plots. Results obtained thus far confirm seasonal variation and the basic soil-cesium-loss relationship derived earlier.

Greenhouse studies of radiocesium uptake by plants using a split-root technique have been initiated. The technique allows control of soil moisture at predetermined tensions and permits an evaluation of the role of soil moisture in radiocesium uptake. Laboratory studies of cobalt sorption reactions point to the conclusion that small amounts of sesquioxides of iron and aluminum influence the reaction of the element in tracer concentrations.

2. Disposal by Hydraulic Fracturing

Two injections of medium-level waste concentrate were made during the past year. In the first, on December 12 and 13, 1966, a total of 96,000 gal of slurry, containing 20,000 curies of cesium, was pumped into a slot at a depth of 872 ft, which already contained 215,000 gal of grout from previous experimental injections. In the second, on April 20 and 24, 1967, 230,400 gal of slurry, containing principally 60,000 curies of cesium, was injected into a new slot at 862 ft. The injection plant operated without incident, and the slurry composition that was used appeared to be satisfactory. Measurements in the gamma-ray and rock-cover monitoring wells show that better instrumentation is now required, but every indication is that the operation is well within the limits of safety.

The oil-field technique of hydraulic fracturing has been proposed as a method for measuring the state of stress in the earth's crust. Hydraulic fracturing would have several distinct advantages over existing methods, because the stress itself can be measured rather than the strain of elastic rocks, which is then reduced to stress by use of Hooke's law. The research and development proposed will extend the present limited applicability of earth-stress measurement by hydraulic fracturing and enable the method to become a standard tool for fundamental studies of earthquakes and other geophysical processes, and for gathering design information for underground structures.

3. Disposal in Natural Salt Formations

The second and third sets of Engineering Test Reactor fuel assemblies have been installed in the arrays in the mine at Lyons, Kansas. The first set was returned to Idaho in October 1966. Both the second and third sets contained about 1.5 million curies at the time they were installed. Radiation doses to personnel were low, and no serious problems were encountered.

Doses to the salt exceeded the minimum goal of 5×10^8 rads, and the last two sets of fuel were returned to Idaho in June 1967. Peak array temperatures reached about 200°C after a power boost in January 1967.

The first two objectives of Project Salt Vault – the demonstration of the feasibility and safety and the demonstration of handling equipment and techniques – have been achieved.

Salt flows (thermal expansion and plastic flow) resulted in increased separation (sag) rates of the

2-ft-thick salt layer in the roof. The installation of roof bolts in the entire experimental area eliminated any possible hazard from this source due to startup of the heated pillar test. The heated pillar test was started November 14, 1966, with a power input of 33 kw and is proceeding in expected fashion; that is, greatly increased transverse expansion rates of the pillar produce pillar spalling and large vertical thermal expansion of the floor in the adjoining rooms.

Small quantities of water trapped in negative crystal cavities in the salt have been found to migrate toward a heat source. The water inflow rate in the main and electrical arrays appears to be between 0.3 and 3 ml day^{-1} $hole^{-1}$. In the old mine floor array the water inflow rate is about 40 to 90 ml day^{-1} $hole^{-1}$ due to the presence of water in the embedded shale.

The array in the old mine floor is behaving similarly to the other arrays, except for slightly higher temperature rises, more water inflow, and no roof separation (due to a thicker roof beam).

A detailed stratigraphic study has been completed of the salt section extending from 30 ft below the floor of the old mine workings to 10 ft above the ceiling in the demonstration site, a total thickness of 75 ft. Halite is by far the predominant mineral.

Additional laboratory tests on pillar models have indicated the importance of simulation of roof and floor in quasi-plastic rocks like salt.

Calculations of the gross salt mine space for the projected United States nuclear power economy to the year 2065 indicate that by 2065 an area about 7 miles square (49 square miles, a very small portion of the available area) will have been committed for waste disposal. Only about a third of that will have actually been used at that time, assuming 30 years' interim storage before disposal.

4. Application of Mineral Exchange to Reactor Technology

The behavior of sulfur hexafluoride (SF_6) and methyl iodide (CH_3I) in an Idaho soil was studied. The SF_6 showed little, if any, interaction with the soil material. Methyl iodide was retained to the extent that its movement was about 0.6 that of air.

Curium solutions of various pH levels were passed through columns of hydrobiotite. Instead of normal chromatographic breakthroughs, a constant leakage of curium occurred. The distribution of the curium along the column indicates that a radiocolloid is formed and that the hydrobiotite column acts as a filter.

Several adsorbents have been compared with attapulgite (presently in use) as cleanup agents for organic reactor coolants. Bentonite, activated bauxite, and spent cracking catalyst appear to be superior to attapulgite. Evaluation is based on color, melting point, and molecular weight of the effluent coolant.

5. Engineering, Economic, and Safety Evaluations

Investigation has continued on the degree of safety associated with present methods of radioactive waste management. Studies of ^{85}Kr and ^{3}H have been concerned with acceptable rates of release from a hypothetical fuel-reprocessing plant located in Oak Ridge. A general procedure was developed for estimating permissible atmospheric releases on the basis of average annual meteorological conditions that influence a continuously operating plant. The procedure considers cloud depletion of ^{85}Kr and ^{3}H by washout, fallout, and adsorption on particulate matter in the atmosphere, and buildup of contaminants on the ground surface.

Continuous disposal of ^{85}Kr to suitable geologic formations may be one possible means of reducing or avoiding atmospheric release. Although the apparent advantages of underground disposal are its relative simplicity and its effectiveness, one severe requirement imposed on any disposal formation is that it must be essentially free of vertical channels. The mechanisms considered by which ^{85}Kr may be retained underground include containment and adsorption. In the absence of vertical convective transport, movement is influenced only by molecular diffusion. These mechanisms have been evaluated theoretically for quantities of ^{85}Kr and volumes of off-gas assumed to be produced at a 10 metric ton/day reprocessing plant. Measurements were made of krypton and xenon adsorption by various soil materials.

As a part of the long-range waste management study, projections were made of the nuclear power requirements by regions and of the reactor mix that may accommodate these requirements.

Evaluation of tank safety has been extended to thermal considerations in the event of a leak of

high-level wastes. Preliminary calculations were made for leaks of various sizes using a spherical shell geometry. Transient temperatures are being estimated for various source geometries and heat sinks by use of the computer program TOSS (Transient or Steady State).

6. Earthquakes and Reactor Design

Specific information on earthquake characteristics as they influence site selection, site evaluation, design of nuclear installations, and design of seismic shutdown systems is provided in a state-of-the-art paper on earthquakes and reactor design.

7. Dose-Estimation Studies Related to Proposed Construction of an Atlantic-Pacific Interoceanic Canal with Nuclear Explosives

The phase I dose-estimation studies related to the radiological-safety feasibility of excavating an Atlantic-Pacific interoceanic canal are summarized. Information developed includes methods for estimating external and internal dose equivalents, quantifying the transfer of radionuclides through critical exposure pathways, and identifying the radionuclides likely to be critical, and criteria for evaluating the radiological safety of the operation.

8. Related Cooperative Projects

Representatives of other agencies continued to participate in the Radioactive Waste Disposal Section's studies. Three alien guests were in residence during the year. Members of the section participated in the ASCE Committee on Sanitary Engineering Aspects of Nuclear Energy and in the American Standards Association.

One member served as assistant news editor for the United States for *Health Physics* and as an assistant editor of *Nuclear Safety*. Two members of the section taught courses at the University of Tennessee. Two members of the section participated part time at the Nuclear Safety Information Center.

PART II. RADIATION ECOLOGY

9. Responses of Animal Populations to Ionizing Radiation

Time-related responses in peripheral blood of four species of indigenous mammals were followed after whole-body irradiation. Total leukocyte number in all irradiated groups dropped sharply by one day postirradiation. Decreases in number of lymphocytes primarily accounted for the decrease in total number of leukocytes. By day 20, recovery in leukocyte number was evident for all species (49 to 82% of original values). Erythrocyte count and associated values (hemoglobin concentrations and hematocrits) decreased by day 20 in the rice rat, but these values were not significantly lower in the other species. These studies suggest that the greater radiosensitivity of the rice rat may be attributable to the radiosensitivity of the hematopoietic system of this species.

Loss rates of ^{59}Fe at 25°C were determined in seven species of native rodents in an effort to establish a suitable index to radiation damage in erythropoietic tissues and hemoglobin synthesis in free-ranging animals. Animals were injected peritoneally, and whole body counted until 114 days postinjection. Excretion rates were low for all animals tested. Irradiation (whole body) resulted in decreases in λ_b ranging from 1.9 to 4.4% by day 5 except in *M. musculus*, in which no change occurred. It appears that radiation effects on iron metabolism cannot be detected with this technique, on a short-term basis at least, in animals irradiated at relatively low levels.

The postirradiation survival of brown crickets in a grassland habitat was compared with that in laboratory experiments. Irradiated crickets were released into a field pen and then recaptured nightly in traps. In the laboratory similarly irradiated crickets were maintained at optimum rearing temperatures. Recaptures of crickets suggested a 50% survival time of about 11 days in the meadow environment compared with 21 days in the laboratory. The decreased survival time in the pens indicates that additional mortality factors were operating there; a possibility is predation by wolf spiders, which were observed feeding on these crickets. Further studies were completed on life history stage responses of evergreen bagworms to gamma radiation. For a single end point, LD_{50-20}

day mortality, sensitivities between egg and larval stages varied by a factor of nearly 35.

Fecundity of the mosquito fish, *Gambusia affinis affinis*, which live in White Oak Lake was evaluated. These fish receive approximately 130 rads/year from internal emitters and may receive as much as 10 rads/day from bottom sediments in certain parts of the lake. Fecundity, or brood size, was found to be greater in *Gambusia* from White Oak Lake than in a control population. The average number of viable embryos per fish from White Oak Lake was 44.4 ± 1.83; the average number from the control area was 32.1 ± 1.49. Besides the brood size, percent of dead embryos and abnormalities were greater in the White Oak Lake population. Increased brood size of the chronically irradiated fish may reflect a population adjustment to the increased mortality (exploitation) produced by ionizing radiation.

A comparison was made of the movement of ^{106}Ru, ^{60}Co, and ^{137}Cs in arthropod food chains on White Oak Lake bed. Distribution of ^{137}Cs among biota in the bed was similar to that previously reported. Compared with ^{137}Cs, more efficient food chain movement was suggested by the data for ^{106}Ru and ^{60}Co. Uptake from soil was greater for these latter radioisotopes than for radiocesium. Transfers from vegetation to herbivores and from herbivores to predators also appeared more efficient for ^{106}Ru and ^{60}Co than for ^{137}Cs. In particular, ^{106}Ru concentrations in predators were almost three times higher than those in herbivores. Consequently, the relative abundances of the three radioisotopes became rearranged by food chain processes. Ruthenium-106 had twice the concentration of ^{137}Cs in soils; in predators ^{106}Ru was 20 times more abundant than ^{137}Cs.

10. Responses of Plants to Ionizing Radiation

Responses to fast-neutron radiation in terms of growth, morphological, or mortality criteria have been measured for locally important tree species. These species represent ten families of wide taxonomic distribution. The extreme radiosensitivity of the conifers (*Pinus*) was apparent, with lethal doses being about 12 times less than the average lethal dose for the deciduous species. The most sensitive deciduous trees tested were dogwood (*Cornus florida*), sassafras (*Sassafras albidum*), and sweetgum (*Liquidambar styraciflua*). Doses required to produce lethality and severe growth effects in these species averaged 33 and 35% lower, respectively, than those required to produce these end points in the other deciduous trees. The most resistant species tested were mimosa (*Albizzia julibrissin*) and red oak (*Quercus rubra*). Doses producing lethality and severe growth effects in these species averaged 40 to 57% higher, respectively, than those for other deciduous species.

Nuclear criteria for genotypes of *Populus deltoides* (eastern cottonwood) were investigated to establish whether chromosome-volume differences existed in our populations, which consist of 30 clones representing ecotypes from six states. All clones had the diploid (38) number of chromosomes. The range of the interphase chromosome volumes with their associated standard errors was 2.38 ± 0.07 to 4.24 ± 0.16 μ^3. These two extreme values suggest that a difference in radiosensitivity may exist between these clones due to this 1.8 factor of increase in chromosome size. However, the other clones tested had chromosome volumes differing from one another only by a factor of 1.4 or less. Past work has shown that size differences of this magnitude are not likely to correlate well with exposure predictions for growth or mortality end points.

11. Radionuclide Cycling in Terrestrial Ecosystems

Five years of research, including laboratory experiments on insect feeding, have clarified many problems related to the animal food chains in the ^{137}Cs-tagged forest. Over 2 $\mu c/m^2$ of foliage consumption was necessary to maintain radioactivity levels in canopy insect populations, even though the total activity represented in them was very small (about 0.004 $\mu c/m^2$ at any one time). The contributions of insects, and probably of other animals, to the export of radioactivity from the forest appeared small (less than 0.1 $\mu c/m^2$) by comparison with the measured export in blowing leaves which fell outside the plot boundaries in autumn (5.3 $\mu c/m^2$ in 1963; less in later years). Litter falling inside the plot contributed about 5 $\mu c/m^2$ to animal food chains (especially ground insects and millipedes), which eventually return radiocesium to the litter layer or underlying soil.

Equations that were used previously in mathematical models for accumulations of nutrients in soils, plants, and animals were extended to overall analysis and prediction of radiocesium in and around the tagged forest. The continued decreases in radioactivity of tree foliage imply readjustment toward lower levels of activity throughout the animal food webs. In spite of the tendency of soil minerals to fix cesium ions, recycling into plant roots may lead to an almost steady state, at levels less than 1% of the first year levels of activity, between the fifth and tenth year of the experiment. One model prediction indicates that continued input of activity to the soil may be balanced by radioactive decay in approximately seven years.

Studies on the distribution of three alkali metals (cesium, potassium, and sodium) in arthropod food chains showed that trophic processes do not result in increased concentration of ^{137}Cs and K between arthropod links in the food chains. Since fallout ^{137}Cs often has been reported to be accumulated in vertebrate food chains, it is apparent that the faunistic composition of environmental pathways must be considered before the fate of ^{137}Cs in trophic levels of ecosystems can be assessed.

Laboratory studies of ^{187}W retention were performed with two species of insects to determine what magnitude of food chain transfer might be expected in tungsten-tagged environments. The biological half-lives for tungsten, based on the mean retention estimates at each counting time, were 48 hr for *Acheta* and 58 hr for *Oncopeltus*. Percentage error was found to be about 20%. Radiotungsten absorption and retention parameters appear similar to those for radiocesium in these two insects. From these measurements it is inferred that radiotungsten movements through the arthropod portions of food chains may approximate movement of radiocesium.

12. Radionuclide Cycling in Aquatic Ecosystems

Several types of experiments were done to clarify the respective roles of fish flesh and blood in Sr uptake and turnover in bluegills (*Lepomis macrochirus* Rafinesque). Specific activities or radiostrontium-to-total-Sr ratios were used to determine whether the Sr in flesh and blood was in equilibrium with that in water. The blood incorporated radiostrontium rapidly, reaching about two-thirds of the maximum activity level in 24 hr. The concentration factor rose from 0.124 at 1 day to 0.194 at 35 days. The specific activity in the blood did not change appreciably in the test period, rising from 0.47 at 1 day to 0.74 at 35 days. The greatest rate of ^{89}Sr uptake by the flesh occurred in the first 4 days. The second component of the uptake curve was faster for flesh than for blood, and the maximum concentration factor reached after 35 days was 0.121. Extrapolation of the second component indicates that approximately 72 days are necessary for bluegill flesh to reach a concentration factor of 1, which may be expected from stable Sr analyses.

Uptake responses to different environmental Sr concentrations (0.3 to 30,000 ppb stable Sr) were carried out in bluegills. The concentration factor for radiostrontium was virtually constant within this range. This indicates that the readily exchanged Sr fraction was accumulating Sr in direct proportion to that in the environment. Results of the stable Sr analyses indicated that concentration factors of stable Sr were inversely proportional to the Sr concentration in test waters, except at the two highest environmental concentrations, 3000 and 30,000 ppb. The levels of stable Sr in the flesh of the experimental fish did not change significantly. These results showed that the quickly exchanged fraction of Sr in bluegill flesh was a small proportion of the total Sr in flesh.

Experiments on cesium and potassium turnover in white crappie were performed to test a hypothesis that Cs/K ratios will increase at succeeding trophic levels in the food chain. The results do not support this hypothesis. Field studies on trophic-level increases, using White Oak Lake fish, showed no consistent pattern of Cs content with respect to trophic level. Comparison of Cs and ^{137}Cs analyses from fish from the Clinch River (ORNL), Finnish lakes, and Red Lake, Minnesota, showed that trophic-level increases occurred only part of the time. These differences may be the results of different food chains in different habitats, which in turn affect Cs concentration at succeeding trophic levels. Data available at present do not warrant the general application of trophic-level increases to Cs in food chains.

13. Watershed Aquatic Habitat Interactions

A watershed research program was initiated this year which will unify portions of the terrestrial and aquatic ecology research. The Walker Branch

watershed, having a total area of 241 acres and consisting of two smaller watersheds of 95 and 146 acres, was selected for study. Two permanent spring-fed streams drain the area. Research objectives of the project are to (1) relate water quality and productivity of the stream to the productivity and chemical budget of the adjacent terrestrial ecosystem, (2) equate the net loss of chemical elements to the rate of mineral cycling, (3) establish the relationship between the hydrologic cycle and mineral cycle, and (4) provide benchmark information of natural terrestrial-aquatic ecosystems for comparison with those modified by man's cultural practices.

A base map was prepared from an existing detailed topographic map and from aerial photos taken in October 1966 and February 1967. A four-chain grid system was established with permanent corner markers to facilitate positive field location. The overstory vegetation and soil types have been mapped. Five rain gages were installed, and areas around them were fenced and seeded. Access roads were constructed, and preliminary excavations for the two weirs were completed. Weir design, as well as the design for continuous proportional water samplers which are to be installed at the weir site, was completed. A power line to the weir site was designed and is being installed.

14. Theoretical and Systems Ecology

Data on radiant energy input and productivity were utilized to construct a preliminary model of energy flow in *Liriodendron* (tulip poplar) forest. Values for stem production were 9000 kcal m^{-2} $year^{-1}$, canopy 1950 kcal m^{-2} $year^{-1}$, and 1600 kcal m^{-2} $year^{-1}$ for roots. These values correspond to 0.12, 1.6, and 0.12% of the annual (all wavelength) solar energy input to leaves, stems, and roots respectively. A general instructive model describing vertical periphyton growth was developed on the basis of periphyton studies carried on in White Oak Lake.

15. Forest Management

The Forest Management Program, initiated in 1965, has the responsibility for managing 20,900 forested acres adjacent to the ecology study areas on the AEC Oak Ridge Reservation. A self-financing commercial forest program is conducted in harmony with the research objectives of ORNL. Applied forestry research is conducted as needed to solve specific land management problems.

PART III. RADIATION PHYSICS

16. Theoretical Radiation Physics

The problem of double plasmon excitation by a fast electron is considered a framework which allows for damping of the intermediate states by plasmon interactions together with other possible competing processes. The value of the minimum dipole moment required to bind an electron to a finite permanent electric dipole has been established rigorously to be $D_{min} = 1.625 \times 10^{-18}$ esu-cm. Approximating the polarization potential for electron scattering from atoms of $1s^2 2s^2 2p^q$ configuration, using a polarization potential previously calculated for oxygen and the experimental dipole polarizabilities, calculations of the total elastic scattering cross sections for these atoms have been made; agreement with experiment is rather good. A perturbation method has been used to obtain equations for the dynamic distortion of the target system when low-energy electrons or positrons scatter from atomic or molecular systems. The potential energy of the electronic cloud at the nucleus of an atomic system is of interest in beta decay theory; calculations of this energy for a number of different neutral atoms have been made using the Hartree-Fock equations for the atomic system. Work is continuing on the effect of the exclusion principle in intermediate states of scattering of a hot electron on a free-electron gas. Comparisons of the dose distribution in cylindrical and slab phantoms due to protons of energies in the range 250 to 400 Mev have been carried out. A new formulation of the dielectric constant of an absorbing medium has been made. It is predicted that photon absorption by a fast electron may occur with appreciable probability through the intermediary of a virtual plasmon; estimates show that it may be feasible to observe this process experimentally. Plasmon exchange scattering by two colinear fast electrons of slightly different energies appears more difficult to observe experimentally.

Consideration has been given to the process of surface secondary electron emission from metal through the Auger decay of surface plasmons created by fast charged particles. A procedure has been formulated for choosing the normal modes of motion of nuclei in a molecule so that, when subjected to a symmetry operation of the point group of the molecule, they form bases for irreducible representations of the point group. Work on the Klein method for obtaining the potential vs internuclear distance for diatomic molecules is continuing. Molecular structure calculations of magnesium porphin have been carried out; resulting energy levels and oscillator strengths correspond to two prominent strong absorptions near the experimental values. Studies of the passage of high-energy nucleons through multiregion phantoms, corresponding to soft tissue and bone parts, have been made for protons and neutrons with energies up to 400 Mev.

17. Interaction of Radiation with Liquids and Solids

Optical constants in the vacuum ultraviolet have been determined for single crystals of MgF_2 and MgO and thin films of white Sn, amorphous Se, and K. Reflectance techniques were used, except for K, where the critical-angle method yielded the refractive index directly. For critical-angle measurements an angle doubler, an apparatus for moving the detector at twice the angular velocity of the sample, has been designed. In addition, an ellipsometer and ultrahigh-vacuum chamber were constructed, and optical constants of palladium at long wavelengths were determined from analysis of the ellipticity of light reflected from a flat palladium surface. Photoelectric measurements have been made on silver, palladium, and nickel, with photoelectron energy distribution curves being obtained for various incident-photon energies.

To obtain optical constants from reflectance data, a new method of employing the Kramers-Kronig relations has been devised.

Both optical constants over an extended energy range and photoelectron energy distribution curves yield information about the energy-absorption processes taking place when photons interact with the material. Such information can be related to band structure and to absorption cross sections. For each material studied, structure in the optical constants, in the derived energy-loss functions, and in the photoelectron energy distribution curves has been interpreted in terms of excitons, interband transitions, and collective, or plasma, oscillations. In some cases comparison has been made with characteristic electron energy loss measurements published in the literature. An attempt was made to identify photon excitation of surface plasmons in aluminum using data obtained previously. Positive identification was not possible due to the existence of an interband transition near the surface-plasmon energy.

18. Atomic and Molecular Radiation Physics

The minimum molecular electric dipole moment which is necessary to bind an electron has been calculated and found equal to 1.639 Debye units. An analysis of electron swarm data for electrons traveling through polar gases provided the first experimental evidence for this value.

Investigations of low-energy electron attachment to aromatic molecules have been extended from the halogenated benzene derivatives to benzene itself, naphthalene, and napthalene derivatives. Electron capture in the diatomic molecules HX and DX (X = halogen) revealed new electron attachment processes and provided most interesting results for direct dissociative electron attachment to molecules. Capture cross sections (corrected for the finite width of the electron pulse) as a function of electron energy have been obtained for these molecules. Electron capture in chlorinated linear hydrocarbons provided interesting results which will form the basis of an attempt to relate electron capture with the toxic action of these molecules. Further, a new technique has been developed which allows determination of thermal electron attachment to molecules and thermal electron diffusion under field-free conditions.

Nondissociative electron attachment to O_2 in O_2-C_2H_4 and O_2-C_2H_4-H_2O mixtures has been studied, and the efficiencies of O_2, C_2H_4, and H_2O as stabilizing agents for O_2^{-*} have been investigated. Electrons were found to attach to polyatomic molecules with high probability and for times of the order of 10^{-5} sec. The product of the capture cross section and the corresponding negative ion lifetime has been found to be a strong function of the molecular electron affinity. From a theoretical expression relating the capture cross section, the negative ion lifetime, and the electron

affinity, a calculation has been made of the electron affinity of sulfur hexafluoride, nitrobenzene, diacetyl, and glyoxal. In this respect new experiments have been initiated to study collisional detachment of electrons from negative ions in an effort to measure molecular electron affinity directly.

Short-lived negative ion resonances have been discovered in benzene, seven benzene derivatives, and naphthalene. For benzene derivatives for which dissociative attachment is possible, autoionization and dissociation were found to be in competition. The temporary negative ion resonances observed in benzene and naphthalene gave a lower limit to the electron affinities for these molecules equal to -1.4 and 0.8 ev respectively.

Excitation of hydrogen halide molecules, benzene, seven benzene derivatives, and naphthalene has been studied at the threshold of excitation processes using SF_6 as a scavenger of low-energy electrons. Important results have been obtained, especially with respect to temporary negative ion resonances and triplet state excitation of molecules. The emission from organic liquids excited by electron impact has been found to be completely due to excimers. The characteristic monomer emission observed under ultraviolet and x-ray excitation was completely absent under intense electron bombardment. Ion recombination is believed to be the origin of the excimer emission, while strong ionization quenching of excited monomer molecules is believed to be responsible for the absence of monomer emission. A nanosecond pulsed electron source for scintillation decay time measurements has been developed and will aid our luminescence studies of polyatomic molecules.

Finally, studies have been made of sensitized ionization of molecules, molecular decomposition, and the yields of resolved transitions in gases.

19. Graduate Education and Vocational Training

In the Graduate Education and Vocational Training Program, eight AEC Health Physics Fellows from Vanderbilt University, four from the University of Tennessee, and one from the University of Rochester came to ORNL for summer training in applied health physics and research. Final writing and editing were completed on the book "Principles of Radiation Protection: A Textbook in Health Physics." Page proof was received and publication is expected in time for use during the academic year 1967–68. Nineteen colleges and universities were visited, and health physics research and career opportunities were discussed. Twenty-two graduate students conducted thesis research in the Health Physics Division for the M.S. or Ph.D. during the year. A total of 56 university personnel ranging from undergraduates to professors spent last summer in the Health Physics Division. Several of our staff assisted the UT Physics Department in writing three research proposals to government agencies. A new undergraduate curriculum in health physics was set up at UT with our help. The Division cooperated with Oak Ridge Associated Universities in screening of applicants for USAEC Fellowships; participation in the conference on "Principles of Radiation Protection," which attracted approximately 100 faculty members; and presentation of courses of up to ten weeks duration in health physics for 32 state personnel. Lectures were given at four Medical Radioisotopes Courses, attended by 60 physicians. The Division assisted in the presentation of an eight-week course in health physics for college and university staff members who have responsibility for campus radiation safety. At ORNL, Division personnel participated in the presentation of a two-week course in Radiation Safety for Laboratory staff.

20. Physics of Tissue Damage

In the Physics of Tissue Damage Program, studies of electron transport through tin metallic layers were extended with a new ultrahigh vacuum system and a new electron gun capable of supplying electrons of as little as 1 ev at an arbitrary angle to the layer. An enhancement of surface-plasmon excitation was noted as the electron beam impinged at glancing (as opposed to normal) angles, whereas the absorption due to L-shell ionization decreased. The former behavior was in qualitative accord with theoretical expectations, whereas the latter was not and is not understood. In measurements on amino acid films, electrical characteristics were noted as follows: band gap, 2.7 ev; resistivity, 10^{16} ohm-cm; field strength at

breakdown, 10^5 v/cm. An electron irradiation system was constructed which prevented light from the electron gun from shining on the amino acid target. Optical measurements of the ratio of phosphorescence to fluorescence for tryptophan and tyrosine films showed that the ratio is independent of electron energy from 30 ev to 100 kev, implying that optical excitation is determined entirely by low-energy secondary electrons. The reflectivity of liquid water was measured at angles of 20, 45, and 70° to the normal and in the wavelength region between 1000 and 3000 A. Peaks in reflectivity at 2100, 1700, and 1000 A are attributed tentatively to triplet excitations, singlet excitations, and ionization in the liquid respectively. A peak at 1250 A is unidentified.

Eleven scintillator solutes were studied in the solvent 2-ethylnaphthalene, with emphasis on emission intensities, quenching effects, and pulse heights. This solvent, which emits from excimer formation, was found to be highly efficient and to resist quenching to a much greater extent than other scintillating materials. A preliminary study of light emission from silver irradiated by 200-ev electrons showed a peak at 3900 A, in contrast to the peak at 3300 A found from high-energy (>10-kev) irradiation. Further study is required in order to decide whether this peak arises from surface-plasmon decay or bremsstrahlung. Electron slowing-down spectra from beta-ray sources in aluminum were used to calculate the number of K ionizations (~ 3), L ionizations (~ 300), and plasmon excitations ($\sim 18{,}000$) which arise as an Mev beta ray slows down in aluminum. Virtually all beta-ray energy ultimately goes to plasmon formation.

PART IV. RADIATION DOSIMETRY

21. Ichiban Studies

The major emphasis of the program during fiscal year 1967 was on shielding studies associated with the survivors who were exposed in reinforced concrete or other massive structures, liaison, depth-dose calculations, and dosimetry related to Operation HENRE. The calculation of the shielding provided by large structures requires a knowledge of (1) the geometry of exposure (from ABCC records), (2) the energy and angular distribution of the neutrons and gamma rays (from previous dosimetry studies), and (3) the attenuation and buildup factors for the building materials for the exposure geometry. The latter subject was studied extensively both in the laboratory and during Operation HENRE. Two liaison trips to Japan made it possible for ORNL and ABCC to work efficiently on a joint basis. Calculations of depth-dose distributions for various neutron energies and irradiation geometries were continued (see "Dosimetry Applications," Sect. 23).

22. Spectrometry and Dosimetry Research

Spectrometry research for both directly ionizing particles and indirectly ionizing particles and quanta continued to be an important part of the dosimetry program. Silicon diodes were the primary tools for directly ionizing radiations. Neutron spectrometry research was directed to magnetic analyzing devices for elastically scattered protons and to ^{6}LiI scintillation systems. A new detector system for nuclear accidents is based on the use of rhodium. Much of the overall effort was directed to spectrometry for Operation HENRE (see "Dosimetry Applications," Sect. 23). For these studies, the ^{6}LiI spectrometer was most useful because of its great sensitivity compared with other systems.

23. Dosimetry Applications

Development of integrating or "passive" systems of dosimetry for personnel and nuclear accidents was continued, primarily with solid-state devices; these include metaphosphate glass for gamma radiation and fission-foil–solid-state (glass, plastic, etc.) detectors for neutrons.

Intensive intercomparisons of dosimetry systems were completed; both domestic and foreign groups used the HPRR in joint evaluations of a wide variety of systems. These studies are important both as a basis for evaluating the dosimetry systems and as a forum for information exchange. Depth-dose studies were continued for a tissue medium for an assortment of sizes and geometries, and calculations of radiation dose to many varieties of seeds irradiated at the HPRR were made. Measurements of neutron fluence and dose distributions near thick targets of copper and carbon bombarded by 60- and 80-Mev alpha particles were made at the Oak Ridge Isochronous Cyclotron. A more

sensitive Geiger-Mueller tube was adapted to the "Phil" system by designing appropriate shields for eliminating thermal-neutron response and for flattening the response vs photon energy to match the tissue dose curve. A series of measurements were made to determine the exchangeable and total sodium in the human body by isotopic dilution and neutron activation techniques; the study was conducted because a British group reported experimental values which were sufficiently lower than any previous values to require changes in previous ORNL data.

24. HPRR and DLEA Operations

The Health Physics Research Reactor continued to serve as the radiation source for a large fraction of the world's dosimetry research. An increasing percentage of the reactor operations is in the pulsed mode. The DOSAR Low-Energy Accelerator has proved to be a versatile and highly reliable source of low-energy charged particles and 3- and 14-Mev neutrons.

PART V. INTERNAL DOSIMETRY

25. Internal Dose Estimation

Calculation of the average beta-particle energy in beta decay has been computerized, and graphs of the ratio of average energy to end-point energy are presented for allowed, first-forbidden unique, and second-forbidden unique transitions. Computer codes have been developed which calculate the percentages per decay and respective energies of x rays, gamma rays, internal conversion electrons, and Auger electrons for electron capture decay and gamma-ray internal conversion. Illustrative computer outputs are presented.

When a gamma emitter is present in an organ of the body, one needs to know what fraction of the energy released is absorbed in various tissues of the body in order to estimate dose to those tissues. Many oversimplified methods have been used in the past to estimate these "absorbed fractions" as they are often termed, for example, a single interaction calculation, a "straight-ahead" model of scattering, or the use of an "effective radius." This paper defines a mathematical model of the human body and 23 organs, each having approximately the correct size and shape, and a computer code estimates dose to each of these organs from a source uniformly distributed in any one of them. The principal limitation is that the phantom is homogeneous, and efforts are under way to remedy this. However, for energies above 0.2 Mev, the mass absorption coefficients of bone and soft tissue are not very different, and so only sources at or above 0.2 Mev have been used thus far. In general, the "absorbed fractions" obtained by these more exact, multicollision-type estimates are lower than values obtained by the use of an "effective radius" as defined by the ICRP and NCRP, the new values being generally about half those estimated by that procedure.

A Monte-Carlo-type code has been developed at ORNL which permits one to estimate dose in tissue phantoms for a wide variety of exposure situations. This is a report on dose in an anthropomorphic tissue phantom which has approximately the dimensions and masses of "Standard Man." The incident photons emanate from an external point source which is positioned at various distances up to 2 m from the phantom and at several heights. The phantom is divided into 160 subregions. The volume elements nearest the surface of the trunk section have a thickness of 1 cm, and the dose in these volume elements may be expected to approximate the reading of a dosimeter exposed on that portion of the surface of the body. Thus the variation of dosimeter readings when the dosimeter is worn in different positions on the body surfaces can be estimated and compared with the distribution of dose within the body. Each point source is monoenergetic, and the energy of the photons is varied from 0.07 to 1 Mev. The dose at a specified site within the phantom may differ as much as an order of magnitude from the dose indicated by a dosimeter worn at certain locations on the surface of the phantom, the difference depending on the energy of the source and its position in relation to the phantom and the position of the dosimeter.

After an intake of cesium, this element is eliminated over a period of time. It has been found by Richmond *et al.* that a one- or two-exponential retention function is usually sufficient to fit the observed data. This retention model is valid for adults and children, but the elimination rates are different in each case. In this report a mathematical compartment model is proposed which allows compartment size or growth to be included naturally. This model is applied to the retention of ^{137}Cs by humans from birth through adulthood.

The biological half-times predicted with this model compare favorably with experimental values, although there is still much variation of the observed half-times within an age group. The implications of this model in regard to dose from single and continuous intakes are examined.

Detailed estimates are provided of dose within the body from administration of Neohydrin labeled with ^{197}Hg or ^{203}Hg. Such estimates are of interest in deciding the relative merits of the two compounds for extensive clinical use. Dose estimates to (1) cortex of kidney, (2) medulla of kidney, (3) bladder, and (4) ovaries are provided per millicurie-hour of residence of the source in blood (early phase), in cortex, in medulla, and in the bladder (excretory phase). The dose from photons is estimated using the Monte Carlo technique. These estimates are used with available data on residence times to obtain a dose estimate for a typical case. However, they can be easily adjusted in other proportions appropriate for the elimination rates of a particular patient.

The accuracy of computer codes based on excretion data following a single intake to blood for estimating a systemic body burden of plutonium is considered (1) by fitting power functions to data of individuals resulting from a single intake to blood and comparing these functions to determine individual differences, (2) by analyzing day-to-day fluctuations to determine confidence bands about the power functions which include a preassigned percentage of the data, (3) by using computer methods to predict intake or body burdens for known cases where the predictions can be checked, and (4) by using only portions of the excretion data to reveal inaccuracies due to inavailability of all the excretion data. The use of these data on fluctuations of day-to-day excretion and on individual differences to estimate body burdens by computer methods is being explored.

26. Stable Element Metabolism

Long-Term Study of Intake and Excretion of Stable Elements

Statistical studies of the daily elemental dietary intake and urinary and fecal excretion of two men on *ad libitum* diets over a period of four months indicate the influence of the time of intake, of intake of other elements, and of other factors on the excretion of an element. Equations relating these factors have been developed.

Tissue Analysis Laboratory

In the tissue analysis program, attention has been directed to the detection of trace elements in bone. The overall sensitivity has been improved by developing a chemical preconcentration procedure.

PART VI. HEALTH PHYSICS TECHNOLOGY

27. Aerosol Physics

Studies of the adhesion of solid particles to other particles and to solid surfaces have been extended to provide a better understanding of the basic physical mechanisms. Results of earlier ad hoc studies have confirmed the importance of capillary and electrostatic forces; thus, the major emphasis of the present work has been directed toward capillary and electrical phenomena. A theoretical treatment of the capillary force between two spheres of equal radii has shown that there is a maximum size capillary that can exist between two contacting spheres of radius R and that the maximum adhesion force is $5.329R\gamma_s$, where γ_s is the average surface free energy of the solid. A new analog method was developed for determining the charge area density on a conductive particle in contact with a charged conductive surface. The apparatus is described as a coulometric electrolytic tank and employs electrodeposition of metals onto models of the particle shapes under study. The surface mass density of deposited metal is determined by removing known segments of the deposit and weighing them on an ordinary laboratory balance; the distribution of mass per unit area on the model is analogous to the distribution of charge per unit area in the electrostatic case. The interfering effect of ionic diffusion is reduced by proper selection of the plating bath parameters and by control of the maximum current density. The validity of the method is demonstrated by comparing the analog solution for a hemisphere on a plane with the classical solution for a charged plane having a hemispherical boss. Obviously, departure from the known solution for a hemisphere, resulting from diffusion effects, could be treated as a calibration, providing correction factors useful for other geometries; however, the degree of error is seen to be small, and one may determine the surface charge density of rather complex

particle shapes to within less than about 10% error by this method.

The exploding-wire aerosol generator, described in previous reports, has been redesigned, resulting in a more compact, versatile, and portable device. A commercially available 2800-j capacitor and trigger unit form the central core of the exploding-wire device. Various control circuits are included in the new design to improve the safety features developed in operations of the earlier model.

Aerosols generated by the exploding-wire device are being used in a study of the interaction of airborne vapors with particulates. The rate of disappearance of free iodine vapor from a cylindrical tank is about nine times that of sulfur dioxide vapor from the same aerosol chamber in the absence of significant concentrations of condensation nuclei. When nuclei of platinum for iodine and either platinum or ferrosoferric oxide (Fe_3O_4) for sulfur dioxide are added to the chamber, the rate of equilibration of the vapor with the airborne nuclei is about ten times faster in the case of sulfur dioxide. As an adjunct to this study a screening test is being carried out by passing the vapor through a deposit of exploding-wire particulates collected on a membrane filter. Initial studies have been done using 2 different concentrations of sulfur dioxide and 17 different particulate compositions. The preliminary work shows a variety of interactions, some being proportional to concentration and others more related to time of contact.

Investigations of the retention times of particles adhering to the skin have been extended to include estimates of initial retention after impaction at approximately the terminal velocity of the particle in air. All particles less than about 180 μ in diameter were retained, whereas none larger than about 700 μ were retained when the removal force was equal to the force of gravity.

Particle retention time data were combined with measurements of the dose rate in tissue produced by a neutron-irradiated reactor fuel particle to provide an estimate of dose to the skin as a result of "hot" particles being deposited on the skin. The particles were irradiated for 20 min, simulating a short operating time, and, because of the rapid decay of the contained fission products, the expected dose from a given particle depends on the time, after shutdown of the reactor, at which first contact is made with the skin and upon the time of retention. The results are given in terms of the expected dose averaged over an area of 1 cm^2 at a depth of 7.6 mg/cm^2, and the upper and lower limits on the dose are indicated for one standard deviation of the estimate.

28. Applied Internal Dosimetry

During the period June 1, 1966, through May 31, 1967, a total of 896 whole-body counts were made involving 744 persons. Only 10.2% of the persons counted showed detectable amounts of radionuclides other than normal levels of ^{40}K and ^{137}Cs (6 to 9 nc of ^{137}Cs in 1966). Two employees, whose exposure by inhalation of $^{90}SrTiO_3$ particles in January 1964 has been described in earlier reports, have been recounted at approximately monthly intervals for 1260 days; the half-time for lung clearance at the end of the report period appears to be in excess of 1800 days.

The elimination of ^{203}Hg from the body was observed by whole-body counting using a 6-ft arc geometry during the period from 30 to 190 days after injection for medical purposes. In this period the body burden changed by more than two orders of magnitude, and the indicated effective half-life was 25.1 days; based on this, the biological half-life is calculated to be 54 days. Effective half-lives were observed to be 24 days for retention in the liver and 53 days in the kidney region.

The attenuation of x rays from a $^{238}PuO_2$ microsphere was observed as a function of depth in various absorbers simulating tissue as well as in polyvinyl chloride. Because of the presence of chlorine atoms, attenuation is significantly greater in polyvinyl chloride, for which the half-value layer is 120 mg/cm^2 as compared with 680 mg/cm^2 for the other materials. Calibration of a wound probe using the microsphere source indicates that the least detectable amount of ^{239}Pu in a wound varies from 0.01 nc at a depth of 1 mm to 2.4 nc at 33 mm, based on three standard deviations of the background.

A new procedure has been developed to analyze environmental samples for radioactive strontium. The radioisotopes of strontium, barium, and radium are removed from the dissolved sample by retention on a cation exchange resin, and separation of these elements is effected by elution at controlled pH. The recovery of ^{85}Sr tracer in grass, milk, leaves, feces, and bone samples was observed to be greater than 99%.

25. Internal Dose Estimation

W. S. Snyder
S. R. Bernard
Mary Jane Cook
L. T. Dillman[1]
H. L. Fisher, Jr.[2]
Mary R. Ford
C. F. Holoway
Isabel H. Tipton[3]

CALCULATING THE EFFECTIVE ENERGY PER RADIOACTIVE DECAY FOR USE IN INTERNAL DOSE CALCULATIONS

L. T. Dillman[1]

In making internal dose calculations, it is necessary to determine the effective energy deposited in the organ of reference per radioactive decay. This requires detailed knowledge concerning the decay scheme of the radionuclide involved. Even when decay schemes are well established, considerable tedious work may be involved in computing the effective energy per disintegration. This is particularly true when significant gamma-ray internal conversion or electron-capture processes occur. These processes give rise to x rays and Auger electrons of varying intensities, and the calculation of these intensities is tedious.

This paper describes three computer programs which have been devised as aids to the calculation of the energy of the particles released for each of the following three processes: (1) electron or positron emission, (2) electron capture, and (3) internal conversion of gamma rays. The ultimate goal is a computer code which uses nuclear decay data as input information and calculates the effective energy per decay for the particular organ or organs of interest. The present programs are initial steps toward this goal.

[1]Research participant and consultant to ORNL from Ohio Wesleyan University.

[2]U.S. Public Health Service.

[3]Physics Department, University of Tennessee.

Electron or Positron Emission

For β^+ or β^- decay, one needs the ratio of the average energy of the particle to the end-point energy for each transition under consideration. James *et al.*[4] have computed this ratio for allowed, first-forbidden unique, and second-forbidden unique β^- transitions and have presented their results in graphical form. Their graphs give this ratio as a function of energy for six values of atomic number. Loevinger[5] gives graphs of this ratio as a function of energy for allowed β^+ transitions. A computer code has been written which extends these previous compilations in several ways.

First of all the computer code may be used for any atomic number and for any end-point energy and thus obviates the necessity of graphical interpolation. Second, the code includes first-forbidden unique and second-forbidden unique β^+ transitions. Third, the code calculates the fraction of the emissions in which the initial energy of the β^+ or β^- particle is below a fixed value of energy, for example, 0.03 Mev. This is done because beta radiation of low energy is generally weighted with a quality factor, QF, in estimating dose equivalent; QF is the symbol used for the linear-energy-transfer-dependent factor by which absorbed doses are to be multiplied to obtain, for purposes of radiation protection, a quantity that expresses the dose equivalent delivered to tissue on a common scale for all ionizing radiations. In

[4]M. F. James, B. G. Steel, and J. S. Storey, *Average Electron Energy in Beta Decay*, AERE-M 640 (1960).

[5]R. Loevinger, *Phys. Med. Biol.* 1, 330 (1957).

addition, the absorbed dose may be further multiplied by modifying factors, MF, to take account of other factors that are necessary for calculation of the dose equivalent. For example, ICRP and NCRP assign a QF of 1.7 for beta particles of end-point energy below 0.03 Mev, whereas those above 0.03 Mev are assigned a QF of 1.0. It would seem logical that all electrons or beta-like particles emitted with an initial energy above 0.03 Mev should be assigned a QF of 1.7 for the energy absorbed after they have been degraded to energies below 0.03 Mev; provision is made for evaluating such a part of the energy so this weighting can be used if desired. The discontinuous change in QF at 0.03 Mev is based on quite limited experimental evidence. It may be desirable in the future to use a QF which is a continuous function of energy or which is discontinuous at an energy value different from 0.03 Mev. The code is so written as to make incorporation of either of these a relatively simple matter.

Unlike the work of James *et al.*,[4] the present procedure incorporates a screening correction due to the atomic electrons, and the complicated mathematical functions needed for first- and second-forbidden unique transitions and for the Fermi function are computed from the fundamental equations rather than by using the tables of Rose *et al.*[6] These functions are somewhat dependent on mass number for a given atomic number, and the tables of Rose *et al.*[6] use an average value for the mass number associated with a given atomic number. Use of the fundamental equations leads to greater precision. The ratio of average β^- energy to the end-point energy is quite insensitive to the screening correction, but the ratio of average β^+ energy to the end-point energy is appreciably affected by the screening correction at low values of the end-point energy. Loevinger *et al.*[5] made a screening correction for positrons which was based on the work of Reitz.[7] Reitz's screening correction has been seriously questioned in more recent work by Durand[8] and Brown.[9] A screening correction of the form widely used before the work of Reitz[7] and which is in agreement with the work of Durand[8] has been used in the present work.

Figures 25.1 through 25.6 give the ratios of average β^- energy to end-point energy and of average β^+ energy to end-point energy as determined by this code for allowed, first-forbidden unique, and second-forbidden unique transitions. These ratios are plotted vs energy for ten values of the atomic number of the daughter nuclide. The equations used by the code are given in Appendix A.

Electron Capture

When electron capture occurs, x rays and Auger electrons are generated. Smith *et al.*[10] have developed equations for the calculation of the total "beta-type" energy deposition for cases that are extensions of earlier work by Loevinger *et al.*[11] For electron capture, "beta-type" radiation includes Auger electrons and all x rays of energy less than 0.0113 Mev. This division at 0.0113 Mev is based on the fact that at this energy 95% of the electromagnetic radiation is absorbed in 10 mm of water. This distance is comparable with the ranges of many β^- particles in water. In the general case, "beta-type" radiation also includes internal conversion electrons and gamma rays of energy less than 0.0113 Mev.

We have developed a quite general computer program which analyzes the amounts of radiation of various types that are produced when electron capture occurs. The output of the program lists all x rays of energy sufficiently great that they are not "beta type" and gives the numbers of these x rays per disintegration and their respective energies. The output of the program also lists the number per disintegration and associated average energy of all "beta-type" radiation except Auger electrons of energy less than 0.030 Mev. The number per decay and associated average energy of all Auger electrons with energy less than 0.030 Mev is printed separately since these electrons are assigned a QF of 1.7 rather than 1.0, as for other "beta-type" radiation.

[6] M. E. Rose, C. L. Perry, and N. M. Dismuke, *Tables for the Analysis of Allowed and Forbidden Beta Transitions*, ORNL-1459 (1953).

[7] J. R. Reitz, *Phys. Rev.* 77, 10 (1950).

[8] L. Durand III, *Phys. Rev.* 135B, 310 (1964).

[9] L. S. Brown, *Phys. Rev.* 135B, 314 (1964).

[10] E. M. Smith, C. C. Harris, and R. H. Rohrer, *J. Nucl. Med.* 1, 23–31 (1965).

[11] R. Loevinger, J. G. Holt, and G. J. Hine, "Internally Administered Radioisotopes," p. 801 in *Radiation Dosimetry* (ed. by G. J. Hine and G. L. Brownell), Academic, New York, 1958.

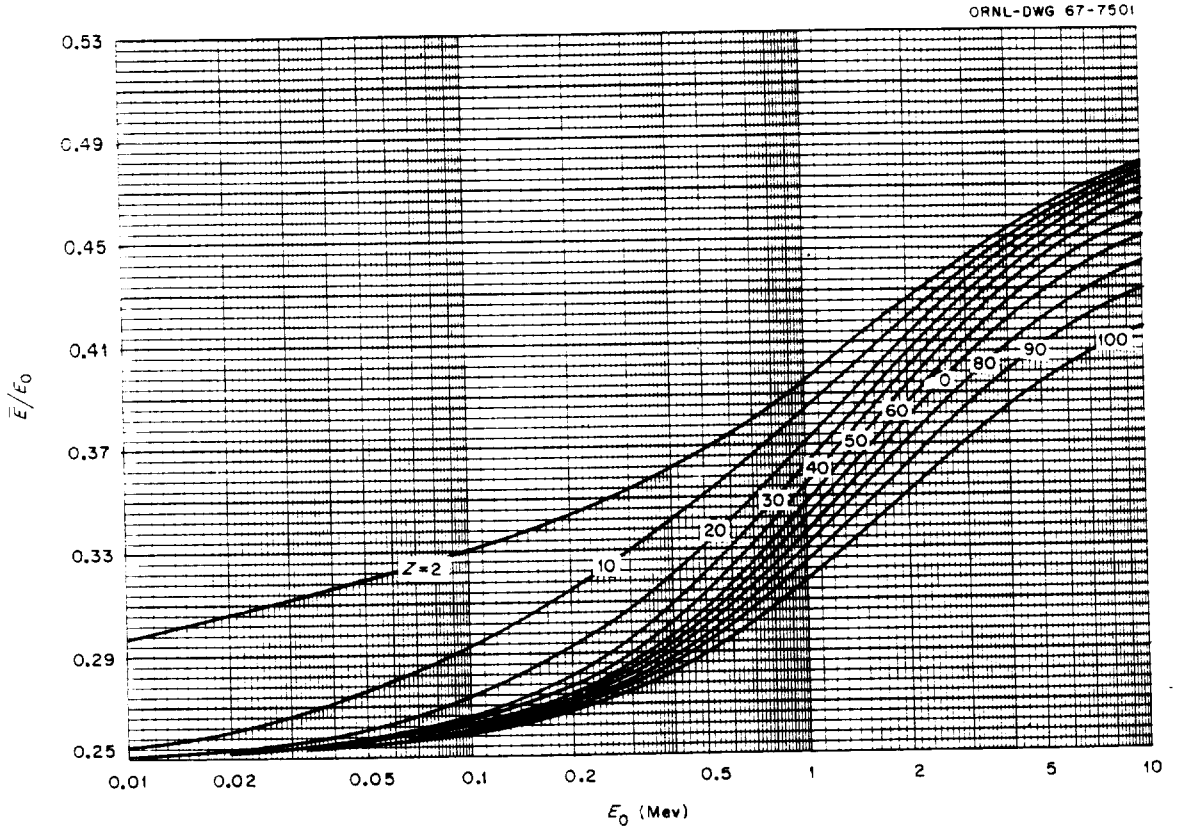

Fig. 25.1. Allowed β^- Transitions.

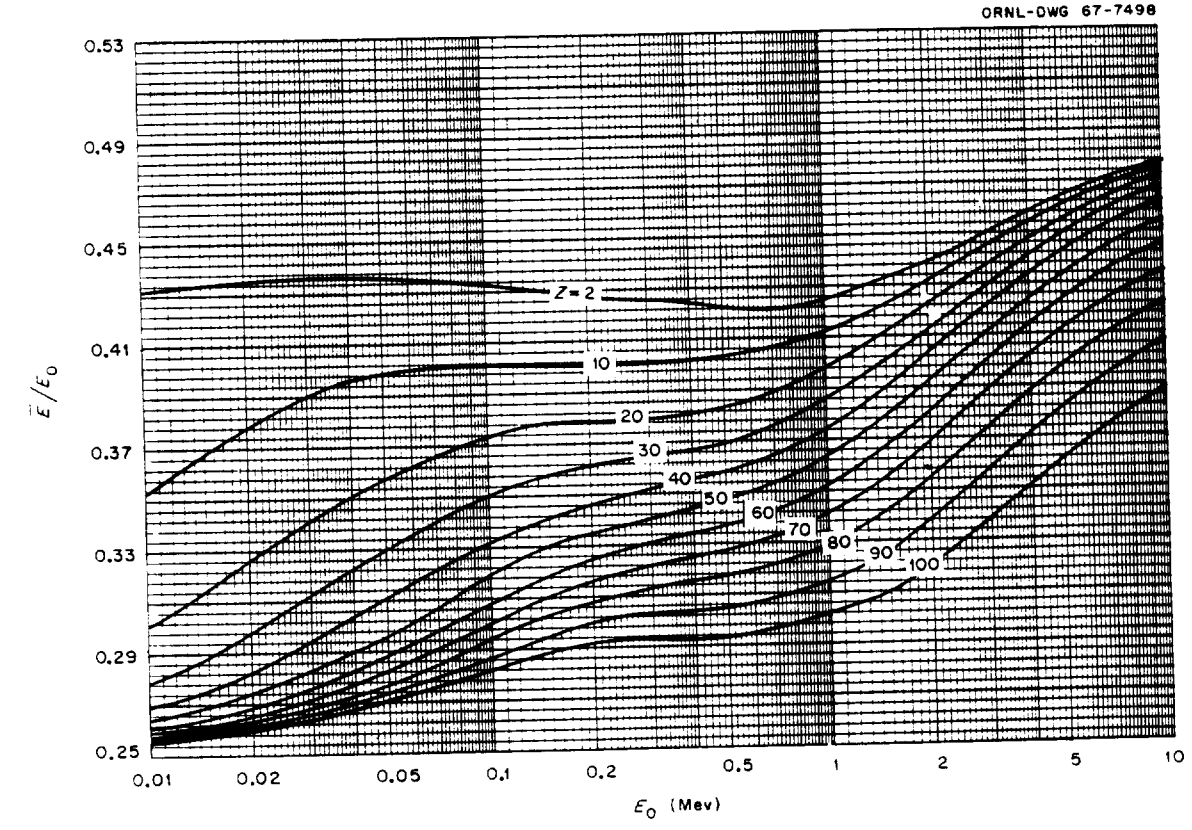

Fig. 25.2. First-Forbidden Unique β^- Transitions.

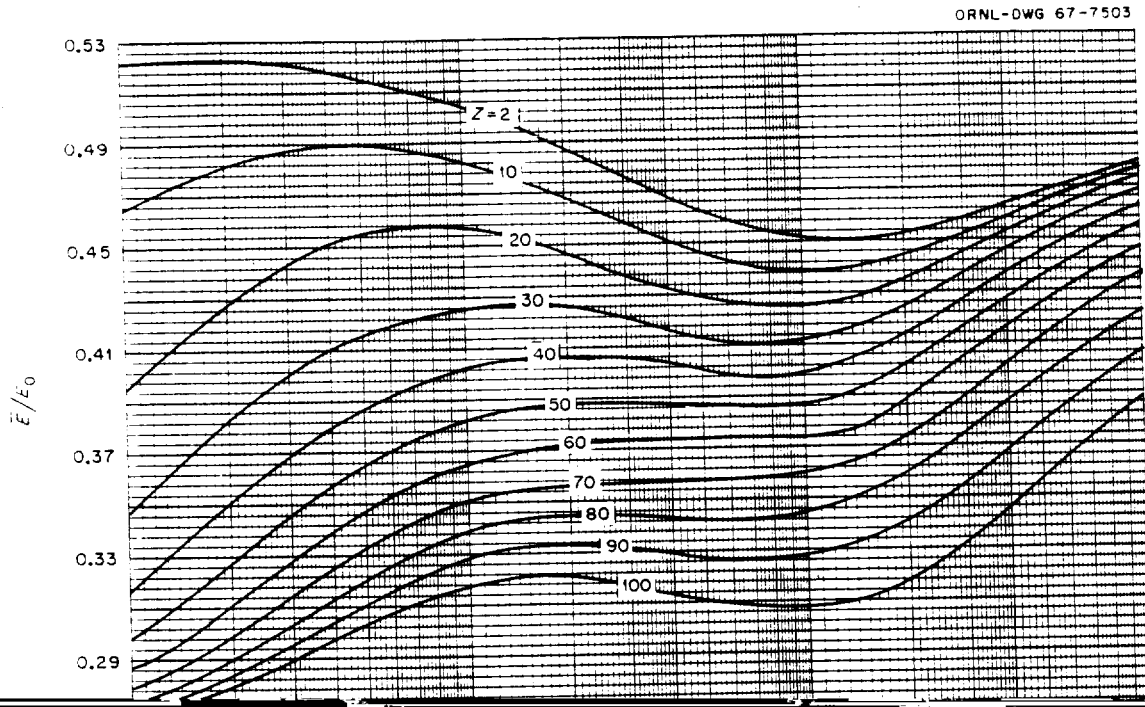
ORNL-DWG 67-7503
0.53
0.49
0.45
0.41
0.37
0.33
0.29
$\bar{E}/E_0$
Z = 2
10
20
30
40
50
60
70
80
90
100

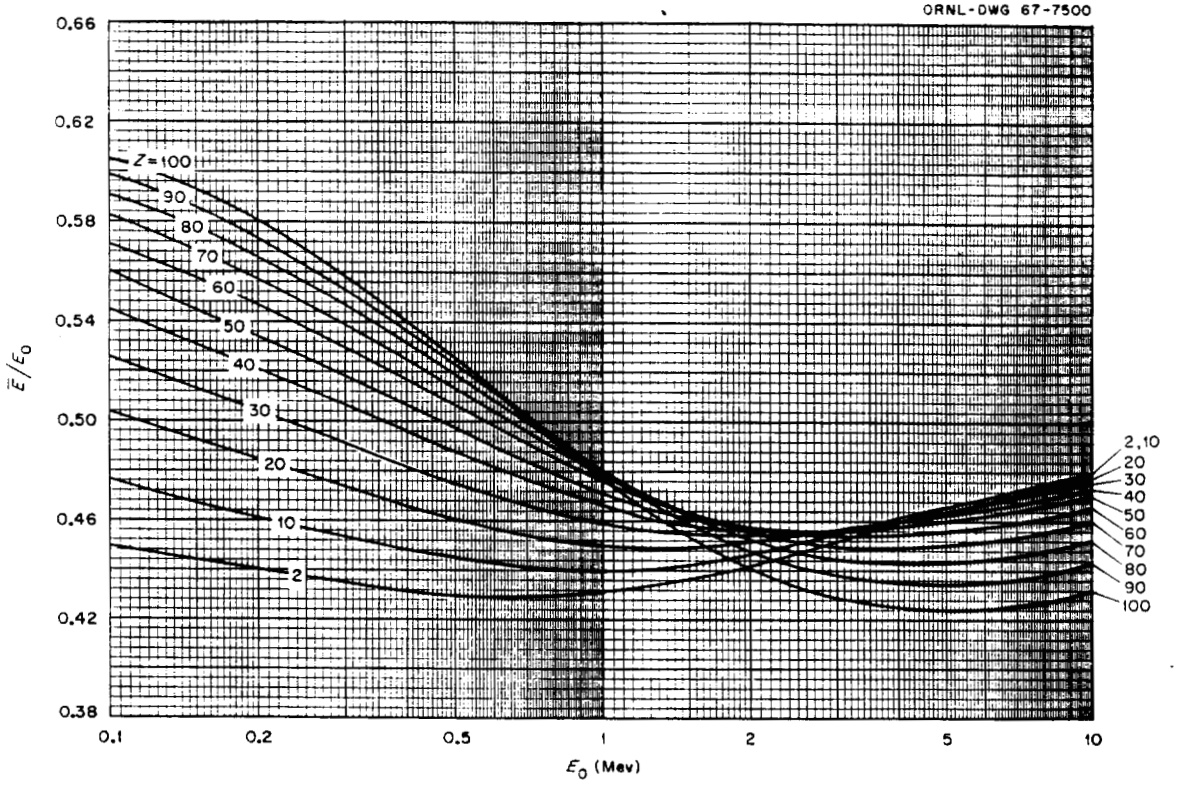

Fig. 25.5. First-Forbidden Unique β^+ Transitions.

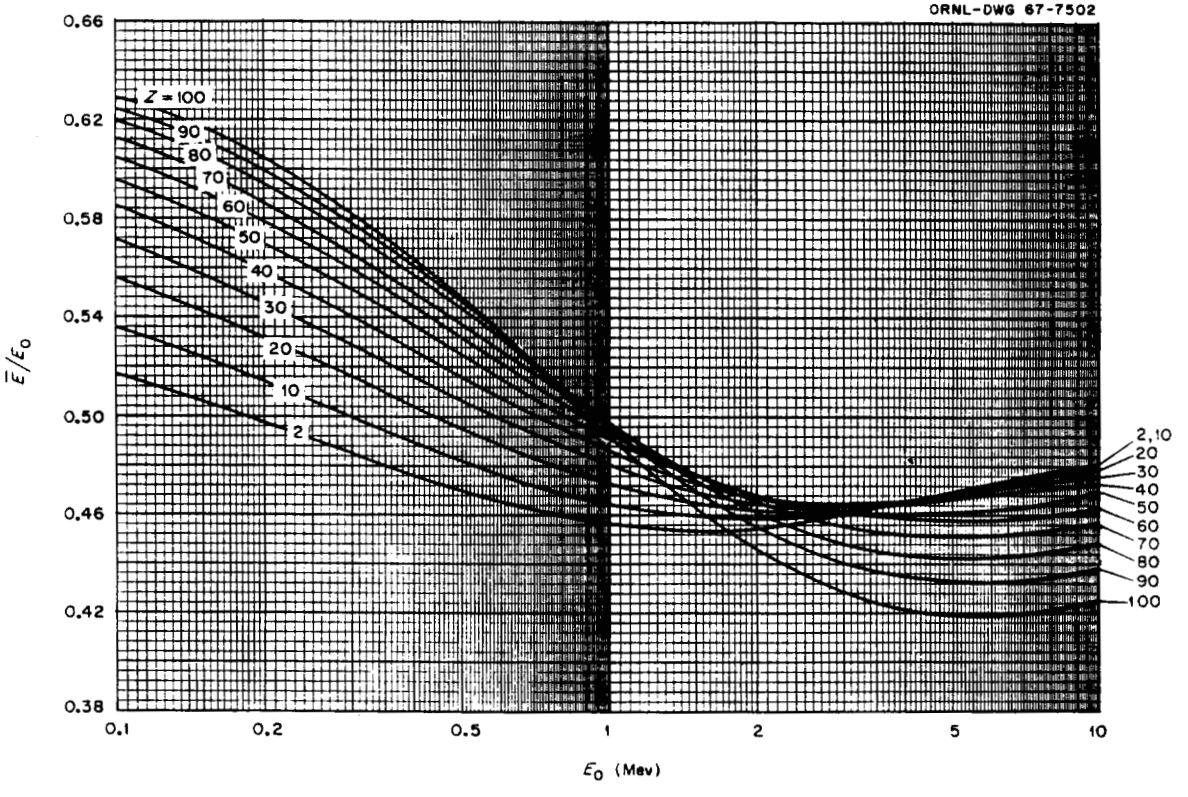

Fig. 25.6. Second-Forbidden Unique β^+ Transitions.

This program extends the work of Smith *et al.*[10] in several ways besides computerization. First of all, their work is limited to atomic numbers less than 82, where the L and M x rays have energies less than 0.0113 Mev, and hence may be considered to be "beta type" and locally absorbed. This limitation is removed in the present work. Second, and most importantly, they state that the fractions f_K, f_L, and f_M, which are the respective fractions of disintegrations that occur by K, L, and M capture, may be determined from $K/L/M$ capture ratios and electron capture branching ratios given in *Nuclear Data Sheets*. However, $K/L/M$ capture ratios are often not given in the *Nuclear Data Sheets*, particularly for the weaker branches. The $K/L/M$ capture ratios as determined from theory are in good agreement with experimental results, but the electron capture branching ratios can be estimated only to orders of magnitude from theory. Hence, the present program uses theoretically computed values of $K/L/M$ capture ratios in conjunction with capture branching ratios given in the *Nuclear Data Sheets*.

The detailed equations involved in the computer program are discussed in Appendix B. The following data for ^{125}I is a typical computer output for electron capture. This example does *not* include the x rays and electrons which are present as a result of the internal conversion of the 0.0353-Mev gamma ray in ^{125}Te which follows the electron-capture process. X rays and electrons arising from internal conversion are included in the example at the end of the following section.

125 I 53 ECA

	FRACTION PER DECAY	ENERGY (MEV)
K-ALPHA1 X-RAYS	.36905	.02747
K-ALPHA2 X-RAYS	.18933	.02720
K-BETA1 X-RAYS	.09964	.03099
K-BETA2 X-RAYS	.02067	.03182
ALL X-RAYS LESS THAN .0113 MEV + ALL AUGER ELECTRONS GREATER THAN .030 MEV	.12913	.00483
ALL AUGER ELECTRONS LESS THAN .030 MEV	2.79170	.00233

The computer output illustrated above is mostly self-explanatory. 125 I 53 means that we are dealing with ^{125}I which has an atomic number of 53; ECA is a mnemonic notation indicating that electron capture is the process under investigation.

Internal Conversion

When internal conversion occurs, one is again faced with the problem of computing the fraction per decay of primary vacancies made in the K, L, and M shells, that is, f_K, f_L, and f_M respectively. Once these fractions are established, the calculations are exactly the same as outlined in the latter part of Appendix B. These fractions may be determined from experimental information concerning the fraction of unconverted gamma transitions per decay, f_r, and experimental information concerning internal conversion coefficients α_K, α_L, α_M, or α_K and $K/L/M$ conversion coefficient ratios. Unfortunately, experimental information concerning internal conversion coefficient parameters is found in many different forms or may be unmeasured. The present computer program does two things in regard to this problem.

First of all, if experimental information is available, the computer will accept a wide variety of forms of the data. The following forms of input data, all of which are sufficient to determine f_K, f_L, and f_M, are accepted by the computer:

1. α_K, α_L ;
2. α_K, K/L ;
3. α_K, K/L, K/M ;
4. α_K, $K/(L+M)$;
5. α_K, K/L, $K/(L+M)$.

For forms 1, 2, and 4, the empirical fact that conversion in the M shell is nearly always about one-third of the conversion in the L shell is used. For example, for form 1 of the input data, we have

$$f_K = f_r \alpha_K ,$$

$$f_L = f_r \alpha_L ,$$

and

$$f_M = \tfrac{1}{3} f_L \ .$$

Forms 3 and 5 of the input data are sufficient to determine f_K, f_L, and f_M uniquely. For example, we have for form 3 of the input data

$$f_K = f_r \alpha_K \ ,$$

$$f_L = f_K/(K/L) \ ,$$

and

$$f_M = f_K/(K/M) \ .$$

Second, the computer program accepts the theoretically computed values of the internal conversion coefficients. We have an entirely separate computer program which computes theoretical internal conversion coefficients by interpolation (cubic equation least-squares fit to the four nearest tabulated values) of the tables compiled by Sliv and Band.[12] This program is a modification of a similar one obtained from the Nuclear Data Group at ORNL. The difficulty with using theoretically computed internal conversion coefficients is that many transitions are admixtures of two different multipolarities, and at the present time it is usually impossible to determine from theory the relative amounts of components of the admixture. A common admixture is magnetic dipole and electric quadrupole radiation. We shall illustrate how the computer program deals with this problem by considering such an admixture.

A quantity called the mixing ratio, δ^2, which is the ratio of intensity of $E2$ (electric quadrupole) radiation to $M1$ (magnetic dipole) radiation, is often experimentally measured and available in the literature. From this the internal conversion coefficients α_K and α_L may be determined by

$$\alpha_K = \frac{\alpha_K(M1) + \delta^2 \alpha_K(E2)}{1 + \delta^2} \ ,$$

and

$$\alpha_L = \frac{\alpha_L(M1) + \delta^2 \alpha_L(E2)}{1 + \delta^2} \ .$$

The computer uses the value of δ^2 and theoretically evaluated internal conversion coefficients in the K and L shells to determine α_K, α_L, and α_M. If α_K or K/L or other experimental quantities concerning internal conversion are available in addition to δ^2, the computer uses theoretically evaluated internal conversion coefficients only to supplement the experimental information and make possible a unique determination of α_K, α_L, and α_M.

If no quantities concerning internal conversion parameters have been measured, the computer assumes no mixing of multipolarities (e.g., it would assume 100% $M1$ where $M1$ and $E2$ are a possible mixture) and uses theoretically determined values of α_K, α_L, and α_M. This can, of course, sometimes lead to significant errors, but for most cases it represents the best estimate available in the complete absence of measured data.

The final output of the program is similar to that for electron capture, and since the electron capture decay of ^{125}I, which was illustrated above, results in an internally converted 0.0353-Mev gamma ray, the kind of output obtained is illustrated below:

[12] L. A. Sliv and I. M. Band, issued in U.S.A. as Report 57ICC K1, Physics Department, University of Illinois (K shell). The L shell results appear in Report 58ICC L1.

125 I 53 GEC

	FRACTION PER DECAY	ENERGY (MEV)
GAMMA RAY	.07020	.03530
K-ALPHA1 X-RAY	.37207	.02747
K-ALPHA2 X-RAY	.19087	.02720
K-BETA1 X-RAY	.10045	.03099
K-BETA2 X-RAY	.02083	.03182
ALL X-RAYS AND/OR GAMMA RAYS LESS THAN .0113 MEV + ALL AUGER AND/OR INTERNAL CONVERSION ELECTRONS GREATER THAN .0300 MEV	.26822	.01951
ALL AUGER AND/OR INTERNAL CONVERSION ELECTRONS LESS THAN .030 MEV	3.44394	.00263

The letters GEC are a mnemonic notation to indicate we are dealing with a gamma ray following electron capture. The computer output for the electron capture decay of ^{125}I may be added to this computer output to give the total distribution of radiations emitted in the case of ^{125}I decay. This gives the following results:

Radiations Present in ^{125}I Decay

	FRACTION PER DECAY	ENERGY (MEV)
GAMMA RAY	.07020	.03530
K-ALPHA1 X-RAY	.74112	.02747
K-ALPHA2 X-RAY	.38020	.02720
K-BETA1 X-RAY	.20009	.03099
K-BETA2 X-RAY	.04150	.03182
ALL X-RAYS AND/OR GAMMA RAYS LESS THAN .0113 MEV + ALL AUGER AND/OR INTERNAL CONVERSION ELECTRONS GREATER THAN .0300 MEV	.39735	.01474
ALL AUGER AND/OR INTERNAL CONVERSION ELECTRONS LESS THAN .030 MEV	6.23564	.00250

The last two rows of information are sufficient to determine the total "beta-type" radiation emitted by ^{125}I and give 21.4 kev/disintegration. This compares quite favorably with the value of 20.8 kev/disintegration computed by Smith *et al.*[10]

A number of extensions and improvements in these programs are possible, and further work is in progress. These programs are written in FORTRAN IV and are available from the author.

Appendix A: Beta Decay

The following notations are used:

V_0 = screening potential due to atomic electrons (mc^2 units)

W_0 = end-point total energy (mc^2 units)

W = total energy of negatron or positron (mc^2 units)

ρ = momentum of negatron or positron (mc units)

Z = atomic number of daughter nucleus; Z must be taken positive for negatron emission and negative for positron emission

$F(Z, W)$ = Fermi function

α = fine structure constant = 1/137

R = nuclear radius

A = mass number

$\bar{E}$ = average kinetic energy of the negatron or positron (mc^2 units)

E_0 = end-point kinetic energy (mc^2 units)

The units used throughout the following equations are those in which m (electron mass), c (velocity of light in vacuo), and $\hbar$ (Planck's constant divided by 2π) are assigned values equal to 1. In these units $E = W - 1$ and $\rho^2 = W^2 - 1$.

Neglecting screening corrections, the ratio $\bar{E}/E_0$ in allowed beta decay is given by

$$\frac{\bar{E}}{E_0} = \frac{\bar{W} - 1}{E_0}, \tag{1}$$

where

$$\bar{W} = \frac{\int_1^{W_0} W\, N(W)\, dW}{\int_1^{W_0} N(W)\, dW}, \tag{2}$$

and

$$N(W) = F(Z, W)\, \rho W (W_0 - W)^2, \tag{3}$$

with

$$F(Z, W) = 2(1 + \gamma_0)\, (2\rho R)^{2(\gamma - 1)}\, e^{\pi y} \times \left[\frac{|\Gamma(\gamma_0 + iy)|}{\Gamma(2\gamma_0 + 1)} \right]^2. \tag{4}$$

In this equation for $F(Z, W)$, $\gamma_0 = [1 - (\alpha Z)^2]^{1/2}$, $R = \frac{1}{2} \alpha A^{1/3}$, and $y = \alpha ZW/\rho$.

When screening is taken into account, Eq. (3) becomes

$$N(W) = F(Z, W - V_0)\,[(W - V_0)^2 - 1]^{1/2} \times (W - V_0)\,(W_0 - W)^2, \quad (5)$$

where V_0 is the screening potential in mc^2 units. The screening potential used in the present work is

$$V_0 = \frac{1.13\,|Z|^{4/3}}{\alpha^2}, \quad (6)$$

where V_0 must be taken positive for electrons and negative for positrons. When Eq. (5) is substituted into Eq. (2), it can be shown that the result is equivalent to

$$\bar{W} = \frac{\int_{1 - V_0}^{W_0 - V_0} (W + V_0)\,F(Z, W)\,W\rho(W_0 - W - V_0)^2\,dW}{\int_{1 - V_0}^{W_0 - V_0} F(Z, W)\,W\rho(W_0 - W - V_0)^2\,dW}. \quad (7)$$

Equation (7) in combination with Eq. (1) was used to determine $\bar{E}/E_0$ for allowed transitions.

For first-forbidden unique transitions, Eq. (3) is modified by a shape function a_1, namely,

$$N(W) = F(Z, W)\;a_1 \rho W (W_0 - W)^2, \quad (8)$$

where

$$a_1 = (W_0 - W)^2 L_0 + 9L_1, \quad (9)$$

and for second-forbidden unique transitions, there is a similar modification by a shape function a_2, where

$$a_2 = (W_0 - W)^4 L_0 + 30\,(W_0 - W)^2 L_1 + 225 L_2. \quad (10)$$

The complicated functions L_0, L_1, and L_2 are determined from

$$L_\nu = \frac{1}{2\rho^2 F(Z, W) R^{2\nu}} (g^2_{-\nu - 1} + f^2_{\nu + 1}). \quad (11)$$

The subscript ν may have the value 0, 1, or 2.

Functions f and g are determined from

$$f_n = (W - 1)^{1/2} Q_n \times \left\{ \text{imaginary part}\,[S_n\,{}_1F_1(a, b; z)] \right\} \quad (12)$$

and

$$g_n = (W + 1)^{1/2} Q_n \times \left\{ \text{real part}\,[S_n\,{}_1F_1(a, b; z)] \right\}, \quad (13)$$

where

$$Q_n = \frac{(2\rho R)^{\gamma_n}}{W^{1/2} R}\, e^{\pi y/2}\, \frac{|\Gamma(\gamma_n + iy)|}{\Gamma(2\gamma_n - 1)},$$

$$S_n = e^{-i\rho R + in}(\gamma_n + iy),$$

$$a = \gamma_n + 1 + iy,$$

$$b = 2\gamma_n + 1,$$

$$z = 2i\rho R,$$

$$\gamma_n = (n^2 - \alpha^2 Z^2)^{1/2},$$

$$e^{2i\eta} = \frac{-n + iy/W}{\gamma_n + iy},$$

and ${}_1F_1(a, b; z)$ is the confluent hypergeometric function, which can be represented by

$${}_1F_1(a, b; z) = \frac{\Gamma(b)}{\Gamma(a)} \sum_{m=0}^{\infty} \frac{\Gamma(a + m)}{\Gamma(b + m)} \frac{z^m}{m!}.$$

The subscript n in the functions f_n and g_n takes on the values -3, -2, -1, $+1$, $+2$, and $+3$ for the various calculations necessary to compute L_0, L_1, and L_2.

When screening is taken into consideration and one integrates from $1 - V_0$ to $W_0 - V_0$, as in Eq. (7), the shape factors represented by Eqs. (9) and (10) become, respectively,

$$a_1 = (W_0 - W - V_0)^2 L_0 + 9L_1 \quad (14)$$

and

$$a_2 = (W_0 - W - V_0)^4 L_0 - 30(W_0 - W - V_0)^2 L_1 + 225 L_2 \quad (15)$$

Thus, finally, for first-forbidden unique transitions, one has

$$\frac{\overline{E}}{E_0} = \frac{\int_{1 - V_0}^{W_0 - V_0} (W + V_0)\, F(Z, W)\, W p a_1 (W_0 - W - V_0)^2\, dW}{\int_{1 - V_0}^{W_0 - V_0} F(Z, W)\, W p a_1 (W_0 - W_0 - V_0)^2\, dW} , \quad (16)$$

where a_1 is given by Eq. (14). Equation (16), in conjunction with Eq. (2), was used to determine $\overline{E}/E_0$ for first-forbidden unique transitions.

For second-forbidden unique transitions, a_2 as given by Eq. (15) is used in Eq. (16) in place of a_1, and the calculations otherwise proceed in a similar fashion.

Appendix B: Electron Capture

When orbital electron capture occurs, vacancies are created in the various electronic shells. The probability is highest for vacancies to be made in the K shell, if energetically possible. However, a significant number of primary vacancies often are made in the L and M shells. As we shall see, the contributions due to still higher shells are nearly always negligible. For the present work these small contributions may be included with the M-shell contribution.

The $K/L/M$ capture ratios have been studied on the basis of theory by Brysk and Rose[13] and by Bahcall.[14] A number of the results of Brysk and Rose are contained in *Nuclear Spectroscopy Tables*, by Wapstra *et al.*,[15] on pages 59–61. Table 25.1 gives the notations which will be used in the remaining parts of Appendix B.

In Table 25.1, items 4 through 9 are functions of the atomic number and have been tabulated in the literature. Items 4 to 7 may be found in *Nuclear Spectroscopy Tables*,[15] and items 8 and 9 may be extracted from graphs in Chap. XXV, Part A, of *Alpha, Beta and Gamma-Ray Spec-*

[13] H. Brysk and M. E. Rose, *Rev. Mod. Phys.* 30, 1169 (1958).

[14] J. N. Bahcall, *Phys. Rev.* 132, 362 (1963).

[15] A. H. Wapstra, G. J. Nijgh, and R. Van Lieshout, *Nuclear Spectroscopy Tables*, p. 61, Interscience, New York, 1959.

Table 25.1. Notations Used in Appendix B

1. E_n = energy difference of the nuclear levels involved in the nth electron capture branch
2. N_n = the fraction of times the parent nucleus decays via electron capture to the nth branch
3. $\epsilon_{L_I}/\epsilon_K$, $\epsilon_{L_{II}}/\epsilon_{L_I}$, $\epsilon_{L_{III}}/\epsilon_{L_I}$, $\epsilon_{M^+}/\epsilon_L$ = the ratios of electron captures in the various shells or subshells; ϵ_{M^+} means electron capture in the M and all higher shells
4. L_{L_I}/L_K, $L_{L_{II}}/L_{L_I}$, $9L_{III}/L_{L_I}$ = the ratios of certain needed atomic wave function parameters
5. ω_K and ω_L = the K and L shell fluorescent yields respectively
6. E_K, E_{L_I}, $E_{L_{II}}$, $E_{L_{III}}$, E_M = the binding energies in the various shells; E_M is an average over the subshells
7. $K_{\alpha 2}/K_{\alpha 1}$, $K_{\beta 1}/K_{\alpha 1}$, $K_{\beta 2}/K_{\alpha 1}$ = ratios of numbers of $K_{\alpha 1}$, $K_{\beta 1}$, and $K_{\beta 2}$ x rays to $K_{\alpha 1}$ x rays respectively
8. a_{KLX}/a_{KLL} and a_{KXY}/a_{KLL} = ratios of numbers of KLX and KXY Auger electrons to KLL Auger electrons respectively
9. R_{11}, R_{12}, R_{22}, R_{13}, R_{33} = ratios of numbers of KL_1L_1, KL_1L_2, KL_2L_2, DL_1L_3, and KL_3L_3 Auger electrons to KL_2L_3 Auger electrons respectively

trometry, edited by K. Siegbahn. These parameters for each value of Z have been punched onto IBM cards and are used as input data for the computer code.

Electron capture transitions, like other beta transitions, are classed into allowed, first-forbidden, first-forbidden unique, etc., types depending upon spin and parity changes between the nuclear levels involved in the transition. The $K/L/M$ capture ratios are about the same for first-forbidden and allowed transitions; they are also about the same for first-forbidden unique and second-forbidden transitions. Hence we shall consider $K/L/M$ ratios for three cases: allowed, first-forbidden unique, and second-forbidden unique transitions.

Allowed Transitions. – The ratio of capture in the L_{I} shell to that in the K shell is given by

$$\frac{\epsilon_{L_{\mathrm{I}}}}{\epsilon_K} = \frac{L_{L_{\mathrm{I}}}}{L_K}\left(\frac{E_n - E_{L_{\mathrm{I}}}}{E_m - E_K}\right)^2 \times \left(1 + \frac{2.81}{Z} + \frac{13.76}{Z^2} + \frac{75.2}{Z^3}\right) , \quad (1)$$

where the polynomial in inverse powers of Z (atomic number) is a correction to the theory of Brysk and Rose[13] which takes into account the effects of electron exchange and imperfect atomic overlap. This correction was developed by Bahcall,[14] who shows that Eq. (1) agrees with experiment within experimental error.

The ratio of electron capture in the L_{II} subshell to that in the L_{I} subshell is

$$\frac{\epsilon_{L_{\mathrm{II}}}}{\epsilon_{L_{\mathrm{I}}}} = \frac{L_{L_{\mathrm{II}}}}{L_{L_{\mathrm{I}}}} . \quad (2)$$

Electron capture in the L_{III} subshell does not occur in allowed transitions.

We shall designate the ratio of electron capture in M and higher shells to electron capture in the L shell by $\epsilon_{M^+}/\epsilon_L$, and, as indicated above, this has been tabulated as a function of Z.

Designating the total electron capture by ϵ, one may easily show that

$$\frac{\epsilon}{\epsilon_K} = 1 + \frac{\epsilon_{L_{\mathrm{I}}}}{\epsilon_K}\left(1 + \frac{\epsilon_{L_{\mathrm{II}}}}{\epsilon_{L_{\mathrm{I}}}}\right) \times \left(1 + \frac{\epsilon_{M^+}}{\epsilon_L}\right) . \quad (3)$$

Hence the number of vacancies made in the K shell per decay, f_K, is given by

$$f_K = \sum_n N_n \frac{\epsilon_K}{\epsilon} = \sum_n N_n \left[1 + \frac{\epsilon_{L_{\mathrm{I}}}}{\epsilon_K} \times \left(1 + \frac{\epsilon_{L_{\mathrm{II}}}}{\epsilon_{L_{\mathrm{I}}}}\right)\left(1 + \frac{\epsilon_{M^+}}{\epsilon_L}\right)\right]^{-1} . \quad (4)$$

The number of primary vacancies made in the L shell per decay, f_L, is

$$f_L = \sum_n f_{K_n} \frac{\epsilon_{L_{\mathrm{I}}}}{\epsilon_K}\left(1 + \frac{\epsilon_{L_{\mathrm{II}}}}{\epsilon_{L_{\mathrm{I}}}}\right) . \quad (5)$$

The number of primary vacancies made in the M and higher shells per decay, f_{M^+}, is

$$f_{M^+} = \sum_n (N_n - f_{K_n} - f_{L_n}) . \quad (6)$$

In Eqs. (4) to (6) the summation over n is necessary if there is more than one electron capture branch in the decay.

First-Forbidden Unique Transitions. – For first-forbidden unique transitions, the following equations apply:

$$\frac{\epsilon_{L_{\mathrm{I}}}}{\epsilon_K} = \frac{L_{L_{\mathrm{I}}}}{L_K}\left(\frac{E_n - E_{L_{\mathrm{I}}}}{E_n - E_K}\right)^4 \quad (7)$$

and

$$\frac{\epsilon_{L_{III}}}{\epsilon_{L_I}} = 0.511^2 \left(\frac{9L_{L_{III}}}{L_{L_I}}\right) \frac{\left(E_n - E_{L_{III}}\right)^2}{\left(E_n - E_{L_I}\right)^4} ; \quad (8)$$

$\epsilon_{L_{II}}/\epsilon_{L_I}$ and $\epsilon_{M^+}/\epsilon_L$ are the same as for allowed transitions. It follows that the number of vacancies made in the K shell per decay is

$$f_K = \sum_n N_n \left[1 + \frac{\epsilon_{L_I}}{\epsilon_K} \left(1 - \frac{\epsilon_{L_{II}}}{\epsilon_{L_I}} + \frac{\epsilon_{L_{III}}}{\epsilon_{L_I}}\right)\left(1 + \frac{\epsilon_{M^+}}{\epsilon_L}\right)\right]^{-1} , \quad (9)$$

$$f_L = \sum_n f_{K_n} \frac{\epsilon_{L_I}}{\epsilon_K} \left(1 + \frac{\epsilon_{L_{II}}}{\epsilon_{L_I}} + \frac{\epsilon_{L_{III}}}{\epsilon_{L_I}}\right) , \quad (10)$$

and f_{M^+} is given by Eq. (6).

Second-Forbidden Unique Transitions. – For second-forbidden unique transitions, the following equations apply:

$$\frac{\epsilon_{L_I}}{\epsilon_K} = \frac{L_{L_I}}{L_K} \left(\frac{E_n - E_{L_I}}{E_n - E_K}\right)^6 \quad (11)$$

and

$$\frac{\epsilon_{L_{III}}}{\epsilon_{L_I}} = \frac{10}{3} \cdot 0.511^2 \frac{\left(E_n - E_{L_{III}}\right)^4}{\left(E_n - E_{L_I}\right)^6} ; \quad (12)$$

$\epsilon_{L_{II}}/\epsilon_{L_I}$ and $\epsilon_{M^+}/\epsilon_L$ are the same as for allowed transitions. Using these results, Eqs. (6), (9), and (10) then apply to give f_K, f_L, and f_{M^+}.

Once f_K, f_L, and f_{M^+} are found by the above equations, we use the results to determine the relative numbers of various x rays and Auger electrons which will be produced. This proceeds as follows:

First of all, it is a simple matter to program the computer, using the information listed in item 7 of Table 25.1 as input, to compute the relative yields of $K_{\alpha 1}$, $K_{\alpha 2}$, $K_{\beta 1}$, and $K_{\beta 2}$ x rays arising from vacancies in the K shell. Let us call these relative yields, normalized to 1, $N_{\alpha 1}$, $N_{\alpha 2}$, $N_{\beta 1}$, $N_{\beta 2}$ respectively. Similarly, one may use the information listed in item 6 of the table to determine the respective energies of these x rays.

Second, the computer uses the information listed in item 8 of Table 25.1 to determine the relative intensities of the KLL, KLX, and KXY Auger electrons. Let us call these relative intensities, normalized to 1, N_{KLL}, N_{KLX}, and N_{KXY} respectively. Similarly one may use the information listed in items 6 and 9 to determine a weighted average energy associated with each of these Auger electron groups.

Then the fractions of $K_{\alpha 1}$, $K_{\alpha 2}$, $K_{\beta 1}$, and $K_{\beta 2}$ x rays per decay and the fractions of KLL, KLX, and KXY Auger electrons per decay, which may be represented by $f_{\alpha 1}$, $f_{\alpha 2}$, $f_{\beta 1}$, $f_{\beta 2}$, f_{KLL}, f_{KLX}, and f_{KXY}, respectively, are

$$f_{\alpha 1} = f_K \omega_K N_{\alpha 1} , \quad (13)$$

$$f_{\alpha 2} = f_K \omega_K N_{\alpha 2} , \quad (14)$$

$$f_{\beta 1} = f_K \omega_K N_{\beta 1} , \quad (15)$$

$$f_{\beta 2} = f_K \omega_K N_{\beta 2} , \quad (16)$$

$$f_{KLL} = f_K (1 - \omega_K) N_{KLL} , \quad (17)$$

$$f_{KLX} = f_K (1 - \omega_K) N_{KLX} , \quad (18)$$

$$f_{KXY} = f_K (1 - \omega_K) N_{KXY} . \quad (19)$$

Then the total vacancies per decay made in the L shell, n_L, are given by

$$n_L = f_L + f_{\alpha 1} + f_{\alpha 2} + 2f_{KLL} + f_{KLX} , \quad (20)$$

and the fraction per decay of L x rays, f_{LX}, is

$$f_{LX} = n_L \omega_L , \quad (21)$$

whereas the fraction per decay of LXY Auger electrons, f_{LXY}, is

$$f_{LXY} = n_L (1 - \omega_L) . \quad (22)$$

We make the approximation in this code that for

both x-ray and Auger processes, only M-shell electrons are involved in the transitions which result from vacancies in the L shell.

The total vacancies per decay made in the M shell, n_M, is

$$n_M = f_M + f_{21} + f_{KLX} + 2f_{KXY} + f_{LX} + 2f_{LXY} . \quad (23)$$

The very low-energy x rays and Auger electrons which result from these vacancies in the M shell will be completely absorbed locally, and we assign an energy equal to the average binding energy in the M shell to these processes.

DISTRIBUTION OF DOSE IN THE BODY FROM A SOURCE OF GAMMA RAYS DISTRIBUTED UNIFORMLY IN AN ORGAN

H. L. Fisher, Jr.[16] W. S. Snyder

When a gamma emitter is present in an organ of the body, only a fraction of the emitted gamma energy is absorbed in that organ. Many evaluations of the absorbed fraction have been published, mostly for highly idealized and perhaps oversimplified cases. The use of an effective radius and a spherical geometry is one instance of such drastic simplification. Although an exact theory of gamma photon interaction with matter is known in detail, application of this theory is usually difficult since an enormous amount of mathematical computation is involved. However, by use of a high-speed digital computer these calculations become feasible. A Monte-Carlo-type calculation has been used to estimate the dose in 22 organs and 100 subregions of an adult human phantom for four initial gamma energies. This report is divided into three parts: a description of the phantom, details of the Monte Carlo method used (described previously[17]), and the dose estimates from a gamma source distributed uniformly in the total body and in the skeleton.

The Phantom

Figure 25.7 shows the phantom and the subregions in which dose was determined. The dimensions of the phantom were chosen after consideration of the average size and weight of humans[18–20] and the phantoms designed by Hayes and Brucer.[21] In order to describe the various regions, a coordinate system is needed. As shown in the figure, the origin of the rectangular coordinate system is located at the center of the base of the trunk. The positive z axis extends vertically through the head, the left side of the phantom is taken along the positive x axis, and the rear is taken along the positive y axis. All units of length are in centimeters.

By use of the coordinate system in Fig. 25.7, the body of the phantom may be described as follows. The trunk is an elliptical cylinder given by

$$\left(\frac{x}{20}\right)^2 + \left(\frac{y}{10}\right)^2 \leq 1 ,$$

$$0 \leq z \leq 70 .$$

The head is also an ellipitical cylinder:

$$\left(\frac{x}{7}\right)^2 + \left(\frac{y}{10}\right)^2 \leq 1 ,$$

$$70 < z \leq 94 .$$

The legs are considered together to be a truncated elliptical cone:

$$\left(\frac{x}{20}\right)^2 + \left(\frac{y}{10}\right)^2 \leq \left(\frac{100 + z}{100}\right)^2 ,$$

$$-80 \leq z < 0 .$$

[16] U.S. Public Health Service.

[17] H. L. Fisher, Jr., and W. S. Snyder, *Health Phys. Div. Ann. Progr. Rept. July 31, 1966*, ORNL-4007, p. 221.

[18] P. L. Altman and D. S. Dittmer, *Growth Including Reproduction and Morphological Development*, Biological Handbook, Fed. Am. Soc. Exptl. Biol., Washington, 1962.

[19] W. M. Krogman, "Growth of Man," pp. 712–15 in *Tabulae Biologicae*, vol. XX, ed. by H. Denzer *et al.*, Den Haag, 1941.

[20] "Report of ICRP Task Group on the Revision of Standard Man," in preparation.

[21] R. L. Hayes and M. Brucer, *Intern. J. Appl. Radiation Isotopes* 9, 111 (1960).

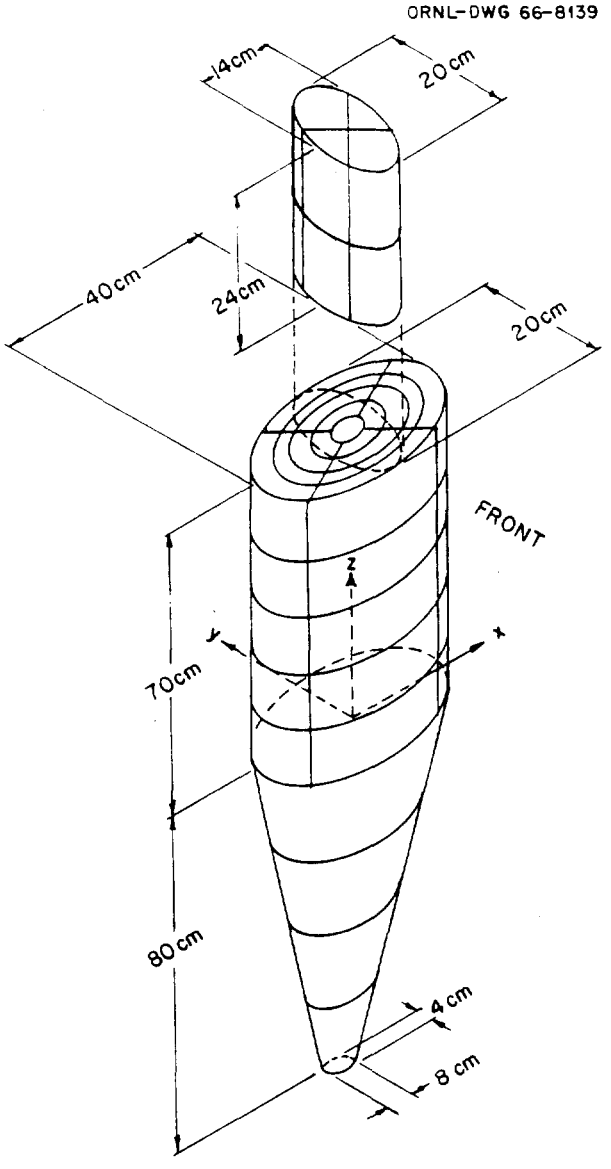

Fig. 25.7. The Adult Human Phantom.

It is now a simple matter for the computer to take any point (x, y, z), substitute it into these inequalities, note whether the inequalities are satisfied, and thereby determine whether this point is inside or outside the phantom and whether it is in the head, trunk, or legs. Except for the head, this phantom is convex. Account has been taken of the photons which transverse the void between the trunk and the head.

The arbitrary subregions into which the phantom was sectioned and in which dose was determined are outlined in Fig. 25.7. The legs were cut into four layers by equidistant horizontal planes; the trunk was divided into five layers by equidistant horizontal planes. Two vertical planes, intersecting at right angles along the central axis of the trunk and having an angle of 45° from either the x or y axis, cut these layers. The final volume element is obtained by four vertical concentric elliptical cutting cylinders. The major axes of these elliptical cylinders are 4, 8, 12, and 16 cm, and the minor axes are 2, 4, 6, and 8 cm. The innermost elliptical cylinder was not cut by the vertical planes. The head was sectioned into two layers equal in thickness and was cut by the same two vertical planes that cut the trunk. Although dose was determined in these arbitrary regions, the results are not presented in this report since the principal purpose is to give organ doses. However, results from the arbitrary regions permit an approximation of the variation of dose throughout the phantom. In particular, if an organ is very small (e.g., ovary, thyroid, pituitary, etc.), the dose estimate may be statistically unreliable on a given calculation, and one may use instead an average dose over one of these layer regions.

Mathematical descriptions of the organs were formulated after consideration of the descriptive and schematic material from several general anatomy references.[22,23] The scaled cross sections of the human body by Eycleshymer and Schoemaker[24] were helpful in locating the positions at which to place the organs as well as an aid in the construction of the organs. The representations of the organs by the mathematical equations given herein are only approximate, and many other geometrically simple approximations might be used. The goal in constructing these mathematical organs was to obtain the approximate size and shape of an average organ through the use of a few simple mathematical equations. If the size and shape approximate those of the real organ, the dose estimate should be correspondingly accurate. To minimize running time and, therefore, cost, the formulas used should be as simple as possible.

The composition of the phantom is tissue[25] of density 1 g/cm^3. There is no low-density area for

[22] H. Gray, *Anatomy of the Human Body*, Lea and Febiger, Philadelphia, 1942.

[23] W. J. Hamilton, *Textbook of Human Anatomy*, Macmillan, London, 1957.

[24] A. C. Eycleshymer and D. M. Schoemaker, *A Cross-Section Anatomy*, D. Appleton-Century, New York, 1911.

[25] "Protection Against Neutron Radiation up to 30 Million Electron Volts," *NBS Handbook* 63, U.S. Dept. of Commerce, 1957.

the lung nor is there a high-density region with modified mass absorption coefficient for bone. However, for gamma energies between 0.2 and 4 Mev, the mass absorption coefficients for bone and soft tissue are essentially the same within several percent. Below 0.2 Mev the photoelectric cross section for bone rises much more rapidly than that for soft tissue. This is one of the major limitations of the present approach. The volume in cubic centimeters of most mathematical organs will be equal to the weight of an average organ in grams. This is not true for the lungs or for regions of bone. The linear dimensions of all organs, including lungs and bones, have been used as the primary basis for developing the mathematical equations.

Figure 25.8 shows an anterior view of some of the larger organs and their positions in the phantom. In the following account, a brief description of each mathematical organ will be given, followed by the mathematical inequalities which must be satisfied for the point (x, y, z) in the coordinate system of Fig. 25.7 to be in the organ. The volumes given were determined by integration.

The volumes of the head, trunk, legs, and total body are 5278, 43,982, 20,776, and 70,036 cm^3 respectively. When there are left and right organs, the equations for only one, the left, will be given. The equations for the other may be obtained by replacing x by $-x$ in the inequalities.

Adrenals. – Each adrenal is half an ellipsoid sitting atop a kidney. The left adrenal is given by

$$\left(\frac{x-4.5}{1.5}\right)^2+\left(\frac{y-6.5}{0.5}\right)^2+\left(\frac{z-38}{5}\right)^2\leq 1,$$

$$z\geq 38$$

The volume of both adrenals is 15.71 cm^3.

Bladder (Urinary). – The bladder plus contents when moderately full is an ellipsoid given by

$$\left(\frac{x}{6}\right)^2+\left(\frac{y+4.5}{4.5}\right)^2+\left(\frac{z-8}{4.5}\right)^2\leq 1,$$

and the volume is 508.9 cm^3.

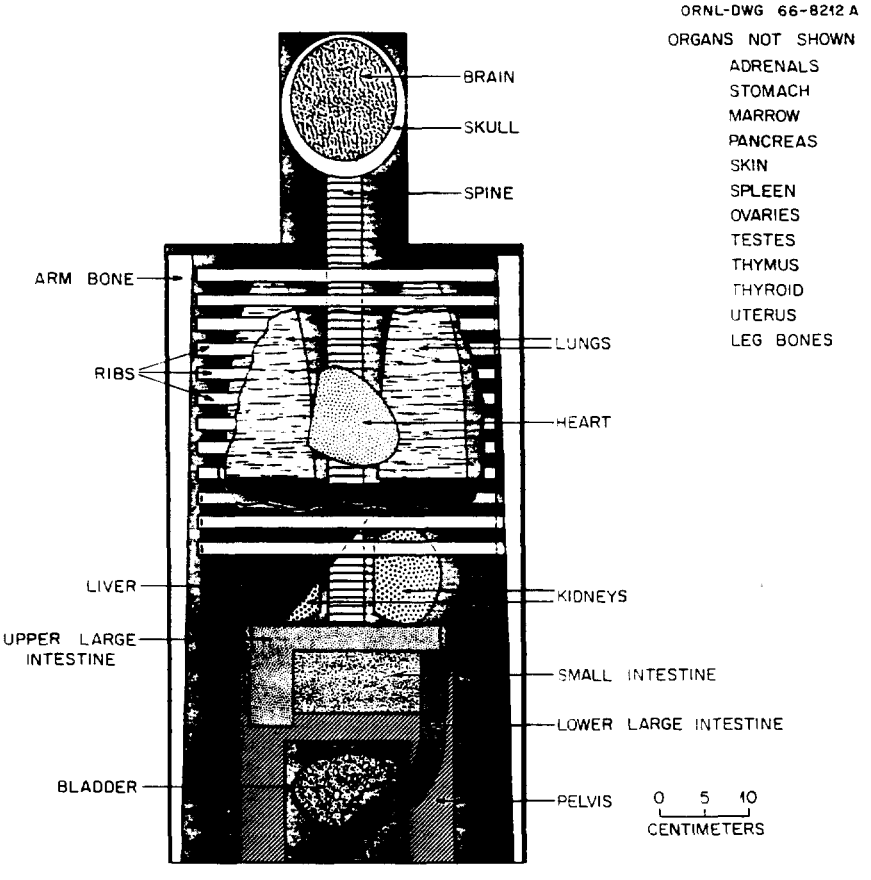

Fig. 25.8. Anterior View of the Principal Organs in the Head and Trunk of the Phantom.

Brain. – The brain is an ellipsoid given by

$$\left(\frac{x}{6}\right)^2 + \left(\frac{y}{9}\right)^2 + \left(\frac{z - 86.5}{6.5}\right)^2 \leq 1 ,$$

and the volume is 1470 cm^3.

Gastrointestinal Tract. – The form of the gastrointestinal (GI) tract given here represents the mass of the tract itself plus the 24-hr average mass of contents. This is a particularly difficult organ to fix since its volume and location are subject to change between individuals as well as in the same individual. The intestines are taken to be in the somewhat-idealized standard positions. The stomach is the most difficult to represent since its volume will change by nearly an order of magnitude several times in 24 hr. The constant-sized and fixed-position stomach given here is, therefore, not very realistic but should suffice for estimating an approximate dose in that region. The stomach is an ellipsoid,

$$\left(\frac{x - 8}{4}\right)^2 + \left(\frac{y + 4}{3}\right)^2 + \left(\frac{z - 35}{8}\right)^2 \leq 1 ,$$

and has a volume of 402.1 cm^3.

The small intestine has not been constructed in detail. Instead the volume occupied by the coils of the small intestine is used. This volume, which lies in the pelvic region, is a section of a circular cylinder given by

$$x^2 + (y + 3.8)^2 \leq (11.3)^2 ,$$

$$-7 \leq y \leq 3 ,$$

$$17 \leq z \leq 27 .$$

Exclude the portion of the large intestine lying in this volume. The volume is 1696 cm^3.

The upper large intestine is simulated by two cylinders, one with its axis vertical representing the ascending colon and the other an elliptical cylinder with its axis horizontal representing the transverse colon. The upper large intestine is the region satisfying (subregion 1)

$$(x + 8.5)^2 + (y + 4.5)^2 \leq (2.5)^2 ,$$

$$15.4 \leq z \leq 24$$

or (subregion 2)

$$\left(\frac{y + 4.5}{2.5}\right)^2 + \left(\frac{z - 25.5}{1.5}\right)^2 \leq 1 ,$$

$$-10.5 \leq x \leq 10.5 .$$

Its volume is 416.3 cm^3.

The lower large intestine is composed of an elliptical cylinder and an S-shaped figure formed from half of a torus. It is the region satisfying (subregion 1)

$$\left(\frac{x - 9.5}{1.6}\right)^2 + \left(\frac{y + 4.3}{2}\right)^2 \leq 1 ,$$

$$13.4 \leq z \leq 24$$

or (subregion 2)

$$0 \leq z \leq 13.4 ,$$

$$\left(\sqrt{E^2 + (z - 6.7 + 6.7m)^2} - 6.7\right)^2 + F^2 \leq (1.6)^2 ,$$

where

$$E = (x - 4.75)\ 0.7090 - (y - 0.4252)\ 0.7053 ,$$

$$F = (x - 4.75)\ 0.7053 + (y - 0.4252)\ 0.7090 ,$$

$$m = 1 \text{ if } E \geq 0 ,$$

$$m = -1 \text{ if } E < 0 .$$

It has a volume of 275.8 cm^3.

Heart. – The heart is half an ellipsoid capped by a hemisphere which is cut by a plane. A rotation and translation are then effected. The heart,

$$x_1 = 0.6943\ (x + 1) - 0.3237\ (y + 3) - 0.6428\ (z - 51) ,$$

$$y_1 = 0.4226\ (x + 1) + 0.9063\ (y + 3) ,$$

$$z_1 = 0.5826\ (x + 1) - 0.2717\ (y + 3) + 0.7660\ (z - 51) ,$$

$$\left(\frac{x_1}{8}\right)^2 + \left(\frac{y_1}{5}\right)^2 + \left(\frac{z_1}{5}\right)^2 \leq 1 ,$$

$$x_1^2 + y_1^2 + z_1^2 \leq (5)^2 \text{ if } x_1 < 0 ,$$

$$\frac{x_1}{3} + \frac{z_1}{5} \geqq -1 \text{ if } x_1 < 0 ,$$

has a volume of 603.1 cm^3.

Kidneys. – Each kidney is an ellipsoid cut by a plane. The left kidney is given by

$$\left(\frac{x-6}{4.5}\right)^2 + \left(\frac{y-6}{1.5}\right)^2 + \left(\frac{z-32.5}{5.5}\right)^2 \leqq 1 ,$$

$$x \geqq 3 .$$

The volume of both kidneys is 288.0 cm^3.

Liver. – The region of the liver is defined by an elliptical cylinder cut by a plane as follows:

$$\left(\frac{x}{16.5}\right)^2 + \left(\frac{y}{8}\right)^2 \leqq 1 ,$$

$$\frac{x}{35} + \frac{y}{45} - \frac{z}{43} \leqq -1 ,$$

$$27 \leqq z \leqq 43 .$$

Its volume is 1614 cm^3.

Lungs. – Each lung is half an ellipsoid with a section in front removed. The defining inequalities for the left lung are

$$\left(\frac{x-8.5}{5}\right)^2 + \left(\frac{y}{7.5}\right)^2 + \left(\frac{z-43.5}{24}\right)^2 \leqq 1 ,$$

$$z \geqq 43.5 ,$$

$$\left(\frac{x-2.5}{5}\right)^2 + \left(\frac{y}{7.5}\right)^2 + \left(\frac{z-43.5}{24}\right)^2 \geqq 1 \text{ if } y < 0 .$$

The volume of both lungs is 3378 cm^3.

Ovary. – Each ovary is an ellipsoid. The left ovary is given by

$$(x-6)^2 + \left(\frac{y}{0.5}\right)^2 + \left(\frac{z-15}{2}\right)^2 \leqq 1 .$$

The volume of both ovaries is 8.378 cm^3.

Pancreas. – The pancreas is half an ellipsoid with a section removed. It is defined by

$$\left(\frac{y}{15}\right)^2 + y^2 - \left(\frac{z-37}{3}\right)^2 \leqq 1 ,$$

$$x \geqq 0 ,$$

$$z \leqq 37 \text{ if } x > 3 .$$

It has a volume of 61.07 cm^3.

Skeleton. – The skeleton consists of six parts – the leg bones, the arm bones, the pelvis, the spine, the skull, and the ribs. Each piece will be described separately. Each arm bone is the frustum of an elliptical cone. The left one is defined by

$$\left[\frac{(1.4/138)(z-69) + (x-18.4)}{1.4}\right]^2 + \left(\frac{y}{2.7}\right)^2 \leqq \left[\frac{138 + (z-69)}{138}\right]^2 ,$$

$$0 \leqq z \leqq 69 .$$

The volume of both arm bones is 956.0 cm^3.

The pelvis is a volume between two nonconcentric circular cylinders described by

$$x^2 + (y+3)^2 \leqq (12)^2 ,$$

$$x^2 + (y+3.8)^2 \geqq (11.3)^2 ,$$

$$y + 3 \geqq 0 ,$$

$$0 \leqq z \leqq 22 ,$$

$$y \leqq 5 \text{ if } z \leqq 14 .$$

Its volume is 606.1 cm^3.

The spine is an elliptical cylinder given by

$$\left(\frac{x}{2}\right)^2 + \left(\frac{y-5.5}{2.5}\right)^2 \leqq 1 ,$$

$$22 \leqq z \leqq 78.5 ,$$

and has a volume of 887.5 cm^3.

The rib volume is that region between two concentric right vertical elliptical cylinders. This

region is sliced by a series of equispaced horizontal planes into slabs, every other slice being a rib. The statements that must be satisfied are

$$\left(\frac{x}{17}\right)^2 + \left(\frac{y}{9.8}\right)^2 \leq 1 ,$$

$$\left(\frac{x}{16.5}\right)^2 + \left(\frac{y}{9.3}\right)^2 \geq 1 ,$$

$$35.1 \leq z \leq 67.3 .$$

$$\text{Integer}\left(\frac{z - 35.1}{1.4}\right) \text{ is even} .$$

The total rib volume is 694.0 cm^3.

Each leg bone is the frustum of a circular cone. The left one is

$$\left(x - 10 - \frac{8}{79.8} z\right)^2 + y^2 < \left(3.5 + \frac{2.5}{79.8} z\right)^2 ,$$

$$-79.8 \leq z \leq 0 .$$

The volume of both is 2799 cm^3.

The skull is the volume between two nonconcentric ellipsoids defined by

$$\left(\frac{x}{6}\right)^2 + \left(\frac{y}{9}\right)^2 + \left(\frac{z - 86.5}{6.5}\right)^2 \geq 1 ,$$

$$\left(\frac{x}{6.8}\right)^2 + \left(\frac{y}{9.8}\right)^2 + \left(\frac{z - 85.5}{8.3}\right)^2 \leq 1 ,$$

and has a volume of 846.6 cm^3.

Dose to the entire skeleton is determined by adding together the energies deposited in each part of the skeleton and dividing by the volume of the skeleton, as follows. Let E_i be the energy (in Mev) deposited in region i having a volume V_i. Then the dose in rads to n such regions is

$$D_n = 1.6 \times 10^{-8} \frac{\sum_{i=1}^{n} E_i}{\sum_{i=1}^{n} V_i} .$$

The proportion of marrow in each bone of the skeleton has been given by Mechanik.[26] Using average values for this proportion, f_i, and assuming that the marrow in each region receives the average dose received by that region, the marrow dose is

$$D_n = 1.6 \times 10^{-8} \frac{\sum_{i=1}^{n} f_i E_i}{\sum_{i=1}^{n} f_i V_i} .$$

The proportions, f_i, are skull 0.2, spine 0.5, leg bones 0.4, arm bones 0.3, rib 0.4, and pelvis 0.45.

Skin. – The so-called skin of the phantom was constructed to give the dose at the surface. This region is a layer about 0.2 cm thick just inside the surface of the phantom. For a point to be located in skin, it must be in one of the following six subregions:

1. $z \geq 93.8$;
2. $70 < z < 93.8$,
$$\left(\frac{x}{6.8}\right)^2 + \left(\frac{y}{9.8}\right)^2 \geq 1 ;$$
3. $z \geq 69.8$,
$$\left(\frac{x}{6.8}\right)^2 + \left(\frac{y}{9.8}\right)^2 \geq 1 ;$$
4. $0 < z < 69.8$,
$$\left(\frac{x}{19.8}\right)^2 + \left(\frac{y}{9.8}\right)^2 \geq 1 ;$$
5. $z \leq -79.8$;
6. $-79.8 < z \leq 0$,
$$\left(\frac{x}{19.796}\right)^2 + \left(\frac{y}{9.799}\right)^2 \geq \left(\frac{98.485 + z}{98.485}\right)^2 .$$

The total volume of skin is 2677 cm^3.

[26] N. Mechanik, "Untersuchungen über des Gewicht des Knochenmarkes des Menschen," *Z. Anat. Entwicklungsgeschichte* 79(1), 58–99 (1926).

Spleen. – The spleen is defined by the ellipsoid

$$\left(\frac{x-11}{3.5}\right)^2+\left(\frac{y-3}{2}\right)^2+\left(\frac{z-37}{6}\right)^2 \leqq 1$$

and has a volume of 175.9 cm^3.

Testes. – The left testis, an ellipsoid, is given by

$$\left(\frac{x-1.3}{1.3}\right)^2+\left(\frac{y+2.2}{1.5}\right)^2+\left(\frac{z+2.3}{2.3}\right)^2 \leqq 1 .$$

The volume of both testes is 37.57 cm^3.

Thymus. – The thymus is formed by the ellipsoid

$$\left(\frac{x+2}{3}\right)^2+\left(\frac{y+6}{0.5}\right)^2+\left(\frac{z-60.5}{4}\right)^2 \leqq 1$$

and has a volume of 25.13 cm^3.

Thyroid. – The lobes of the thyroid lie between two concentric cylinders and are formed by a cutting surface. The inequalities for this organ are

$$x^2+(y+6)^2 \leqq (2.2)^2 ,$$

$$x^2+(y+6)^2 \geqq (1)^2 ,$$

$$y+6 \leqq 0 ,$$

$$70 \leqq z \leqq 75 ,$$

$$[(y+6)-1\times 1]^2 \geqq 2[x^2+(y+6)^2]T^2 ,$$

where

$$T=\frac{2(\sqrt{2}-2)}{5}(z-70)+1 \text{ for } 0 \leqq z-70 \leqq \frac{5}{4},$$

$$=\frac{2(2-\sqrt{2})}{15}(z-70)+\frac{2\sqrt{2}-1}{3} \text{ for } \frac{5}{4}< z-70 \leqq 5 .$$

The volume is 19.89 cm^3.

Uterus. – The uterus is an ellipsoid cut by a plane and is given by

$$\left(\frac{x}{2.5}\right)^2+\left(\frac{y+2}{5}\right)^2+\left(\frac{z-14}{1.5}\right)^2 \leqq 1 ,$$

$$y \leqq -4.5 .$$

It has a volume of 66.27 cm^3.

A computer code has been written which takes a point (x, y, z) and applies the tests for each organ sequentially. For points distributed uniformly in the entire phantom, a CDC 1604 computer using this code can classify the points as to their organ location at an average rate of about 10,000 per minute.

Gamma Dose to Organs

Whole-Body Source. – A source of gamma photons uniformly distributed in the phantom was programmed for the computer. The first objective was to estimate the fraction of the emitted energy that would be absorbed in the phantom. Determination of dose to individual organs will be given later. Photons were given an initial energy E_0, and the energy they imparted in the phantom was recorded. This procedure was followed for seven different initial energies – 0.02, 0.05, 0.2, 0.5, 1.0, 2.0, and 4.0 Mev. There were 1000 photons generated at each energy.

The fractional energy absorption by the total body, which is defined as the ratio of the energy emitted per photon to the average energy absorbed by the total body per photon, was determined from the Monte Carlo data. These results are given in Fig. 25.9. One standard deviation for our data points is less than 1.6% of the mean. An interpolating curve passing through the data points permits the estimation of the fractional energy absorption at other energies. A large number of gamma-emitting radionuclides produce gamma photons with energies in the range 0.1 to 1 Mev, and for such photons the total-body fraction absorption is about 35%. At higher energies the mean free path is larger, permitting a larger percentage of such photons to escape from the phantom and resulting in a lower fractional absorption.

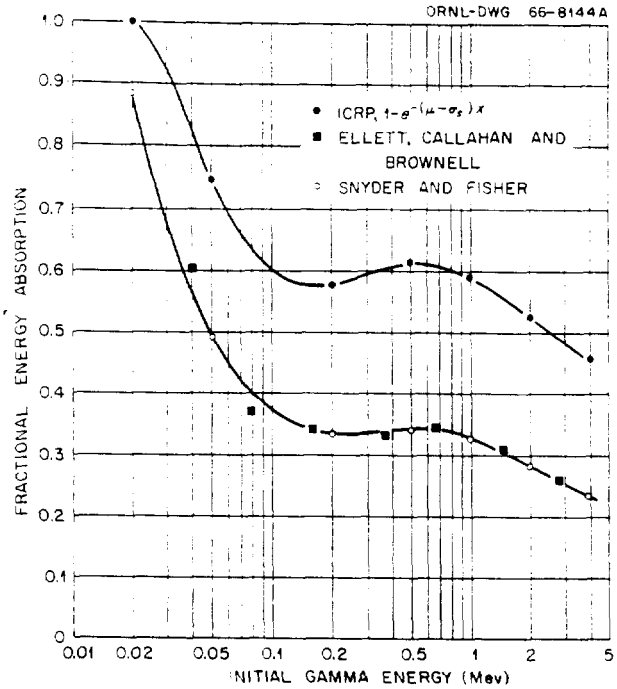

Fig. 25.9. Fractional Gamma Energy Absorption by the Total Body.

Toward lower photon energies, the photoelectric cross section rises steeply, producing an increasing fractional absorption which reaches about 90% at 0.02 Mev.

Also shown in Fig. 25.9 are the Monte Carlo results of Ellett, Callahan, and Brownell[27] for a source uniformly distributed in an ellipsoid. Although their phantom was an ellipsoid, its mass was nearly the same as the mass of the phantom used here, and the fractional absorptions are very similar to those predicted in this paper. The upper curve in Fig. 25.9 gives the fractional energy absorption predicted from the ICRP first-collision formula. In deriving this formula, three major assumptions were made. First, the organ or body is assumed to be spherical. Second, the entire organ or body burden is located at the center of the sphere. Third, a first-collision-dose calculation is then effected to obtain the formula giving the fractional energy absorption:

$$AF = 1 - e^{-(\mu - \sigma_s) r},$$

where r is the radius of the sphere (effective radius), μ is the total gamma cross section at E_0, and σ_s is the Compton scattering cross section at E_0.

It is evident from Fig. 25.9 that the ICRP formula gives a conservative estimate of the fractional absorption, since the Monte Carlo results are seen to be about 55% of those of the ICRP method at intermediate gamma energies.

With the source again uniformly distributed in the phantom, dose to 22 organs was determined. To obtain estimates of dose to individual organs with, at most, 10% statistics required the generation of a larger number of source photons than had been generated in the first case. This was done for initial photon energies of 0.05, 0.2, 0.5, and 1.0 Mev. The number of source photons produced at each energy was 20,000, 30,000, 30,000, and 40,000 respectively.

These results are presented graphically in Figs. 25.10 to 25.13 to permit interpolation. The source is distributed uniformly in the entire phantom, and the dose to various organs in rads per photon emitted by the source is given on the ordinate. The bars on the Monte Carlo data points represent one standard deviation on either side of the mean as estimated from the Monte Carlo calculation. When no bars are given, σ is less than 2%.

Organs located near the center of the phantom, such as the uterus and ovaries, receive a dose of about 1.5 times that of the total body. Most of the organs, however, receive a dose of 1.2 to 1.4 times that of the total body. Of the phantom's organs, the brain receives the lowest dose, 0.45 times that of the total body. This is followed closely by skin, with 0.55 times the body average.

Even with 40,000 initial photons, some organs do not receive a sufficient number of photon collisions to determine the dose received to within 10%. This may be due to the small size of the organ or to its distance from many source photons. An alternative to producing more source photons is to increase the volume in which dose is estimated. This latter procedure was followed. When the standard deviation of dose exceeded 10%, the dose in the arbitrary region(s) (Fig. 25.7) encompassing the organ was taken as the best available estimate of dose received by that organ. When this procedure was necessary, these dose estimates shown in the graphs bear the name of the organ followed by the word "region."

[27] W. H. Ellett, A. B. Callahan, and G. L. Brownell, *Brit. J. Radiol.* 38, 541–44 (1965).

The doses received by the group of organs listed in Fig. 25.13 varied little from each other. Rather than give the doses to each organ individually, the doses received by these organs will lie in the range between the dashed curves in Fig. 25.13.

It is possible to examine the doses received by the organs for very low-energy photons analytically, bypassing the Monte Carlo procedure. At low

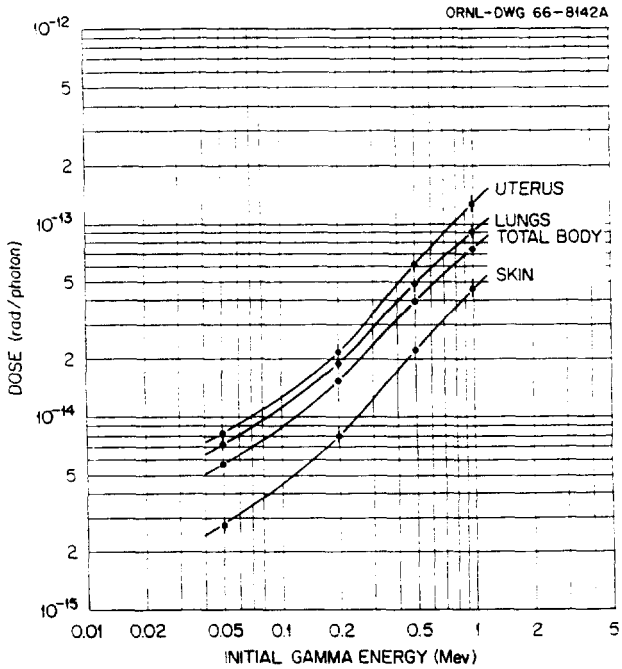

Fig. 25.10. Gamma Dose from a Source Uniformly Distributed in the Body.

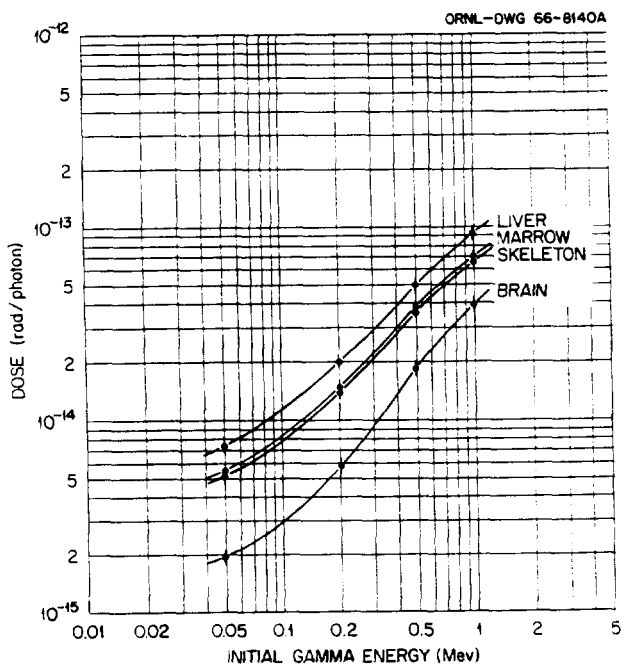

Fig. 25.11. Gamma Dose from a Source Uniformly Distributed in the Body.

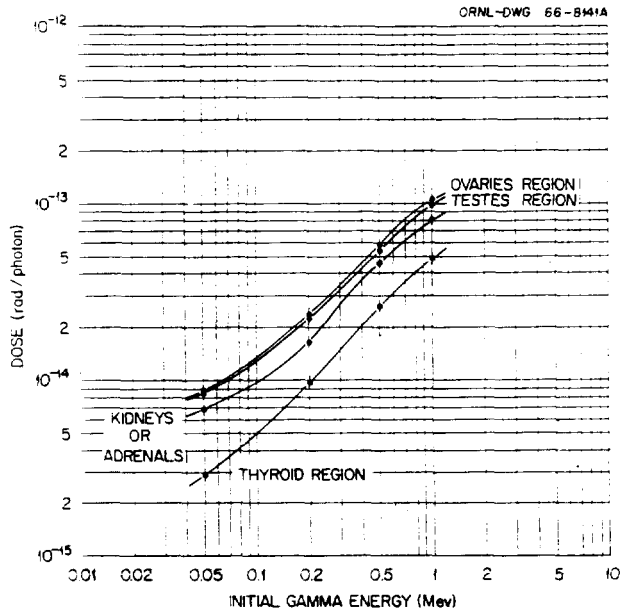

Fig. 25.12. Gamma Dose from a Source Uniformly Distributed in the Body.

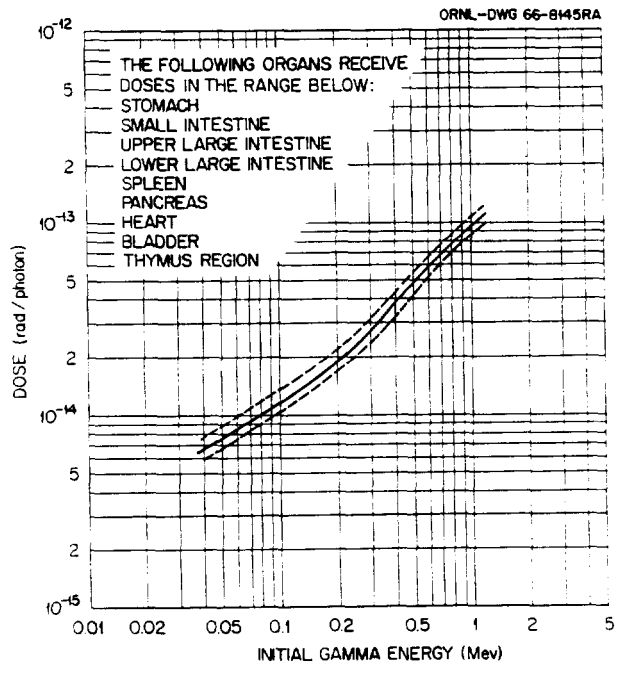

Fig. 25.13. Gamma Dose from a Source Uniformly Distributed in the Body.

photon energies the total cross section is composed almost entirely of that contributed by the photoelectric effect. In addition, the numerical value of this cross section becomes very large, resulting in a small range of the gamma photons before absorption.

If there is a homogeneous medium, infinite in extent, containing a source uniformly distributed throughout which is emitting gamma photons isotropically of energy E_0 Mev at the rate of N_0 per unit time per unit volume, then under steady-state conditions the energy emitted per unit time per unit volume will be equal to the energy absorbed per unit time per unit volume. The dose rate in rads per unit time in any region is then

$$D = \frac{N_0 E_0}{\rho} \; 1.6 \times 10^{-6} \; \frac{\text{erg}}{\text{Mev}} \frac{\text{g rad}}{100 \text{ erg}}$$

$$= 1.6 \times 10^{-8} \; \frac{N_0 E_0}{\rho} \; ,$$

where ρ is the density of the medium (g/cm^3). Suppose now that instead of an infinite medium, there is a finite volume of mass W_T grams. Also, suppose that the mean range of the photon is small compared with the dimensions of the volume, so that the result discussed above applies far from the surfaces in the interior with only a small error. If the source produces photons homogeneously distributed in this medium at the rate of n photons per unit time, then the normalized dose in rads per photon for any interior volume which is far from the boundary of the phantom as compared with the mean free path of the photon is

$$D_p = \frac{D}{n} = 1.6 \times 10^{-8} \; \frac{N_0 E_0}{n\rho} = 1.6 \times 10^{-8} \; \frac{E_0}{W_T} \; .$$

In the case of a gamma source in the total body, the dose to interior organs should asymptotically approach

$$D_p \text{ (rads/photon)} = 2.28 \times 10^{-13} \; E_0 \text{ (Mev)}$$

as the mean free path approaches zero. At 0.01 Mev and below, the mean free path of photons in tissue is less than 0.25 cm, and this formula should yield a more reliable result than could be obtained by Monte Carlo even with large photon sample sizes.

The above does not apply to organs located near the surface. Even in this case, however, one may obtain information as to the surface dose by examining a special case. Suppose that a medium, infinite in extent, is cut by a plane and one half of the medium is removed. The dose rate at the newly formed surface will be one-half of the equilibrium dose rate in the infinite medium, by symmetry. The normalized dose at such a surface of a large finite volume is, therefore,

$$D_{ps} = 0.8 \times 10^{-8} \; \frac{E_0}{W_T} \; .$$

Although the phantom has no such plane surface, the radius of curvature of the elliptical cylinder of the trunk is large compared with the mean free path of low-energy gamma photons. An approximate surface dose for a source distributed uniformly in the total body is, therefore,

$$D_{ps} \text{ (rads/photon)} = 1.14 \times 10^{-13} E_0 \text{ (Mev)} \; ,$$

$$E_0 \leqq 0.01 \text{ Mev} \; .$$

These limiting dose rates appear consistent with the Monte Carlo calculations at 0.02 Mev. The organs inside the rib cage of the trunk received doses within 10% of the predicted equilibrium dose, 4.56×10^{-15} rad/photon, while the skin of the trunk received a dose within 10% of the equilibrium surface dose.

Skeletal Source. – A source of gamma photons uniformly distributed in the skeletal region of the phantom was also simulated on the computer. This program was carried out for five gamma energies – 0.2, 0.5, 1.0, 2.0, and 4.0 Mev.

The fractional energy absorption by the skeleton is given in Fig. 25.14. The standard deviation of the data points is less than 2.5% of the mean. Although there is some variation of the absorbed fraction from 0.2 to 1.0 Mev, as shown in Fig. 25.14, an approximate value of 8% could be used over this energy range with little error. The Monte Carlo estimates given here are about a factor of 2 lower than those given by the first-collision, effective-radius method of the ICRP.

In the energy range under consideration, 0.2 to 4.0 Mev, the gamma cross sections for tissue are very similar to those for bone within several percent. Therefore, there should be little error introduced by the use of a tissue phantom, except for the fact that bone is denser than tissue.

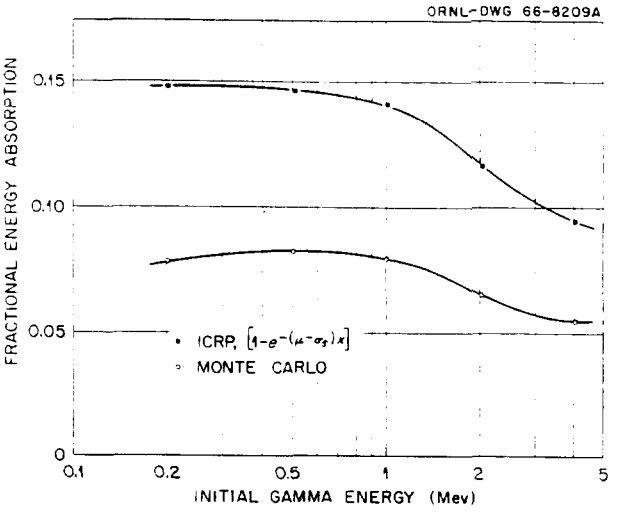

Fig. 25.14. Fractional Gamma Energy Absorption by the Skeleton.

The photoelectric cross section for bone rises steeply with decreasing gamma energy, and although the skeleton is not a compact organ, gamma-ray absorption will be essentially complete at 0.01 Mev and below since the mean free path of these photons will be less than 0.05 cm. In order to obtain a rough estimate for the fractional energy absorption for photons with energies between 0.01 and 0.2 Mev, the entire phantom was considered to be bone. The material in the entire phantom was given the cross section for bone. With the source in bone, the fractional absorption should be more nearly correct for the skeleton than that obtained by using the tissue phantom. However, these results will still be lower than the true values by an undetermined amount for the following reasons. Photons that remain in the skeleton of the phantom will contribute the same amount of energy that a real photon would. However, once a photon escapes from the phantom's skeleton, it will still find itself in a strongly absorbing medium and therefore have a smaller probability of returning to the skeleton than a photon would have if it escaped from skeleton into tissue. A somewhat smaller estimate of the absorbed fraction for the skeleton is obtained, therefore, with the bone phantom at low energies than occurs in the actual situation. With the bone phantom, the fractional energy absorption for the skeleton was 0.81 at 0.02 Mev and 0.41 at 0.05 Mev.

The dose rate to other organs using the skeletal source and the tissue phantom and for energies between 0.2 and 4.0 Mev is given in Figs. 25.15 to 25.18. The notation on these graphs is the same as that described for the total-body source. As expected, the skeleton was the organ with the highest dose. Marrow appears to receive a slightly greater dose than the skeleton but not significantly so. This is because the bones that receive the higher doses happen to contain a greater portion of the marrow. There are compensating factors which would tend to lower the marrow dose, but they are not represented in the model. Marrow is not so uniformly distributed in bone as has been assumed in the model. For a radionuclide that localizes in bone, the marrow should not contain as great a concentration as the bone. This is not the case with the model. Consideration of these factors as well as the Monte Carlo results leads one to believe that the average marrow and average skeletal gamma doses are not very different. The dose estimates to many of the organs or regions were very similar and are not shown separately.

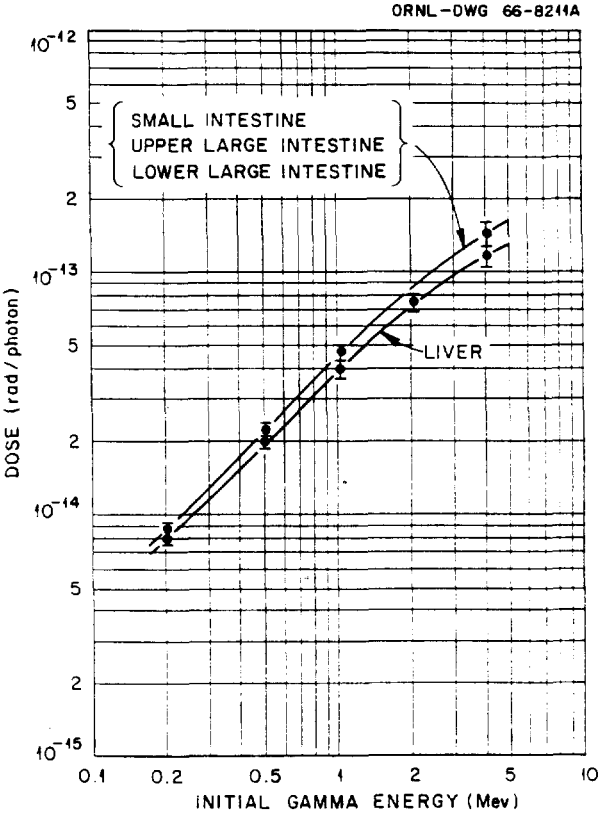

Fig. 25.15. Dose from a Source Uniformly Distributed in the Skeleton.

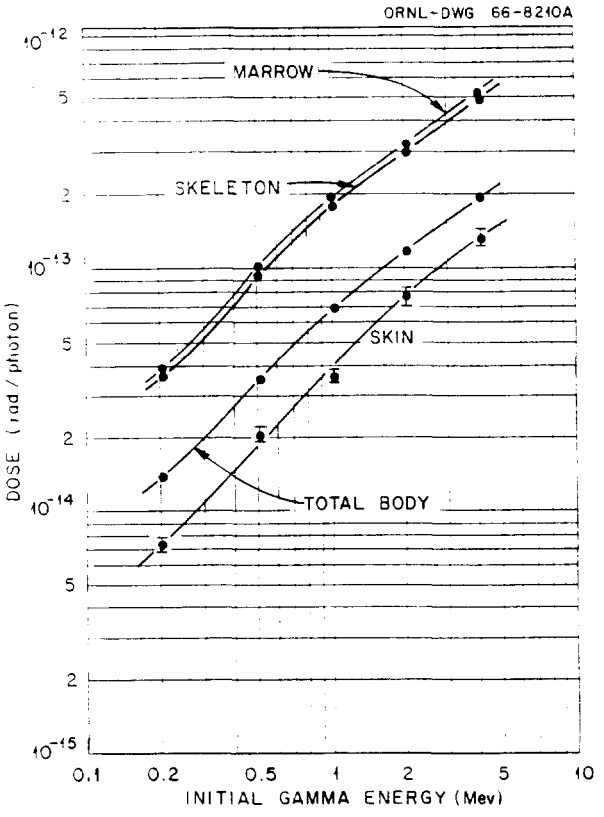

Fig. 25.16. Dose from a Source Uniformly Distributed in the Skeleton.

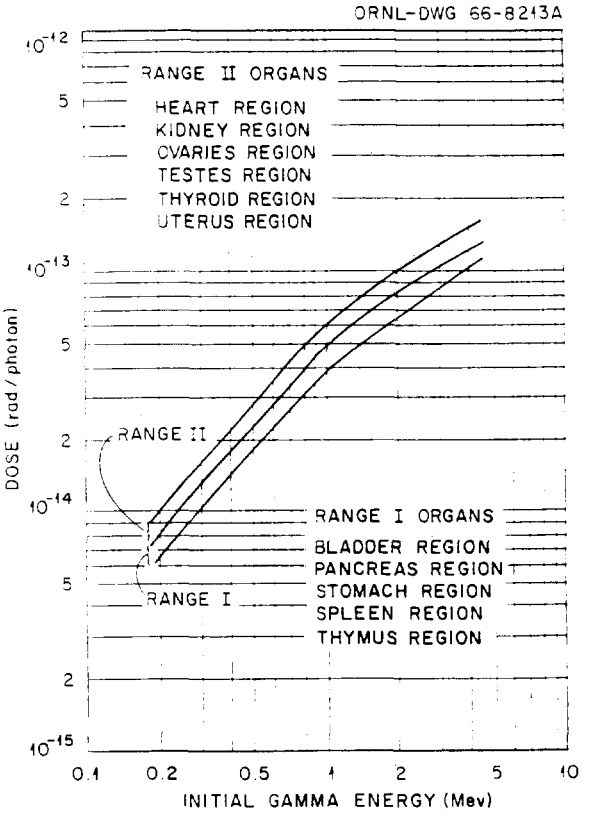

Fig. 25.18. Dose from a Source Uniformly Distributed in the Skeleton.

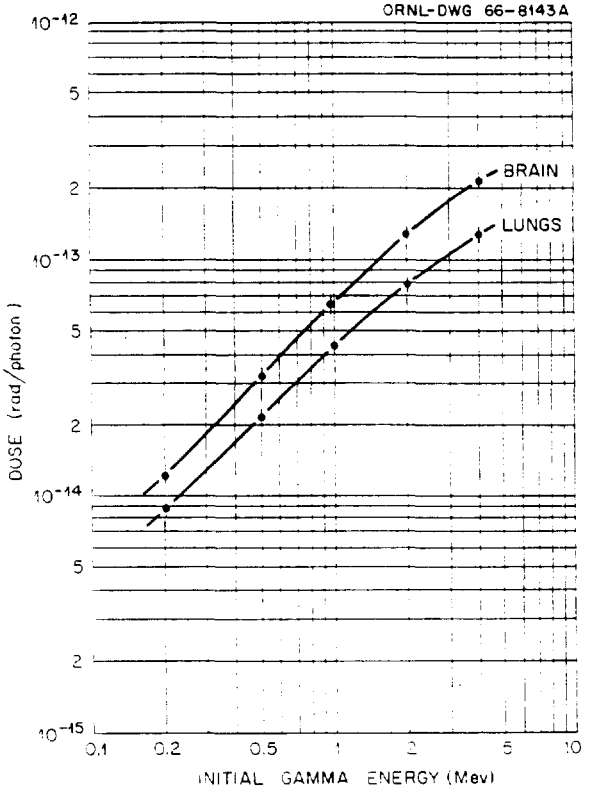

Fig. 25.17. Dose from a Source Uniformly Distributed in the Skeleton.

The doses received by organs listed in the group called range I in Fig. 25.18 received doses between the lower curve and the middle curve in the graph. Similar remarks apply to the organs of range II.

For energies below 0.01 Mev, where absorption is nearly complete, the skeleton would receive a dose in rads per photon of about $1.6 \times 10^{-12} E_0$, where E_0 is the initial gamma energy in Mev. An estimate of dose to the various bones of the skeleton also was obtained from the Monte Carlo code. The part of the skeleton receiving the highest dose was the leg bone, while that receiving the

lowest was rib. For energies between 0.2 and 4.0 Mev, the ratio of the dose in rads per photon of a skeletal part to that of the entire skeleton was formed. These ratios are approximately as follows:

Leg bones/skeleton	$\approx$ 1.4
Spine/skeleton	$\approx$ 1.2
Pelvis/skeleton	$\approx$ 0.8
Arm bones/skeleton	$\approx$ 0.8
Skull/skeleton	$\approx$ 0.6
Ribs/skeleton	$\approx$ 0.5

Conclusion

It appears that a Monte Carlo method of estimating organ doses is feasible under certain conditions. Anatomical differences such as variation of body and organ size have been neglected. Doses have been determined to fixed organ-similar regions of a homogeneous tissue phantom. This gives results that may be extrapolated to many real situations. This paper has examined the dose to organs from gamma sources located in the total body and in the skeleton, although external as well as various other internal sources may be used in conjunction with the Monte Carlo code and phantom.

Acknowledgments

Appreciation is expressed to A. M. Craig, G. G. Warner, and R. T. Boughner of the ORNL Mathematics Division for the programming and computer operations.

THE VARIATION OF DOSE IN MAN FROM EXPOSURE TO A POINT SOURCE OF GAMMA RAYS

W. S. Snyder

A Monte-Carlo-type code has been developed at ORNL which permits one to estimate dose in tissue phantoms for a wide variety of exposure situations. For this paper the code has been used to study the distribution of dose in a homogeneous phantom which has approximately the size and shape of an adult man exposed to a point source of monoenergetic photons.

The trunk of the phantom is taken as a right elliptical cylinder with a height of 70 cm and with semiaxes of the elliptical base as 20 cm and 10 cm (see Fig. 25.19). The arms are considered to be held at the sides and thus are included as part of the above cylinder. The legs are combined to form a truncated elliptical cone, and the head and neck together form a smaller elliptical cylinder. This phantom has about the same masses and dimensions as one designed by Hayes and Brucer[28] and is considered to consist of H, C, N, and O in the proportions given for "Standard Man."[29] Results are presented for the point source positioned directly in front of the phantom at shoulder height or opposite the midpoint of the trunk, and the distance from the midline of the phantom to the source is taken as 1 or 2 m. These four positions, designated *a*, *b*, *c*, and *d*, are shown in Fig. 25.19. The photon energies used are 1.0, 0.5, 0.15, and 0.07 Mev.

A photon is considered to originate at the source position, the direction being chosen from an isotropic distribution, and the coordinates of the point at which the photon strikes the cylinder are computed. This point marks the beginning of what might be termed the "history" of that photon. Successive collision sites are computed, giving the photon the correct probability for the various alternatives that physical theory predicts as being possible. Thus the distances between successive interaction sites, the interaction type (photoelectric effect, Compton scattering, or pair production), and scattering angle are determined in accordance with the values of the cross sections. Each history, then, constitutes a possible path for a photon, and each history is computed in an unbiased manner according to known physical laws. In a large collection of independently calculated histories, the various interactions and distances between interaction sites should be distributed as theory predicts.

The cross sections are taken from *NBS Circular* **583** and its supplement[30] and are programmed on

[28] R. L. Hayes and M. Brucer, *Intern. J. Appl. Radiation Isotopes* **9**, 113–18 (1960).

[29] *Protection Against Neutron Radiation up to 30 Million Electron Volts*, *NBS Handbook* **63**, p. 8, U.S. Dept. of Commerce, NBS, Nov. 22, 1957.

[30] G. W. Grodstein, *X-Ray Attenuation Coefficients for 10 keV to 100 MeV*, *NBS Circular* **583**, 1957; and R. T. McGinnis, *Supplement to NBS Circular 583*, 1959.

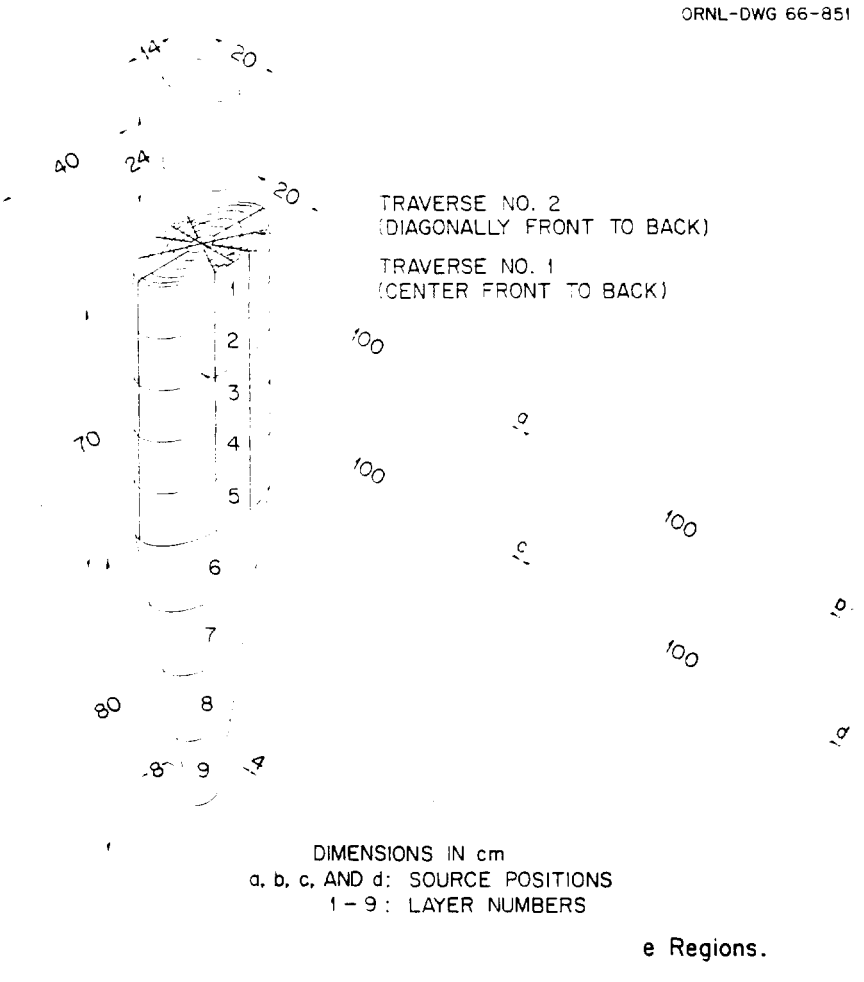

e Regions.

Fig. 25.19. Phantom Dimensions, Source Positions, and Dose Regions.

a separate subroutine. The energy scale is divided into major regions, each corresponding to a decrease of the energy by one-half. Values of the cross sections are listed on magnetic tape at 64 energy values intercalated in each such major region. The machine uses the cross sections corresponding to the nearest listed energy on the magnetic tape. Only the cross sections for the photoelectric effect, pair production, and total cross section are listed, the cross section for Compton scattering being obtained by subtraction.

The trunk region of the phantom is divided into 155 subregions by four equispaced planes perpendicular to the axis of the cylinder, three axial planes making angles of 60° with each other, and five surfaces each of which forms an elliptical cylinder coaxial with the axis of the phantom. The region within the smallest elliptical cylinder was not subdivided by the axial planes in order to improve the statistics on the dose estimates in this region (see Fig. 25.19). The volume elements nearest the surface have a thickness of 1 cm, and the dose in these volume elements may be expected to approximate the reading of a dosimeter exposed on that portion of the surface of the body. These volume elements must be chosen to be large enough so that a significant sample of interactions will occur in the volume to give an acceptably low standard deviation.

The leg region of the phantom is divided into four subregions by three equispaced planes perpendicular to the axis of the cone. The head and neck section, simulated by the smaller elliptical cylinder, is not subdivided.

When an interaction occurs within any one of the volume elements, the energy absorbed in the volume (in Mev) is estimated from the formula

$$E_{\text{absorbed}} = [\sigma_{PE}E_B + \sigma_p(E_B - 1.02) + (\sigma_T - \sigma_{PE} - \sigma_p)E_C]/\sigma_T ,$$

where

τ_T = total cross section,

τ_{PE} = cross section for the photoelectric effect,

τ_p = cross section for pair production,

E_B = energy of the photon before the interaction,

E_C = energy absorbed as a result of a Compton scattering.

The energy absorbed is accumulated for each volume element of the phantom.

When pair production occurs, the positron and an electron are annihilated locally and two photons are released, each having an energy of 0.511 Mev. Photons produced in this way are followed independently, thus producing additional histories. When a photon history has been completed, the total energy contributed to each box by both the parent and the daughter photons, as well as the square of these energies, is accumulated separately. This makes it possible to estimate a variance or standard deviation for the mean energy deposited in each volume element and hence for the average dose in that volume element.

The results obtained are presented in Figs. 25.20 to 25.25. For the trunk section, results are shown graphically for volume elements along two traverses in each layer, one along the minor axis of the elliptical trunk, front to back (traverse 1), and the other running diagonally from front to back (traverse 2) (see Fig. 25.19). Because of the symmetry of the situation, the average dose in any volume element of the trunk can be found from the values given for these traverses. The average dose in the cylinder simulating the head and neck region is shown on the graphs for traverse 1 at the 10-cm position. Results for the leg regions are not presented graphically but are given in a table at the top of the figures. In six cases (E = 0.15

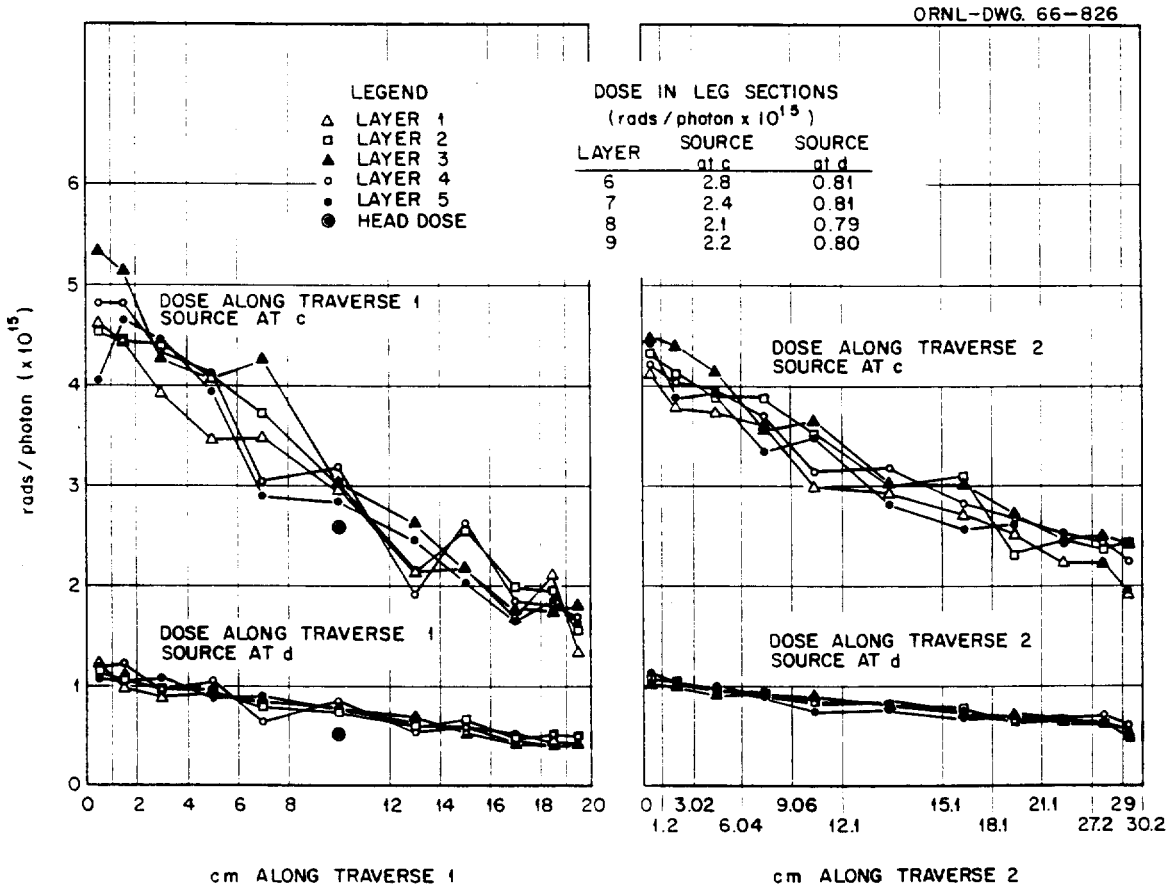

Fig. 25.20. Distribution of Dose in a Tissue Phantom from a Point Source of Photons at Positions c and d, Energy 1 Mev.

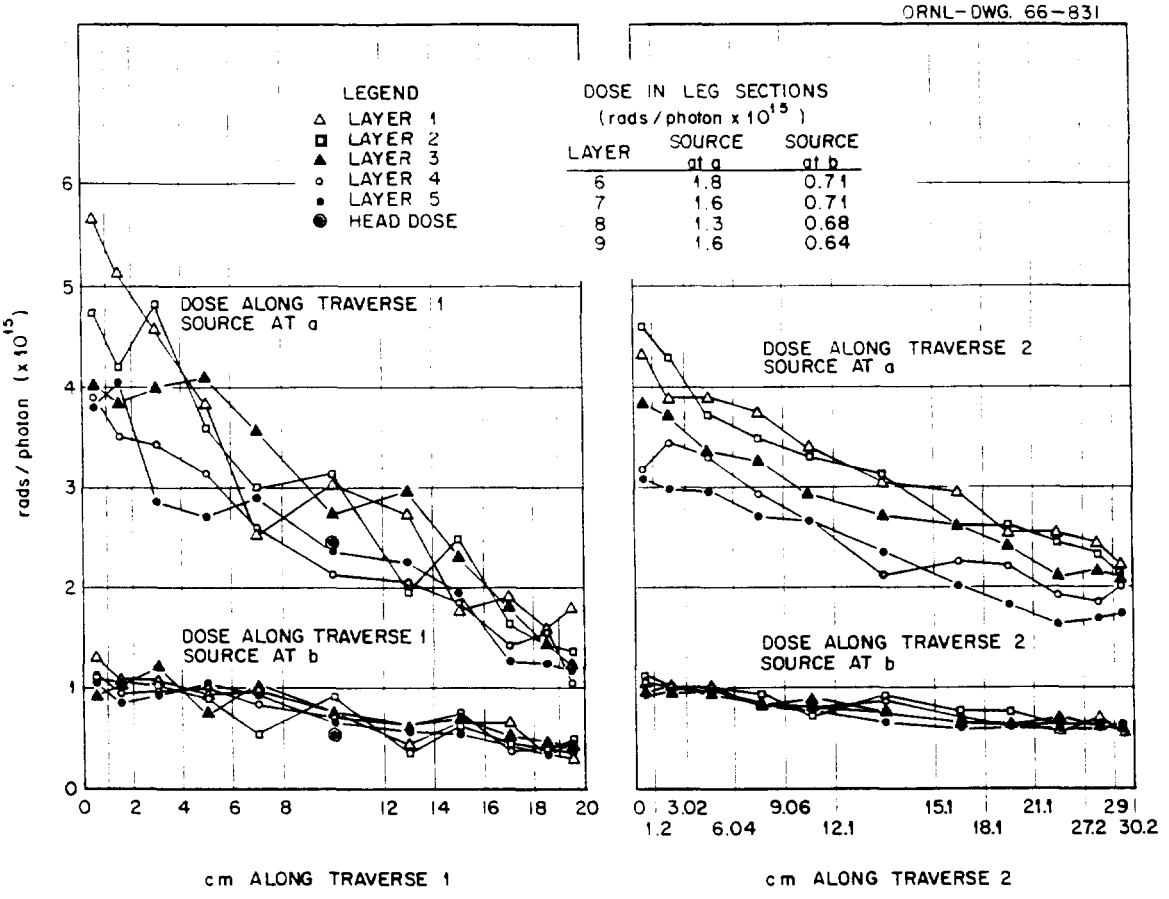

Fig. 25.21. Distribution of Dose in a Tissue Phantom from a Point Source of Photons at Positions *a* and *b*, Energy 1 Mev.

and 1 Mev, source at positions c and *d*; and $E = 0.5$ Mev, source at positions *b* and *d*), 100,000 photons were taken as source; in all other cases 40,000 photons were used. The coefficient of variation (standard deviation expressed as a percentage of the mean) never exceeds 20% for the 40,000 sources nor 11% for the 100,000 sources, and it is much less in the great majority of the volume elements.

The results with the source in positions *b* and *d*, that is, at 2 m from the central axis of the trunk, show less variation from one layer to another than do the results with the source in positions *a* and c. Plausibly, this is due to the fact that the solid angle subtended by similarly placed volume elements in the different layers varies less from one layer to another when the source is 2 m distant than when it is only 1 m distant. Generally, doses to volume elements in the layer at the same height as the source will be higher than at corresponding positions in other layers. However, the statistical fluctuations of the data are so large that one cannot make any very precise interpretation. It is evident that in all cases there is a considerable decrease in dose with distance away from the irradiated surface. In very approximate numbers, the dose to the volume elements near the front exceeds the dose to the volume elements near the back by a factor of about 3 when the source energy is 1 Mev, and the factor increases as the source energy decreases, becoming about a factor of 10 when the source energy is 0.07 Mev. The dose recorded by a film badge might be incorrect by factors of these magnitudes. The dose at corresponding positions varies much less from layer to layer of the trunk section than with depth below the irradiated surface. The variation of dose along traverse 2 is always less than the variation along traverse 1, as would be expected.

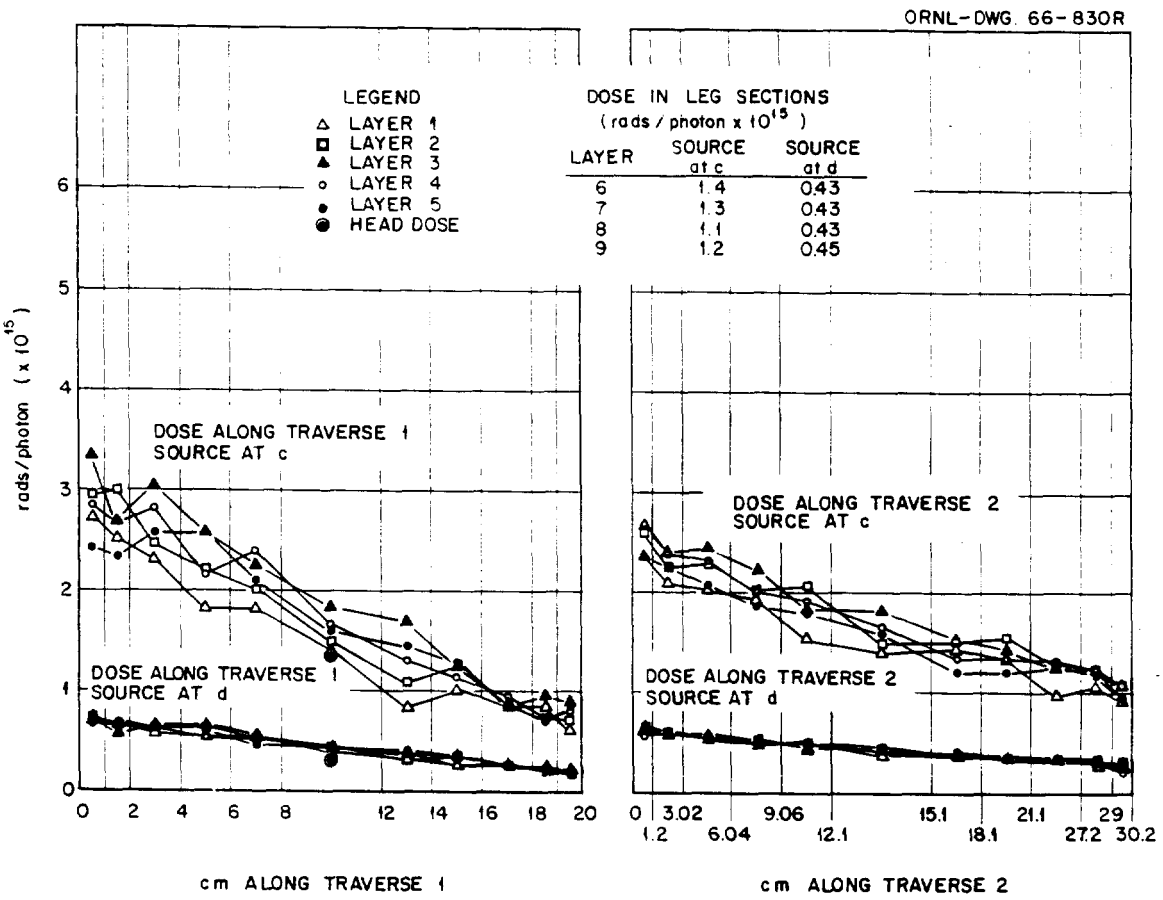

Fig. 25.22. Distribution of Dose in a Tissue Phantom from a Point Source of Photons at Positions c and d, Energy 0.5 Mev.

The average dose in the head region, as well as the average dose in the leg regions, is generally slightly lower than the dose to the central region of the trunk. The dose in the leg region tends to decrease, as would be expected, when the layers are farther from the source.

The results obtained in this study have been compared, insofar as possible, with the results of some other studies. Perhaps the closest check is with a study by Jones,[31] who made measurements of dose on and within a phantom of body size from point sources of photons. He reported the dose only as normalized to a "film badge dose" or to an "air dose," and thus only ratios of doses can be compared. As shown in Fig. 25.26, the data obtained in the present study do not agree very closely with those of Jones; however, there is qualitative agreement. The difference may be plausibly accounted for by the experimental and statistical errors and by the fact that his phantom included a complete set of bones. It appears that the presence of the skeleton significantly alters the dose pattern within the body.

It is planned to extend this study to include more energies and other source positions, such as at the side, on the floor, and above the phantom.

[31] A. R. Jones, *Measurement of the Dose Absorbed in Various Organs as a Function of the External Gamma Ray Exposure*, AECL-2240 (October 1964).

AN AGE-DEPENDENT MODEL FOR THE BODILY RETENTION OF CESIUM

H. L. Fisher, Jr. W. S. Snyder

The retention of radioelements by humans was initially determined for the adult since the pro-

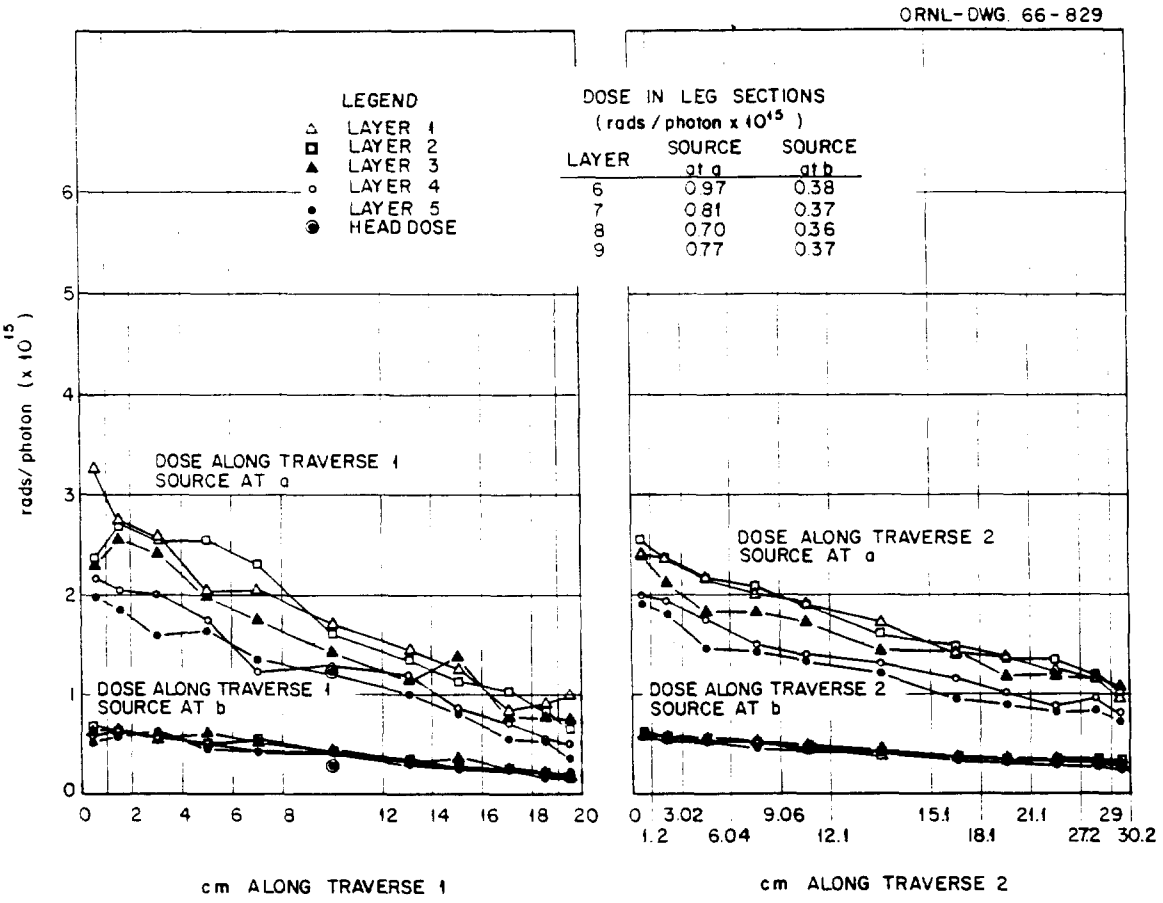

Fig. 25.23. Distribution of Dose in a Tissue Phantom from a Point Source of Photons at Positions *a* and *b*, Energy 0.5 Mev.

tection of radiation workers was a problem of paramount importance and also because more data from accident cases as well as from planned experiments had accumulated for the adult than for individuals of other ages. However, as data accumulated, it was apparent that the retention pattern of a radioelement might vary greatly with age. This appears to be the case for cesium. It is the purpose of this paper to present one theoretical age-dependent compartmental model and apply it to the retention of cesium.

Richmond *et al.*[32] used a two-exponential retention function to fit the observed retention of ^{137}Cs by normal adult males for a period of 550 days after a single oral intake. Except for the

is dominant, contributing more than 99% to the total area under the retention function. Therefore, for purposes of dose estimation or equilibrium level estimation in the adult, the retention of cesium may be considered to be given by a single exponential.

It is well known that a single compartment with an elimination rate proportional to its contents is described by

$$\frac{d}{dt}A(t) = -\lambda\, A(t)\,, \qquad (1)$$

where $A(t)$ is the amount of material in the compartment and λ is the decay constant. This equation has a single exponential as its solution. The

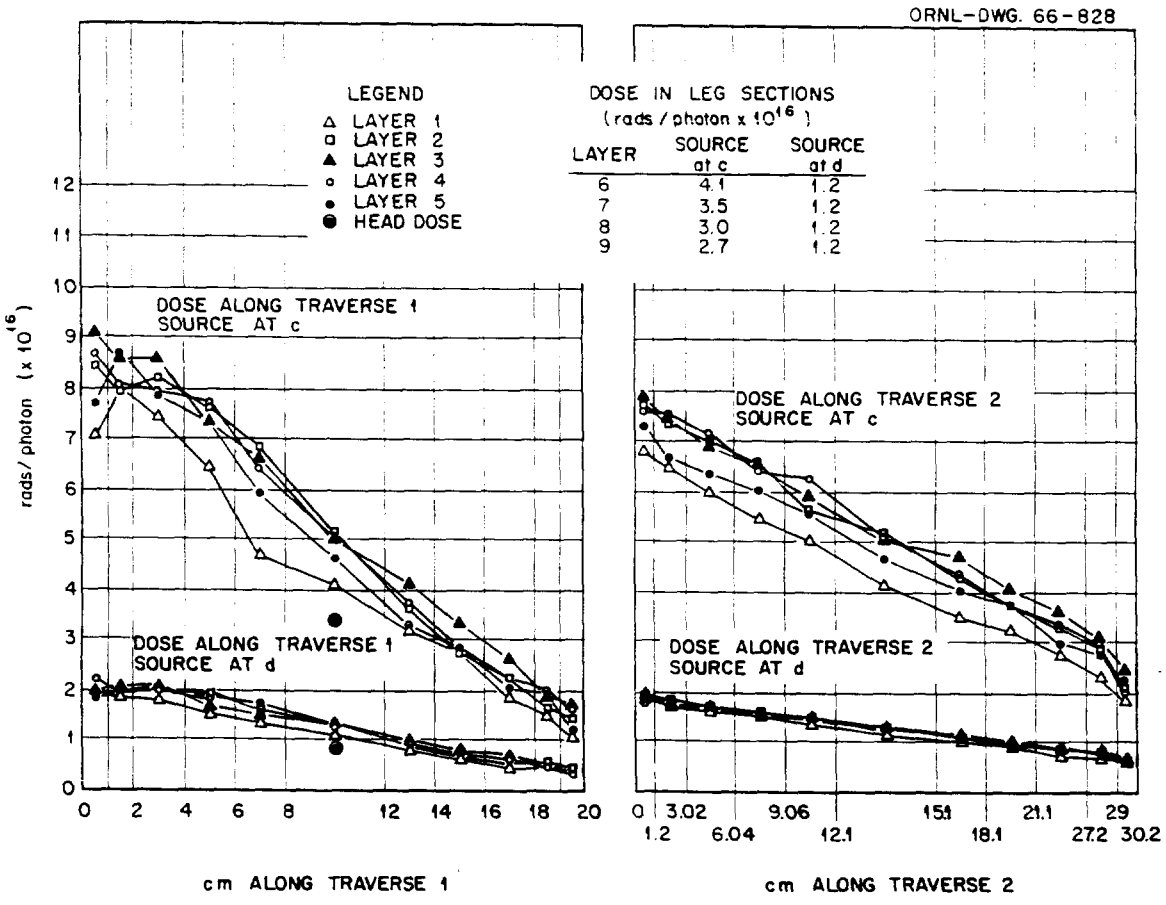

Fig. 25.24. Distribution of Dose in a Tissue Phantom from a Point Source of Photons at Positions c and d, Energy 0.15 Mev.

To introduce the age dependence into the retention function, consider a single compartment with a definite size or volume, but let the size of this compartment vary with time. In order to write a differential equation governing the kinetics of this compartment, it is necessary to make one assumption. Let us assume that the rate of change of a quantity of material introduced into the compartment is proportional to the concentration of the material in the compartment. The kinetic equation is then

$$\frac{d}{dt}A(t) = -\,m\,\frac{A(t)}{W(t)}, \qquad (2)$$

where $W(t)$ is the volume of the compartment and m is the constant of proportionality.

There is now the practical problem of determining what should be used as a measure of compartment size. Many different measures might be proposed, for example, weight, muscle mass, body water, or potassium content. Since cesium is rather uniformly distributed throughout the body, let us take body mass to be a measure of compartment size for cesium. This is not to say that mass has physiological significance in cesium retention. What should be inferred is that the true compartmental volume for cesium is assumed to be proportional to body mass.

Although Eq. (2) may be applied directly, there is a simplification that can be made for ^{137}Cs retention. If at time t the change in the compartmental half-life with time is small compared with this half-life, the compartment may be considered to have a constant half-life for material introduced into the compartment at time t. Therefore,

$$T_{1/2} = \frac{W(t)\ln 2}{m}. \qquad (3)$$

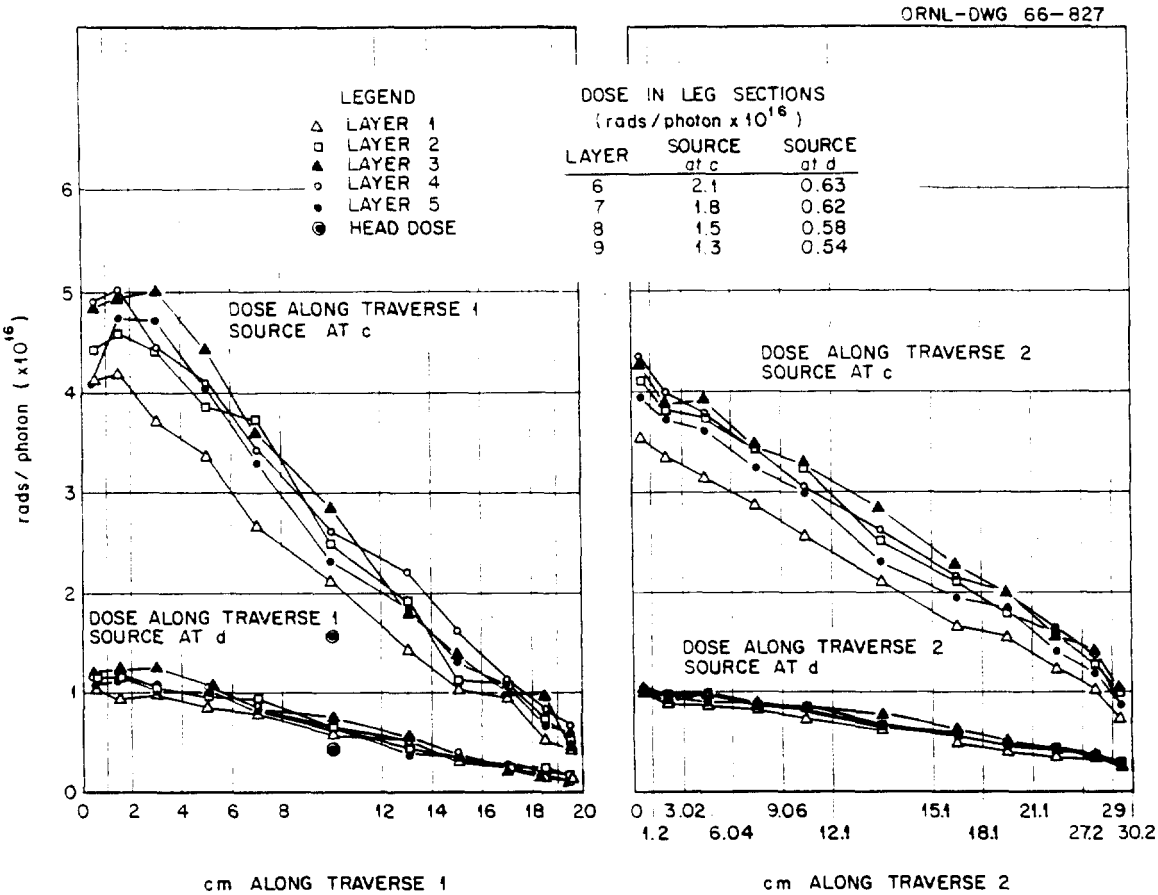

Fig. 25.25. Distribution of Dose in a Tissue Phantom from a Point Source of Photons at Positions c and d, Energy 0.07 Mev.

After this simplification, it follows that for a single intake at any time, the elimination is exponential, with a half-life determinable from the volume of the compartment at that time.

If $W(t)$ is a known function, then after determining the proportionality constant m, the time dependence of the compartmental half-life will be determined. The constant m is determined by using the experimentally determined biological half-life for cesium in the adult male and his body mass.

The adult values for body weight and half-life of cesium are used since they have been the topic of many more experiments and are known more precisely. The mass of the adult male is taken to be 70 kg. Although there is a wide range of biological half-times reported in the literature for cesium in adult males, a representative value of 100 days has been chosen. Having determined m from Eq. (2), the relationship between biological half-life for cesium and body mass is given by

$$T_{1/2}(t) = 1.43W(t) . \qquad (4)$$

This equation was not derived by considering individuals but was determined for the average of populations of various body masses. The equation should only be used to determine the average biological half-life of a group of grossly normal individuals. Such parameters as percent body fat, environmental temperature, or work activity may greatly influence the biological half-life. However, a group of people of the same age chosen randomly should have an average biological half-life for cesium given by Eq. (4).

The growth curve for body mass from infancy to adulthood is given in Fig. 25.27. The curve for

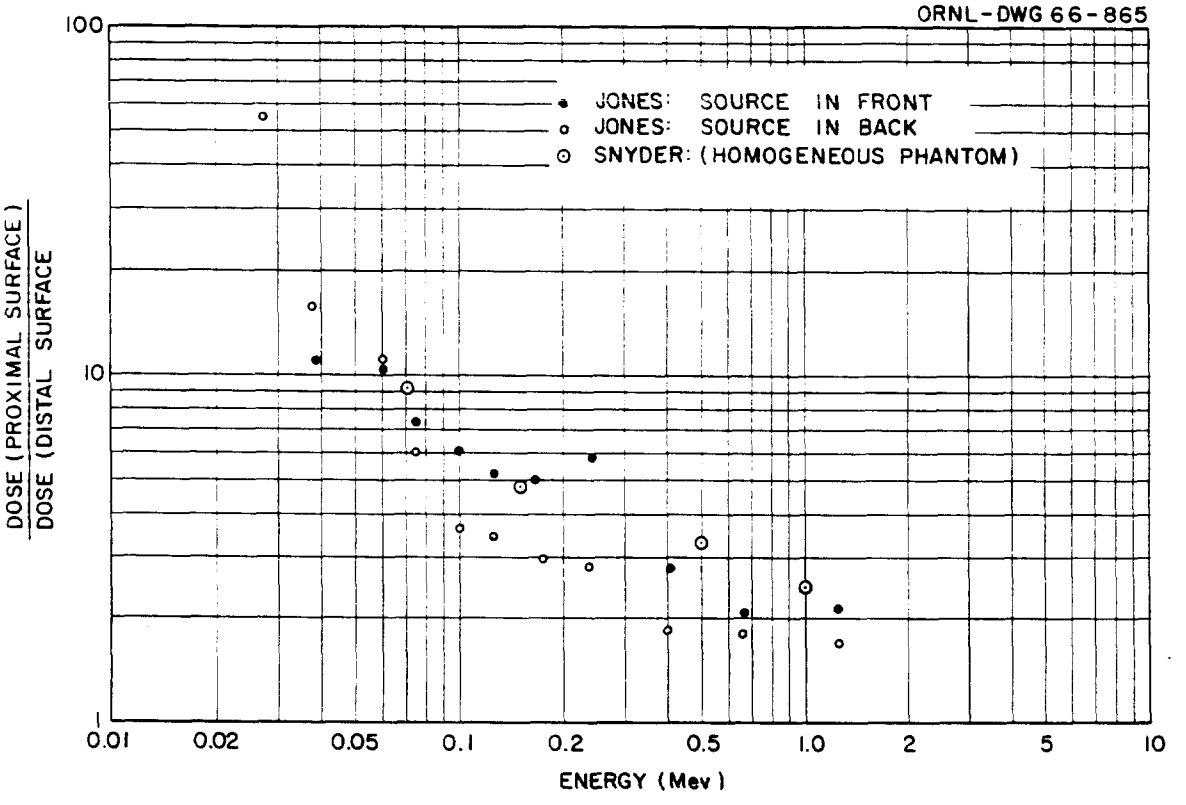

Fig. 25.26. Ratio of Doses on Proximal and Distal Surfaces of a Homogeneous Phantom (Calculated) and of a Phantom with a Skeleton (Experimental).

males is that given by Mitchell;[33] the one for females is taken from ref. 34. Using these curves, the biological half-life for cesium was determined.

In Fig. 25.28 is a comparison of the biological half-life of cesium predicted by the model with some experimental results. The model predicts a cesium biological half-life for the newborn of about 5 days. From this value it increases to the assumed value of 100 days for the adult. Boni[35] has determined the cesium biological half-life of humans from five years of age through adulthood. His method is one in which the body burden of fallout ^{137}Cs, as well as the urinary excretion, is determined. From the single-exponential model and assuming equilibrium conditions, the biological half-life may be determined. For the adult values determined in this way, the range of values about the mean is ±50%. The model given here predicts a half-life about twice as large as Boni's results in the five-to-ten-year age group. However, McGraw[36] has surveyed the literature and given a representative curve for the average half-life. His curve is quite close to the model in the five-to-ten-year age group. It should be pointed out that the variation of the experimental values about McGraw's curve is quite large.

By applying Eq. (4) and using the body weight for females, the half-life of cesium in females was determined and is given in Fig. 25.29. Boni also has measured the biological half-life of cesium in females. As shown, the model predicts a half-life for females of about twice that observed by Boni.

Using measurements of stable cesium in tissue, the daily intake of cesium, and the single-exponential model under equilibrium conditions, Snyder

[33] H. H. Mitchell *et al.*, *J. Biol. Chem.* 158, 625 (1945).

[34] W. S. Spector, *Handbook of Biological Data*, p. 180, W. B. Saunders, Philadelphia, 1956.

[35] A. L. Boni, "Variations in the Retention and Excretion of ^{137}Cs with Age and Sex," presented at Health Physics Society Meeting, 1966.

[36] T. F. McGraw, *Radiol. Health Data* 6(12), 711 (December 1965).

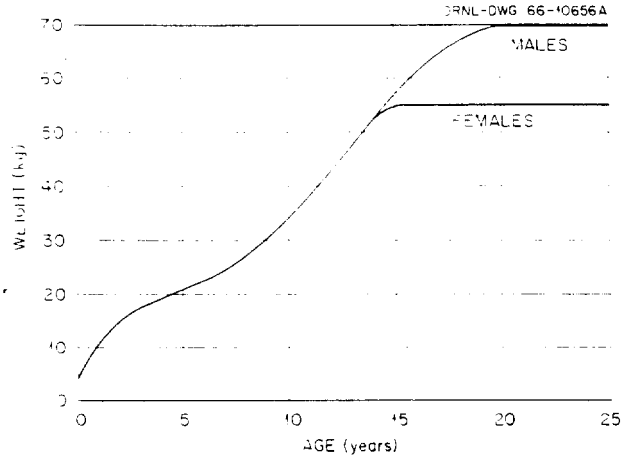

Fig. 25.27. Average Body Weight of Males and Females.

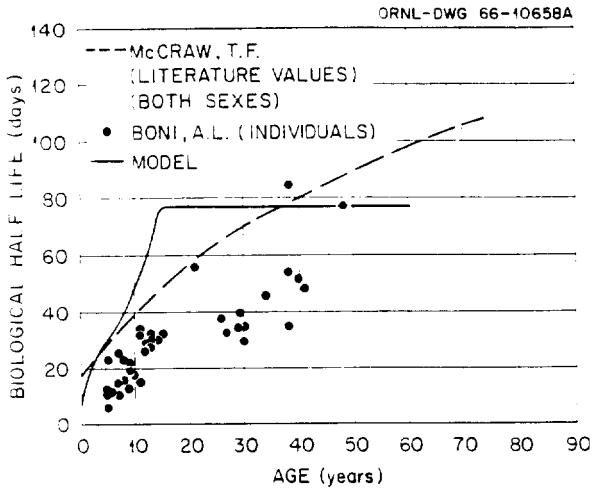

Fig. 25.29. Biological Half-Life of ^{137}Cs in Females.

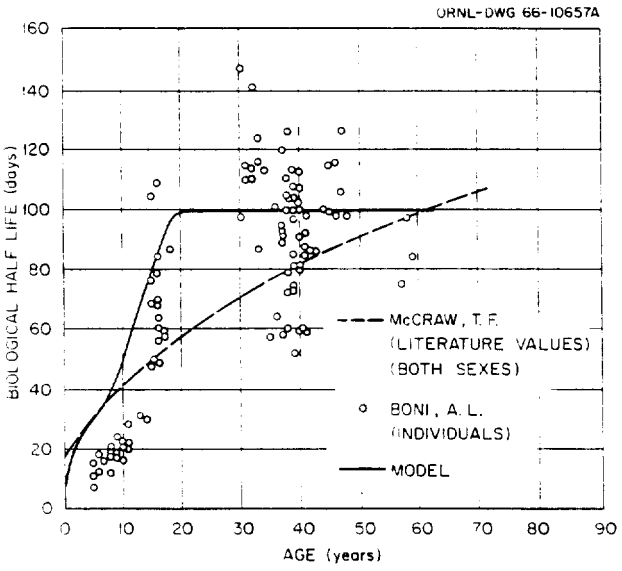

Fig. 25.28. Biological Half-Life of ^{137}Cs in Males.

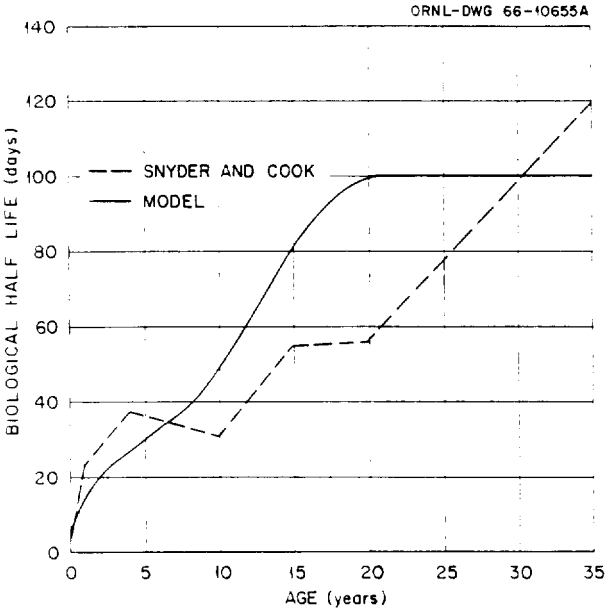

Fig. 25.30. Variation of the Biological Half-Life of Cesium with Age.

and Cook have produced estimates of the biological half-life with age, which are given in Fig. 25.30. During the first five years, the agreement of the model with their values is good. There is agreement for the adult values also; however, the model gives somewhat higher values during the adolescent period.

In this paper we have examined a conceptually very simple age-dependent compartmental model. Application of the model to cesium retention has not been any more successful nor less successful than prior models. It has not explained variation of the biological half-life within an age group. Other parameters besides age are evidently important. However, the model has been derived theoretically with few assumptions, and there is only one arbitrary constant to be determined. The model is capable of accounting for a large part of the variation in half-lives between the various age groups.

Table 25.2. Total Dose Delivered to the Body from a Single Intake of ^{137}Cs

Age (years)	Dose (microrads/μc)		
	Beta	Gamma	Beta Plus Gamma
0	2680	1040	3720
1	2680	1450	4130
5	2680	1650	4330
10	2680	1900	4580
15	2680	2140	4820
20	2680	2390	5070

The total dose delivered to the body of individuals of various ages who have ingested 1 μc of ^{137}Cs has been calculated and is given in Table 25.2. The total dose is directly proportional to half-life and is inversely proportional to body mass. By the model, half-life and mass are proportional. Therefore, total dose is independent of half-life or body mass. This is true when 100% of the emitted energy is absorbed. Beta dose is an example. The fraction of the gamma energy absorbed by the infant is slightly less than half that of the adult, as will be shown later. Therefore, we see the model predicts that for identical single intakes of ^{137}Cs, the infant will receive a beta-plus-gamma total dose of about 75% that of the adult.

Fisher and Snyder[37] have described previously a human phantom and a Monte-Carlo-type calculation which was programmed for a high-speed digital computer. The age-dependent metabolic model described here may be used to estimate the microcurie-days of residence of ^{137}Cs in the body, and the data given in the above report may be used then to obtain an estimate of total dose as well as its distribution in time and in various portions of the body.

Acknowledgment

Appreciation for the coding and computer operations is expressed to Gordon G. Warner of the ORNL Mathematics Division.

[37]H. L. Fisher, Jr., and W. S. Snyder, *Health Phys. Div. Ann. Progr. Rept. July 31, 1966*, ORNL-4007, p. 221.

A DOSIMETRIC STUDY FOR THE ADMINISTRATION OF NEOHYDRIN LABELED WITH ^{203}Hg AND ^{197}Hg

W. S. Snyder Mary R. Ford

Introduction

Brain scanning with the mercurial diuretic chlormerodrin (Neohydrin[38]) labeled with radioactive mercury is now widely used in the localization of intracranial tumors. The isotope of mercury used initially was ^{203}Hg. This isotope was introduced as an agent in brain scanning in 1959 by Blau and Bender,[39] who demonstrated that ^{203}Hg gives a much lower whole-body radiation dose than the conventional agent, ^{131}I-labeled human serum albumin, and it produces scans that compare well with those obtained with ^{131}I. A disadvantage of the mercury, however, is that it accumulates in the kidneys, where it produces a relatively high local dose. More recently, ^{197}Hg has been used. This isotope, because of its shorter half-life and less penetrating radiation, gives a much lower dose to the kidneys than ^{203}Hg. It is considered by some, but not all, clinicians, however, to give less satisfactory scans.[40–42] Because the kidneys lie anatomically not far from the gonads, the magnitude of the genetic dose is a matter of further concern.

Thus an evaluation, with all reasonable precision, of the radiation dose received, especially by the kidneys and gonads, from both ^{197}Hg and ^{203}Hg is needed. We have performed this computation for photons with a Monte-Carlo-type computer code, described previously,[43] which is quite accurate in taking account of the scattering of photons and of the energy deposited in tissue. The dose from beta components is found by conventional techniques, but the estimate is improved

[38]Lakeside Laboratories.

[39]M. Blau and M. A. Bender, *J. Nucl. Med.* 3, 83 (1962).

[40]D. B. Sodee, *J. Nucl. Med.* 5, 74 (1964).

[41]M. Blau and M. A. Bender, *J. Nucl. Med.* 5, 318 (1964).

[42]A. L. Rhoton, Jr., J. Eichling, and M. M. Ter-Pogossian, *J. Nucl. Med.* 7, 50 (1966).

[43]W. S. Snyder, "The Variation of Dose in Man from Unilateral Exposure to Gamma Rays," presented at Tennessee Valley Industrial Health Conference, Gatlinburg, September 30 and October 1, 1965 (submitted to *Health Physics*).

somewhat by use of computer codes to determine the average beta energy and the number and intensity of beta-like radiations. The metabolic model is derived from data on hospital patients, and the dose estimates based on this model can be adjusted easily to take account of elimination rates appropriate for other patients.

Energy Emitted in the Decay of ^{197}Hg and ^{203}Hg

The decay schemes of ^{197}Hg and ^{203}Hg are given below:

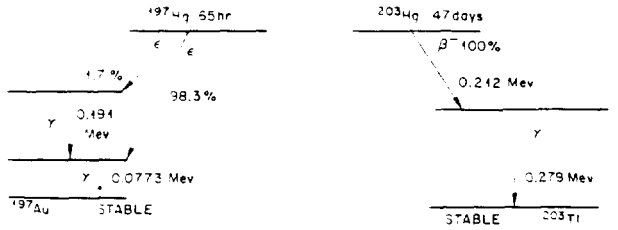

In addition to the energy emitted as shown on the decay schemes, many x rays and Auger electrons of varying energies and intensities arise as a result of gamma-ray internal conversion. This conversion is associated with the gamma decay of both isotopes, and, in the case of ^{197}Hg, the electron capture process accounts for the emission of other x rays and Auger electrons. The calculation of the energy emitted by these processes is tedious and time consuming, and so a computer code developed by Dillman[44] has been used which tabulates the number and energy of these emissions.

The computer output of the gamma and "beta-type" energy emitted per decay of ^{197}Hg and ^{203}Hg is given in Table 25.3. The radiations described as "beta type" include all x rays and/or gamma rays of energy less than 0.0113 Mev, all

[44] L. T. Dillman, "Calculating the Effective Energy per Radioactive Decay for Use in Internal Dose Calculations," this chapter.

Table 25.3. Gammas, X Rays, and "Beta-Type" Energy Emitted by ^{197}Hg and ^{203}Hg

Type of Decay	Radionuclide			
	^{197}Hg		^{203}Hg	
	Energy (Mev)	(%/disintegration)	Energy (Mev)	(%/disintegration)
Gamma	0.191	0.78	0.279	81.6
	0.0773	19.2		
X rays				
$K_{\alpha 1}$	0.0688	37.3	0.0729	6.34
$K_{\alpha 2}$	0.0669	20.5	0.0708	3.50
$K_{\beta 1}$	0.0779	12.9	0.0826	2.23
$K_{\beta 2}$	0.0807	3.47	0.0855	0.63
L			0.01131	5.76
"Beta-type"				
X and/or gamma rays below 0.0113 Mev; Auger and internal conversion electrons above 0.03 Mev	0.0549[a] 0.0158[b]	109[a] 33.5[b]	0.210	19.2
Auger and internal conversion electrons less than 0.03 Mev	0.00398[a] 0.00403[b]	166[a] 203[b]	0.00428	36.6

[a] From gamma decay.

[b] From electron capture.

Table 25.4. Beta Decay of ^{203}Hg

End-Point Energy (Mev)	Fraction per Decay	Betas with Energy Below 0.03 Mev		Betas with Energy Above 0.03 Mev	
		Fraction	Average Energy	Fraction	Average Energy
0.212	1	0.328	0.0249	0.672	0.0490

internal conversion electrons, and all Auger electrons. The output for electrons of energy less than 0.03 Mev is listed separately since these electrons are assigned a quality factor of 1.7 rather than 1 in internal dose calculations.[45] The average energy of the 0.212-Mev beta of ^{203}Hg, also computed by the code of Dillman,[44] is given in Table 25.4. As in the previous case the fraction of the decays in which the initial energy is less than 0.03 is tabulated separately for convenience in applying the quality factor.

Metabolic Characteristics of Neohydrin

The biological data and metabolic characteristics of Neohydrin used in the dose computations are based principally on the clinical experience of Blau and Bender.[39] They found that an injected dose of Neohydrin suitable for scanning purposes (usually 10 μc per kilogram of body weight) is cleared rapidly from the body via the urine and feces. Their data on 20 patients indicate that 50% of the dose is eliminated by the urine during the first 8 hr, and an additional 15% appears in the urine during the next 24 hr. The blood clearance is rapid, with less than 10% remaining after 5 hr. Most of the retained dose accumulates in the kidneys, where about equal amounts are found in the medulla and cortex during the first day. After the first day the concentration in the cortex to that in the medulla is roughly in the ratio of 5/1, and the biological half-life of the long-term component is about 28 days. The remaining few percent of the injected amount is scattered throughout the body, with perhaps some concentrating in the liver.

Based on these data, we have assumed in the computations that 75% of the administered radionuclide is excreted rapidly. Since less than 10% of this 75% is present in blood after 5 hr, according to the curve given in Fig. 2 of Blau and Bender,[39] we have given this deposit an elimination half-time of 1.3 hr. Of the 25% retained, 12% resides in the kidneys with a biological half-life of 28 days – 10% in the cortex and 2% in the medulla. Another 8% is retained in the medulla with a biological half-time of 12 hr. The remaining 5% is assumed to be uniformly distributed in the total body, and this is assigned an elimination half-time of 15 hr, again based on Fig. 2 of Blau and Bender's data.[39]

In addition to these sources of exposure, the urine which flows from the kidneys to the bladder and the amount retained in the bladder will contribute to the dose. This is true especially in the case of the gonads, because they lie in close proximity to the ureter and the bladder. Since the time for urine to pass from the kidneys to the bladder is very short, we have considered the dose from this source to be insignificant, but we have computed the dose from the amount in the bladder. For this computation five voids per day are assumed; that is, 4.8 hr is assumed as a typical period of retention; and because the bladder is near empty during part of each period, 2.4 hr is taken as an average residence time.

Description of the Phantom

The total-body tissue phantom used in the computations is shown in Fig. 25.7. This phantom was designed by the authors for an earlier Monte Carlo computation[46] and is similar to a phantom of Hayes and Brucer.[47] It is considered to consist of H, C, N, and O in the proportions given by standard man and to have a density equal to 1 g/cm^3. The subregions were made originally to show the variation of depth dose from an external source. They are left in these computations to permit the estimation of dose to the ovaries and bladder from the source located in the kidneys.

[45] *Recommendations of the International Commission on Radiological Protection*, ICRP Publication 2, p. 29, Pergamon, London, 1959.

[46] W. S. Snyder, "The Variation of Dose in Man from Exposure to a Point Source of Gamma Rays," presented at Intern. Conf. Radiological Protection in Industrial Uses of Radioisotopes, Dec. 13–15, 1965, Paris (to be published in proceedings).

[47] R. L. Hayes and M. Brucer, *Intern. J. Appl. Radiation Isotopes* 9, 111 (1960).

When an organ is very small or lies at some distance from the source, the dose estimate averaged over the appropriate subregion is statistically more reliable than the dose estimated in the actual organ.

The internal organs of interest here, the kidneys, ovaries, and bladder, have the same location as corresponding organs described in a paper by Fisher.[48] Also, the size and shape of the ovaries and bladder are identical in the two papers; but the kidneys are described here in somewhat more detail, because Neohydrin concentrates in the kidney cortex, and thus it is necessary to identify the different regions, that is, the cortex, medulla, and papillary region.

The structure of the kidneys was determined from several anatomy references and from consultation with Dr. F. Jones, pathologist, University Hospital, Knoxville, Tennessee. In order to formulate this information as well as possible into a simple mathematical expression usable by the computer, the kidney as a whole is assumed to be an ellipsoid cut by a plane parallel to the major axis. With the rectangular coordinate system located at the center of the base of the trunk in the phantom, as shown in Fig. 25.7, the left kidney can be described by the inequalities

$$\left(\frac{x-6}{4.5}\right)^2+\left(\frac{y-6}{2}\right)^2+\left(\frac{z-32.5}{5}\right)^2 \leqq 1 \qquad (1)$$

and

$$x \geqq 4 . \qquad (2)$$

The kidneys are assumed to be alike and equal in volume; the combined volume of the two is 305.8 cm^3.

The human kidney is divided internally into three rather well defined regions: (1) the cortex, (2) the medulla, and (3) the papillary region. The cortex caps and surrounds the medulla, which consists of a series of conical masses termed renal pyramids whose apexes project in the form of renal papilla into the cuplike structure known as the papillary region.

[48] H. L. Fisher, Jr., and W. S. Snyder, "Distribution of Dose in the Body from a Source of Gamma Rays Distributed Uniformly in an Organ," presented at First Intern. Congress on Radiation Protection, Sept. 5–10, 1966, Rome (to be published in proceedings).

ORNL-DWG 67-1768R

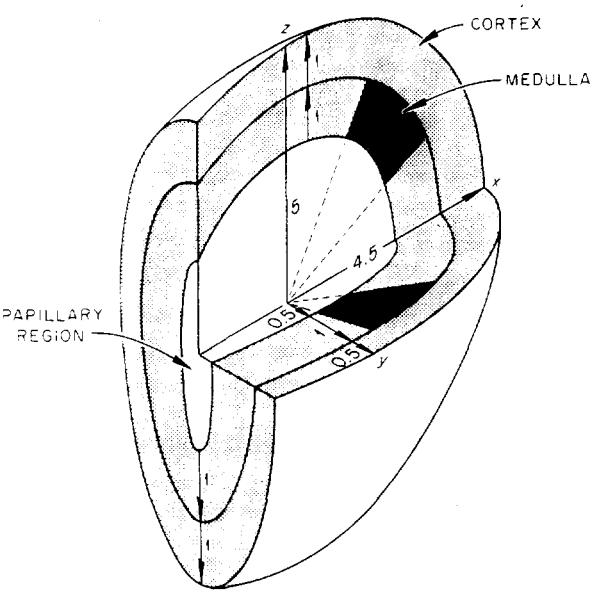

Fig. 25.31. Dosimetric Model of a Human Kidney.

The three sections of the kidney as simulated for computational purposes are shown in Fig. 25.31. The papillary region consists of the points satisfying inequalities (1) and (2) as well as the inequality

$$\left(\frac{x-6}{2.5}\right)^2+\left(\frac{y-6}{0.5}\right)^2+\left(\frac{z-32.5}{3}\right)^2 \leqq 1 , \qquad (3)$$

and the volume is 15.27 cm^3. Thus the papillary region consists of that portion of the entire kidney defined by (1) and (2) which lies inside a smaller ellipsoid having semiaxes 2.5, 0.5, and 3 cm.

The cortex contains an outer band consisting of the points (x, y, z) satisfying the inequalities (1) and (2) as well as the additional inequality

$$\left(\frac{x-6}{3.5}\right)^2+\left(\frac{y-6}{1.5}\right)^2+\left(\frac{z-32.5}{4}\right)^2 \geqq 1 . \qquad (4)$$

The volume is 94.17 cm^3. The cortex also contains certain portions of the medullary band to be described later.

The medulla lies in the space between the ellipsoid defining the papillary region and the ellipsoid defining the inner surface of the outer band of cortex. This medullary band consists of points

(x, y, z) satisfying (1) and (2) but not satisfying either (3) or (4), that is, satisfying the opposite inequalities

$$\left(\frac{x-6}{2.5}\right)^2+\left(\frac{y-6}{0.5}\right)^2+\left(\frac{z-32.5}{3}\right)^2>1\,, \quad (3')$$

$$\left(\frac{x-6}{3.5}\right)^2+\left(\frac{y-6}{1.5}\right)^2+\left(\frac{z-32.5}{4}\right)^2<1\,. \quad (4')$$

However, the medulla does not contain all this band. It consists of portions of circular cones having vertexes at the center of the above ellipsoids and half-angles of 17° 42′ which lie in the band defined above, that is, by inequalities (1), (2), (3′), and (4′). There are some 32 such cones distributed so as not to intersect each other. The total volume is 43.5 cm^3.

The portion of the medullary band which is not included in the cones is the additional part of the cortex mentioned above. This consists of points satisfying inequalities (1) and (2), (3′), and (4′) but not inside the cones of the medulla. The volume of the intermedullary portion of the cortex is 18.8 cm^3.

Dosimetry

By use of the physical and biological data and the geometrical configurations described above, the dose to the cortex and medulla of the kidneys and to the bladder and ovaries has been estimated. Estimates are provided per millicurie-hour of residence of ^{197}Hg and ^{203}Hg in the cortex of the kidneys, in the medulla of the kidneys, in the bladder, and in the total body (blood). These estimates are given in Table 25.5 for Neohydrin labeled with ^{197}Hg and in Table 25.6 for the ^{203}Hg label.

The doses were computed for gamma and x rays by use of the Monte Carlo computer code described previously,[45] and the decay data in Table 25.3 were used as input for each source location. In the case of beta and "beta-type" decays, doses were computed only for the organ containing the source, since the range of these emissions is insufficient – about 0.05 cm for the most energetic – to irradiate the other organs of interest. In estimating the dose from "beta-like" radiation, complete absorption of energy in the source region was assumed.

To find the rads per millicurie of intake by use of Tables 25.5 and 25.6, the rads per millicurie-hour for the tissue of interest must be multiplied by the millicurie-hours of residence of the radionuclides in each of the source organs and the results added. The millicurie-hours are given by

$$I\int_0^\infty R(t)\,dt\,,$$

where I is the intake (mc) and $R(t)$ is the fraction of the intake present in the tissue of interest t hours after intake.

The activity depositing in the kidney is considered in three parts: (1) a fraction of intake K_1 depositing in the cortex with rather long biological turnover time, T_1 days; (2) a fraction of intake K_2 depositing in medulla with a rather short biological turnover time, T_2 days; and (3) a fraction of intake K_3 depositing in medulla with a rather long biological turnover time, T_3 days. The number of millicurie-hours of residence in kidney for any of the above three fractions is given by

$$I\int_0^\infty R(t)\,dt=\frac{24IK_iT_rT_i}{0.693(T_r+T_i)}\,,\quad i=1,\,2,\,3\,, \tag{5}$$

where T_r is the half-time (days) for radioactive decay and

$$R(t)=K_i\exp\left[-\left(\frac{0.693}{T_r}+\frac{0.693}{T_i}\right)\frac{t}{24}\right]$$

for the respective cases.

The activity (mc) excreted into the bladder from the above deposits is given by

$$I\int_0^\infty R(t)\times\frac{0.693}{24T_i}\,dt=\frac{IK_iT_r}{T_r+T_i}\,,\quad i=1,\,2,\,3\,. \tag{6}$$

This expression must be summed for $i = 1, 2, 3$. If this activity is assumed to reside in the bladder for B hr, the total millicurie-hours of residence in the bladder due to activity eliminated from the kidney deposits may be taken as B multiplied by the sum of the expressions in (6). This estimate neglects radioactive decay, which seems justified. Indeed, if one assumes a uniform intake to the

Table 25.5. Radiation Dose to Various Body Organs from an Injected Dose of 1 mc of ^{197}Hg Neohydrin

Organ	Type of Decay	Location of Source: Cortex		Medulla		Bladder		Whole Body		Total (rads/mc)
		Rads/mc-hr	Rads/mc	Rads/mc-hr	Rads/mc	Rads/mc-hr	Rads/mc	Rads/mc-hr	Rads/mc	
Cortex	Gamma	0.037		0.036		1.3×10^{-4}		7.7×10^{-5}		
	β^-	2.0						2.7×10^{-3}		
	Total	2.0	18	0.036	0.10	1.3×10^{-4}	2.7×10^{-4}	2.8×10^{-3}	6.4×10^{-3}	18
Medulla	Gamma	0.044		0.062		1.3×10^{-4}		7.7×10^{-5}		
	β^-			4.4				2.7×10^{-3}		
	Total	0.044	0.37	4.5	13	1.3×10^{-4}	2.7×10^{-4}	2.8×10^{-3}	6.4×10^{-3}	13
Bladder	Gamma	1.5×10^{-4}		1.8×10^{-4}		0.041		8.2×10^{-5}		
	β^-					0.38		2.7×10^{-3}		
	Total	1.5×10^{-4}	1.3×10^{-3}	1.8×10^{-4}	5.2×10^{-4}	0.42	0.85	2.8×10^{-3}	6.4×10^{-3}	0.86
Ovaries	Gamma	2.3×10^{-3}		2.2×10^{-4}		5.1×10^{-3}		1.0×10^{-4}		
	β^-							2.7×10^{-3}		
	Total	2.3×10^{-3}	0.019	2.2×10^{-4}	6.3×10^{-3}	5.1×10^{-3}	0.010	2.8×10^{-3}	6.4×10^{-3}	0.042

Table 25.6. Radiation Dose to Various Body Organs from an Injected Dose of 1 mc of ^{203}Hg Neohydrin

Organ	Type of Decay	Location of Source: Cortex		Medulla		Bladder		Whole Body		Total (rads/mc)
		Rads/mc-hr	Rads/mc	Rads/mc-hr	Rads/mc	Rads/mc-hr	Rads/mc	Rads/mc-hr	Rads/mc	
Cortex	Gamma	0.12		0.11		5.7×10^{-4}		3.1×10^{-3}		
	β^-	2.3						3.1×10^{-3}		
	Total	2.4	144	0.11	1.5	5.7×10^{-4}	1.3×10^{-3}	6.2×10^{-3}	0.015	146
Medulla	Gamma	0.13		0.20		5.7×10^{-4}		3.1×10^{-3}		
	β^-			4.9				3.1×10^{-3}		
	Total	0.13	8.1	5.1	69	5.7×10^{-4}	1.3×10^{-3}	6.2×10^{-3}	0.015	77
Bladder	Gamma	6.7×10^{-4}		6.0×10^{-4}		0.12		3.6×10^{-3}		
	β^-					0.42		3.1×10^{-3}		
	Total	6.7×10^{-4}	0.040	6.0×10^{-4}	8.1×10^{-3}	0.54	1.2	6.7×10^{-3}	0.016	1.3
Ovaries	Gamma	5.9×10^{-3}		5.7×10^{-3}		0.013		4.1×10^{-3}		
	β^-							3.1×10^{-3}		
	Total	5.9×10^{-3}	0.36	5.7×10^{-3}	0.077	0.013	0.029	7.2×10^{-3}	0.018	0.46

bladder for T hr and then a voiding, the correction factor needed to correct for radioactive decay is

$$2\,(T\lambda_r - 1 + e^{-\lambda_r T})/T^2\lambda_r^2\,,$$

and for $T = 4.8$ hr, this is 0.98 and 0.99 for the ^{197}Hg and ^{203}Hg respectively. In addition to activity entering the bladder from the kidney deposits, there is the amount eliminated from the blood, which is assumed to pass through the kidney to the bladder. This is computed by the formula

$$IA \int_0^\infty e^{-(\lambda_r+\lambda_b)t}\lambda_b\, dt = \frac{IA\,\lambda_b}{\lambda_r + \lambda_b}\,, \qquad (7)$$

where $\lambda_r = 0.693/T_r$ is the radioactive decay constant and $\lambda_b = 0.693/T_b$ is the rate of biological elimination. As discussed above, this is used with $A = 0.75$ and $T_b = 1.3$ hr and again with $A = 0.05$ and $T_b = 15$ hr. The sum of the two values obtained from (7) using these data represents the material entering the bladder from blood and must be added to the sum of the three terms obtained from (6). All the activity entering the bladder, that is, the sum of the three terms of (6) and the two terms of (7), is multiplied by B, the residence time in the bladder (i.e., $B = 2.4$ hr), to obtain the total millicurie-hours of residence in the bladder.

In like manner, the millicurie-hours of residence in the whole body (blood) is computed by the formula

$$IA \int_0^\infty e^{-(\lambda_r+\lambda_b)t}\, dt = \frac{IA}{\lambda_r + \lambda_b}\,, \qquad (8)$$

where the terms are defined and used as in (7). In Table 25.7 the numerical values of the constants used in estimating millicurie-hours of residence for the "typical" case described above are given, as well as the corresponding millicurie-hours for each of the reference tissues. These residence times were used to obtain the estimates of dose per millicurie of intake given in Tables 25.5 and 25.6.

If different values of K_i and T_r or of B seem appropriate for a particular patient, formulas (5) and (6) are easily computed to obtain the proper number of millicurie-hours of residence time in the various tissues. Thus the dose estimate is easily adjusted for a particular patient for whom the parameter values given above might not be appropriate. If an entirely different metabolic model is assumed, of whatever kind, and if by its use one can estimate the total millicurie-hours of residence in the various tissues, then, again, one can use the table to obtain the estimate of dose resulting from use of this model. Since individuals may differ rather markedly, there may be cases where this adjustment is of considerable significance.

Table 25.7. Residence Times (mc/hr) of ^{197}Hg and ^{203}Hg in Various Body Organs from an Injected Dose of 1 mc of ^{197}Hg or ^{203}Hg Neohydrin

Organ	Formulas and Constants Used in the Computations	^{197}Hg	^{203}Hg
Total body (blood)	Formula (8)	2.3	2.5
Cortex	Formula (5), $K_1 = 0.10$, $T_1 = 28$ days	8.5	61
Medulla 1	Formula (5), $K_2 = 0.08$, $T_2 = 0.5$ days	1.2	1.4
Medulla 2	Formula (5), $K_3 = 0.02$, $T_3 = 28$ days	1.7	12
Bladder	Formulas (6) and (7), $B = 2.4$ hr	2.1	2.3

USE OF EXCRETION DATA TO PREDICT THE SYSTEMIC BODY BURDEN OF PLUTONIUM

W. S. Snyder Mary R. Ford
G. G. Warner[49]

Health physicists face one of their most difficult problems when they need to estimate the exposure status of an employee who may have been, or is known to have been, exposed to plutonium. In particular, the estimation of the systemic body burden is difficult since the available data suggest that the excretory rate changes, though slowly, with time. Thus, the systemic burden cannot be directly inferred from the excretion rate, but the

[49] Mathematics Division.

time sequence of the exposures is important. In addition, there are wide fluctuations of the amounts excreted per day as have been found in employees[50] as well as in experimental animals.[51] The crowning difficulty is that there are only a few data available which can be used to study the problem and perhaps construct a model.

Langham *et al.*[52] have analyzed the excretion and autopsy data obtained from 15 hospital patients who were given plutonium intravenously. Eleven patients received $^{239}PuNO_3$ complexed with citrate, and four patients received $^{239}PuO_2$. This study provides the best available data on humans concerning retention and excretion as they apply to a systemic burden of plutonium in that the amount entering blood is accurately known, the excretion data are nearly complete, and in six of these cases autopsy data provide evidence on the distribution of the systemic burden as well as a check on the excretion data. These data are limited in three respects: (1) Because the complexing with citrate probably influences the distribution of the systemic burden, emphasizing deposition in bone and deemphasizing deposition in liver, these cases may not be typical of occupational exposure in the majority of cases. (2) The data do not extend very far in time, less than half these patients being available for study up to 40 days postinjection and daily excretion data being available on only two patients for as long as 138 days. (3) These were inactive terminal patients, and this might have some influence on the metabolism and excretion of the plutonium. Langham *et al.*[52] did extend the record by determining the average daily excretion of two of the patients at various times after the close of the experiment and by following the excretion on a few employees who had accumulated measurable amounts of plutonium. He found that by making certain assumptions concerning the employees' exposure, their excretion followed the same trend indicated by the terminal patients. On this basis it is often assumed that the excretion data follow the trend of a power function for times of five years or more, that is, if a unit amount of plutonium enters blood at time $t = 0$, the excretion on day t may be expected to average $at^{-\alpha}$ units, where a and α are constants. As mentioned above, one may expect rather large fluctuations in the day-to-day values.

There is one case of occupational exposure reported in the literature[53] which is not complete enough to be useful for testing or constructing metabolic models but does provide very valuable data. Although neither the exposure nor the amount entering the blood of this employee is known even approximately, the excretion data obtained from scattered samples collected in the course of his employment are available, and the autopsy data are complete and rather detailed. It would be extremely valuable to have more data of this kind, for, although occupational exposures will inevitably lack the precision of the experimental studies, they provide useful data which involve exactly those uncertainties and difficulties the health physicist faces in the practical situation. Hence they are valuable checks on procedures which are proposed for the practical problem of evaluating exposures of plutonium workers. Additionally, one may turn to data on experimental animals to study the problem, but, while valuable, results from animal experiments must be viewed as requiring some confirmation by human data before we can be entirely confident of their applicability to occupational exposure. These remarks are meant to stress the importance of obtaining every bit of human data bearing on the problem whenever possible, as well as to excuse, if excuse be necessary, the analysis which follows and which is open to the charge of overelaboration and refinement of analysis of very few data. However, these are all the relevant data we have found which could be used for this type of analysis.

The first question studied here is that of the extent of individual differences: How different are the 15 patients[52] as far as excretion of plutonium that has entered blood is concerned? The question has been studied previously,[54] and the present studies may be considered as an extension of that study. Langham *et al.*[52] were the first to fit a power function to the excretion data of these patients, that is, to obtain constants a and α so that the function $at^{-\alpha}$ represents approximately

[50] S. A. Beach and G. W. Dolphin, *Assessment of Radioactivity in Man*, vol. II, p. 603, IAEA, Vienna, 1964.

[51] W. J. Bair *et al.*, *Health Phys.* 8, 639 (1962).

[52] W. H. Langham *et al.*, *Distribution and Excretion of Plutonium Administered Intravenously to Man*, LA-1151 (1950).

[53] H. Foreman, W. Moss, and W. Langham, *Health Phys.* 2, 326 (1960).

[54] W. S. Snyder, *Health Phys.* 8, 767 (1962).

the excretion expected on day t. In particular, they gave the three formulas $0.23t^{-0.77}$, $0.63t^{-1.09}$, and $0.79t^{-0.94}$ for urinary, fecal, and total daily excretion respectively. These functions have been extensively used in the interpretation of excretion data to obtain an estimate of body burden. In this study we retain the form of the function, that is, $at^{-\alpha}$, but we analyze the data for each individual to determine what differences exist in the values of a and α that provide the best fit of the function to the data. The values so determined are shown in Table 25.8 together with the values of a and α of best fit when all the data of all the patients are used together.

The values of the parameters a and α given in Table 25.8 are selected in a novel manner. The columns under the subtitle "Point Fit" regard the urinary excretion U_i on day i as a point in a two-dimensional plot, i (days) being the abscissa and U_i (fraction of injected activity excreted on day i) being the ordinate. The values of a and α are chosen to minimize the sum

$$\sum_{i=1}^{n} |U_i - ai^{-\alpha}| = \min , \qquad (1)$$

that is, the sum of the absolute deviations of the data from the formula is minimized. The minimization is accomplished by setting up a mesh, generally on the interval $0 < \alpha < 2$, with a spacing of $\Delta\alpha = 0.01$ for the mesh. A code was designed which selected, in turn, each point of the mesh and, having thus fixed the value of α, used standard techniques to find the minimizing value of the linear parameter a. The value of the sum was computed for each such choice of α and for the minimizing value of a, and the smallest of these values determined the choice of a and α. It is noteworthy that no log transform of the data was used nor was the sum of squares of deviations used. When the formula $at^{-\alpha}$ is used to estimate intake or body burden of an employee, it will be used multiplicatively, and thus any percent deviation by excess or by default of an individual's data from the formula will produce a corresponding percent of error in the estimate. It is for this reason that we chose to minimize the deviations of the data and not the squares of the deviations or the deviations of the logarithms of the data. This procedure produced the values of a and α shown under the subheading "Point Fit."

Table 25.8. Urinary Excretion Formulas, $at^{-\alpha}$, for 15 Individuals Obtained by Minimizing the Sum of the Absolute Deviations

Patient	"Point Fit"		"Area Fit"	
	a	α	a	α
Hp-1	0.24	0.74	0.10	0.42
Hp-2	0.47	1.04	0.17	0.63
Hp-3	0.38	0.99	0.17	0.71
Hp-4	0.44	0.89	0.20	0.54
Hp-5	0.30	1.10	0.11	0.62
Hp-6	0.50	1.21	0.31	0.99
Hp-7	0.24	1.02	0.078	0.64
Hp-8	0.38	0.88	0.16	0.58
Hp-9	0.12	0.48	0.096	0.40
Hp-10	0.41	0.98	0.17	0.60
Hp-12	0.15	0.58	0.087	0.40
Chi-I	0.86	1.85	0.18	0.79
Chi-II	0.25	0.73	0.20	0.66
Chi-III	0.15	0.86	0.071	0.53
Cal-I	0.48	1.19	0.12	0.74
All the patients	0.32	0.93	0.15	0.65

Since the formula $at^{-\alpha}$ is fitted to the 24-hr excretion values, the formula should, strictly, only be used when t is a positive integer, that is, to predict the excretion for a complete day. Thus, it is not a true rate of excretion in the usual sense. When the value of the function does not vary appreciably throughout the day, one may consider it as a rate function and replace the tedious summation of daily values by an integration. Although this procedure is logically based, it points up the basic difficulty of the approach taken here, namely, that excretion is a continuous process and not a discrete one. Even though the individual voids occur at discrete intervals of time, the plutonium is constantly being transferred to the bladder or to the large intestine and is then effectively not a part of the systemic body burden. Thus, it appears more logical on physiological grounds to attempt to determine a true rate of excretion which considers it as a continuous process. Treating the data in this way is in accord with the view

that if a formula is to be used in a certain way, then the procedure used to fit the formula to the data should minimize the deviations from the formula as used; for example, in the present case, if a rate function is wanted so that excretion during a time interval equals $\int f(t)\,dt$ over that time interval, then it is the integral of f that should be used in the minimization process. This is easily done, for if $at^{-\alpha}$ represents the instantaneous rate of excretion, then the excretion over the time interval corresponding to the ith day is given by

$$\int_{i-1}^{i} at^{-\alpha}\,dt = a\left[\frac{i^{1-\alpha} - (i-1)^{1-\alpha}}{1-\alpha}\right]. \qquad (2)$$

The minimizing values of a and α are determined as before, except that the formula

$$\sum_{i=1}^{n}\left|U_i - a\left[\frac{i^{1-\alpha} - (i-1)^{1-\alpha}}{1-\alpha}\right]\right| = \min \qquad (3)$$

is used in place of Eq. (1). The values of a and α so obtained are shown in Table 25.8 under the subheading "Area Fit," for the integral in Eq. (2) represents the area under the curve $at^{-\alpha}$ that corresponds to a daily excretion. It will be noted that there appears to be less spread in the values of a and α for the individual patients when determined in this way than when the "Point Fit" method is used.

As mentioned above, one might prefer to minimize the sum of percent deviations, and the above procedure only minimizes the sum of absolute deviations. It is easy to make the necessary modifications, and thus one obtains

$$\sum_{i=1}^{n}\left|\frac{U_i}{a\,f(i,\alpha)} - 1\right| = \min \qquad (4)$$

with

$$f(i,\alpha) = i^{-\alpha} \text{ or } f(i,\alpha) = \frac{i^{1-\alpha} - (i-1)^{1-\alpha}}{1-\alpha} \qquad (5)$$

and the values of a and α which minimize the sum of the percent deviations. As before, the formula determined by Eq. (4) is to be used essentially by forming sums corresponding to excretion for whole days if $f(i,\alpha) = i^{-\alpha}$ is used, but the second formula given in Eq. (5) is to be used to determine a rate of excretion and the integral used in place of the discrete sum. The values of a and α obtained from Eqs. (4) and (5) for all 15 patients are shown in Table 25.9. This table also contains values of a and α obtained when the data of all patients are used in Eqs. (4) and (5).

Table 25.9. Urinary Excretion Formulas, $at^{-\alpha}$, for 15 Individuals Obtained by Minimizing the Sum of the Percent Deviations

Patient	"Point Fit"		"Area Fit"	
	a	α	a	α
Hp-1	0.28	0.82	0.18	0.65
Hp-2	0.66	1.21	0.17	0.63
Hp-3	0.57	1.20	0.16	0.72
Hp-4	0.44	0.89	0.19	0.56
Hp-5	0.18	0.79	0.11	0.62
Hp-6	0.50	1.21	0.31	0.99
Hp-7	0.48	1.26	0.089	0.75
Hp-8	0.32	0.81	0.23	0.73
Hp-9	0.12	0.47	0.096	0.40
Hp-10	0.73	1.22	0.16	0.72
Hp-12	0.15	0.57	0.12	0.52
Chi-I	0.11	0.61	0.099	0.57
Chi-II	0.17	0.62	0.16	0.60
Chi-III	0.15	0.83	0.083	0.45
Cal-I	0.26	0.88	0.13	0.72
All the patients	0.21	0.73	0.14	0.61

From the data of Tables 25.8 and 25.9, some indication of the extent of individual differences can be observed. Despite the reservations noted concerning the data used here, that is, the sick and immobilized condition of the patients and the limited extent in time of the data, the authors know of no other data available to check on this extent of individual differences. The values of a and α obtained by pooling all the data of all the patients might be considered as "typical" of these parameters so far as our present knowledge permits us to judge. Clearly, the range of the individual values about these "typical" values will produce great differences over long

periods of time, and therefore it is particularly unfortunate that data are not available over a longer period of time. For persons exposed occupationally, the period may extend over many years. For example, in the case reported by Foreman *et al.*[53] the employee worked with plutonium over a period of about 11 years, although not continuously. The data on the isotopic ratio of ^{238}Pu and ^{239}Pu suggest that some of the exposure probably occurred early in this period and that some of it occurred much later. Thus, the formula to be validated should extend over many years – ideally, over a working lifetime.

The previous section was concerned with differences in the broad trends of excretion for different individuals. We turn now to consider the fluctuations of an individual's day-to-day excretion values about his own particular curve. Except for those employees who are subjects of special and intensive study, an individual's excretion curve is unknown, and thus we study also the fluctuation of daily excretion values about the "typical" curve. Some data on this distribution of values appear in Table 25.10, where factors to apply to an individual's curve or to the "typical" curve are given, that is, factors p and P, which correspond to a specified percent of the daily excretion values of the jth individual between $pai^{-\alpha}$ and $Pai^{-\alpha}$, are given. In the case of the "typical" values of a and α, the factors p and P when so applied define a range including a specified percent of all the data of all the patients. The same considerations apply to the formula

$$a\left[\frac{i^{1-\alpha}-(i-1)^{1-\alpha}}{1-\alpha}\right],$$

which is designated in Table 25.11 as the "Area Fit" formula. Values are given only for urinary data, because fecal data are not available in a practical case.

These data are treated more generally by calculating the ratios $R_i = U_i/ai^{-\alpha}$ or $R_i' = (1-\alpha)\,U_i/a\,[i^{1-\alpha}-(i-1)^{1-\alpha}]$ and noting the fluctuations of these ratios. If the ratios R_i, or R_i', are ranked by magnitude, irrespective of the chronological order indicated by i, one has a distribution of values on the real axis. When the ratio R_i equaled 1, the formula predicted the excretion on day i exactly, while values of R_i greater than 1 (less than 1) correspond to cases where the formula predicted too little (too much) excretion. By graphing the cumulative distribution of the R_i or the R_i' for an individual case, one obtains visual presentation of the data. The presentation of these cumulative curves for all the individual cases in one graph produces a complex network of curves, and individual curves are not easily identified. Consequently, only a general region is shown in which all the individual curves lie (see Fig. 25.32 for distribution of values of R_i for the individual cases). Using this region, one can select values of p and P to include any desired percentage of the daily excretion values. Figure 25.33 contains the same presentation for the ratio $R_i' = (1-\alpha)\,U_i/a\,[i^{1-\alpha}-(i-1)^{1-\alpha}]$, and the interpretation is similar. The values of a and α used in Figs. 25.32 and 25.33 are those obtained by minimizing the sum of percentage deviations for the appropriate formula. This would be expected to produce the narrowest region.

The values of a and α may be selected to minimize any one of the four sums defined by Eqs. (1), (3), (4), or (5) when the data of all the patients are used simultaneously. One might expect that the curve so obtained would be more representative of a "typical" or average excretion pattern than any of the individual cases. The values of a and α so obtained are given in Tables 25.8 and 25.9. From these values, the spread of individual fluctuations about the "typical" or group curve is presented in Figs. 25.34 and 25.35. It is evident that the spread of fluctuations is somewhat greater than when the data of each patient are compared with the trend curve obtained by choosing a and α on the basis of his data. The difference in spread of the regions in Figs. 25.34 and 25.35 as compared with the width of the regions in Figs. 25.32 and 25.33 is a measure of the extent of individual differences. In Figs. 25.32 and 25.33, the width is a measure of the extent of daily fluctuations when the curve of best fit for each patient is used for his data. However, in Figs. 25.34 and 25.35, a single formula is used for all the patients, and so the variability due to individual differences is added to the variability due to day-to-day variations.

These data may be used to design a program for a digital computer which uses the entire record of an employee's urinary excretion of plutonium and produces an estimate of his intakes as well as of the plutonium present in bone at any time during exposure or postexposure and which takes into account to some extent the effect of daily fluctuations of data. Other codes of this general type

Table 25.10. Fluctuations of Daily Urinary Excretion Values of Individuals About Their Own Formulas and About the "Typical" Formula of Best Fit–"Point Fit" Formulas Used[a]

Formulas obtained by minimizing the sum of percent deviations

Patient	Percentiles $pf(i)$ and $Pf(i)$ of the Distribution of Excretion Data									
	25%–75%		15%–85%		10%–90%		5%–95%		2.5%–97.5%	
	p	P	p	P	p	P	p	P	p	P
Hp-1	0.93 (1.00)	1.07 (1.15)	0.72 (0.73)	1.10 (1.18)	0.71 (0.71)	1.11 (1.19)	0.65 (0.71)	1.12 (1.20)	0.65 (0.64)	1.17 (1.21)
Hp-2	0.90 (0.66)	1.20 (1.20)	0.77 (0.49)	1.27 (1.37)	0.72 (0.45)	1.33 (1.75)	0.68 (0.41)	1.53 (2.20)	0.66 (0.40)	1.57 (2.27)
Hp-3	0.76 (0.64)	1.08 (1.04)	0.74 (0.61)	1.17 (1.18)	0.65 (0.51)	1.18 (1.37)	0.54 (0.50)	1.27 (2.24)	0.52 (0.43)	1.29 (2.65)
Hp-4	0.82 (1.04)	1.10 (1.72)	0.45 (0.55)	1.25 (1.83)	0.44 (0.54)	1.27 (2.05)	0.34 (0.41)	1.34 (2.30)	0.34 (0.41)	1.34 (2.30)
Hp-5	0.76 (0.56)	1.07 (0.80)	0.73 (0.55)	1.21 (0.86)	0.69 (0.51)	1.22 (0.87)	0.58 (0.45)	1.57 (1.28)	0.45 (0.35)	1.61 (1.38)
Hp-6	0.97 (0.60)	1.03 (0.92)	0.96 (0.54)	1.07 (1.15)	0.93 (0.53)	1.07 (1.32)	0.91 (0.52)	1.17 (1.42)	0.80 (0.48)	1.19 (1.67)
Hp-7	0.86 (0.38)	1.10 (0.58)	0.79 (0.37)	1.14 (1.01)	0.76 (0.35)	1.16 (1.04)	0.72 (0.33)	1.18 (1.43)	0.45 (0.29)	1.33 (1.64)
Hp-8	0.90 (1.03)	1.04 (1.24)	0.85 (0.96)	1.08 (1.30)	0.81 (0.94)	1.17 (1.33)	0.79 (0.86)	1.25 (1.45)	0.63 (0.72)	1.30 (1.80)
Hp-9	0.89 (0.85)	1.12 (1.40)	0.85 (0.74)	1.19 (1.43)	0.77 (0.71)	1.22 (1.47)	0.72 (0.68)	1.28 (1.61)	0.68 (0.66)	1.36 (1.66)
Hp-10	0.96 (0.76)	1.15 (1.18)	0.87 (0.74)	1.17 (1.43)	0.85 (0.72)	1.20 (1.93)	0.74 (0.69)	1.24 (2.27)	0.57 (0.68)	1.27 (2.55)
Hp-12	0.91 (1.00)	1.14 (1.31)	0.82 (0.91)	1.32 (1.61)	0.75 (0.81)	1.56 (1.70)	0.72 (0.76)	2.40 (3.17)	0.68 (0.70)	2.44 (3.25)
Chi-1	0.69 (0.59)	1.31 (1.16)	0.59 (0.48)	1.55 (1.39)	0.52 (0.39)	1.67 (1.46)	0.31 (0.26)	1.96 (1.77)	0.27 (0.22)	2.38 (2.16)
Chi-2	0.63 (0.77)	1.26 (1.53)	0.51 (0.60)	1.46 (1.76)	0.50 (0.55)	1.59 (1.96)	0.47 (0.49)	1.80 (2.12)	0.41 (0.46)	2.08 (2.36)
Chi-3	0.77 (0.44)	1.10 (0.71)	0.69 (0.40)	1.33 (0.75)	0.53 (0.29)	1.88 (1.03)	0.26 (0.14)	1.95 (1.29)	0.26 (0.14)	1.95 (1.29)
Cal-1	0.66 (0.44)	1.20 (0.75)	0.53 (0.38)	1.35 (0.85)	0.41 (0.31)	1.47 (0.93)	0.31 (0.22)	1.61 (1.11)	0.26 (0.20)	1.85 (1.25)

[a]Values in parentheses indicate values of p and P as percentiles of the distribution of values about the "typical" curve, that is, curve of best fit for the data of the group.

Table 25.11. Fluctuations of Daily Urinary Excretion Values of Individuals About Their Own Formulas and About the "Typical" Formula of Best Fit–"Area Fit" Formula Used[a]

Formulas obtained by minimizing the sum of percent deviations

	Percentiles $pf(i)$ and $Pf(i)$ of the Distribution of Excretion Data									
	25%–75%		15%–85%		10%–90%		5%–95%		2.5%–97.5%	
Patient	p	P	p	P	p	P	p	P	p	P
Hp-1	0.89	1.06	0.64	1.12	0.64	1.12	0.57	1.14	0.34	1.16
	(1.01)	(1.28)	(0.73)	(1.31)	(0.73)	(1.36)	(0.64)	(1.38)	(0.49)	(1.41)
Hp-2	0.59	1.06	0.43	1.21	0.39	1.55	0.35	1.76	0.35	2.13
	(0.67)	(1.29)	(0.49)	(1.41)	(0.44)	(1.84)	(0.40)	(2.11)	(0.39)	(2.58)
Hp-3	0.82	1.21	0.77	1.35	0.64	1.44	0.64	1.65	0.55	2.37
	(0.65)	(1.17)	(0.64)	(1.36)	(0.57)	(1.55)	(0.51)	(1.60)	(0.46)	(2.54)
Hp-4	0.68	1.29	0.35	1.39	0.34	1.50	0.26	1.90	0.26	1.90
	(1.07)	(1.93)	(0.55)	(2.03)	(0.54)	(2.07)	(0.41)	(2.68)	(0.41)	(2.68)
Hp-5	0.80	1.05	0.79	1.16	0.70	1.18	0.68	1.20	0.51	1.86
	(0.62)	(0.81)	(0.61)	(0.88)	(0.54)	(0.90)	(0.52)	(0.93)	(0.39)	(1.46)
Hp-6	0.83	1.00	0.81	1.00	0.79	1.02	0.77	1.08	0.67	1.23
	(0.62)	(1.03)	(0.56)	(1.33)	(0.54)	(1.54)	(0.53)	(1.66)	(0.50)	(1.90)
Hp-7	0.96	1.42	0.92	2.05	0.85	2.39	0.73	3.03	0.61	3.14
	(0.38)	(0.62)	(0.36)	(0.98)	(0.35)	(1.20)	(0.33)	(1.66)	(0.28)	(1.86)
Hp-8	0.93	1.07	0.87	1.13	0.83	1.19	0.74	1.30	0.58	1.31
	(0.98)	(1.27)	(0.92)	(1.36)	(0.89)	(1.44)	(0.78)	(1.54)	(0.71)	(2.04)
Hp-9	0.89	1.10	0.85	1.14	0.78	1.18	0.75	1.22	0.69	1.24
	(0.93)	(1.41)	(0.82)	(1.45)	(0.76)	(1.49)	(0.75)	(1.61)	(0.44)	(1.65)
Hp-10	0.94	1.35	0.90	1.68	0.88	1.84	0.84	2.54	0.70	2.62
	(0.77)	(1.21)	(0.76)	(1.55)	(0.73)	(1.73)	(0.70)	(2.65)	(0.69)	(2.90)
Hp-12	0.91	1.18	0.85	1.32	0.77	1.59	0.72	2.34	0.58	2.38
	(1.04)	(1.27)	(0.88)	(1.51)	(0.87)	(1.82)	(0.84)	(2.92)	(0.69)	(2.98)
Chi-1	0.68	1.25	0.56	1.44	0.50	1.58	0.31	1.81	0.27	2.22
	(0.54)	(1.02)	(0.45)	(1.18)	(0.40)	(1.30)	(0.24)	(1.53)	(0.21)	(1.83)
Chi-2	0.63	1.24	0.51	1.44	0.49	1.59	0.47	1.74	0.41	1.97
	(0.74)	(1.45)	(0.59)	(1.69)	(0.57)	(1.84)	(0.55)	(1.99)	(0.48)	(2.23)
Chi-3	0.65	1.01	0.51	1.22	0.35	1.28	0.17	2.40	0.17	2.40
	(0.49)	(0.81)	(0.41)	(0.83)	(0.31)	(1.11)	(0.15)	(1.47)	(0.15)	(1.47)
Cal-1	0.66	1.13	0.58	1.29	0.46	1.42	0.33	1.48	0.30	1.71
	(0.41)	(0.66)	(0.36)	(0.77)	(0.26)	(0.82)	(0.21)	(1.05)	(0.18)	(1.32)

[a]Values in parentheses indicate values of p and P as percentiles of the distribution of values about the typical curve, that is, curve of best fit for the data of the group.

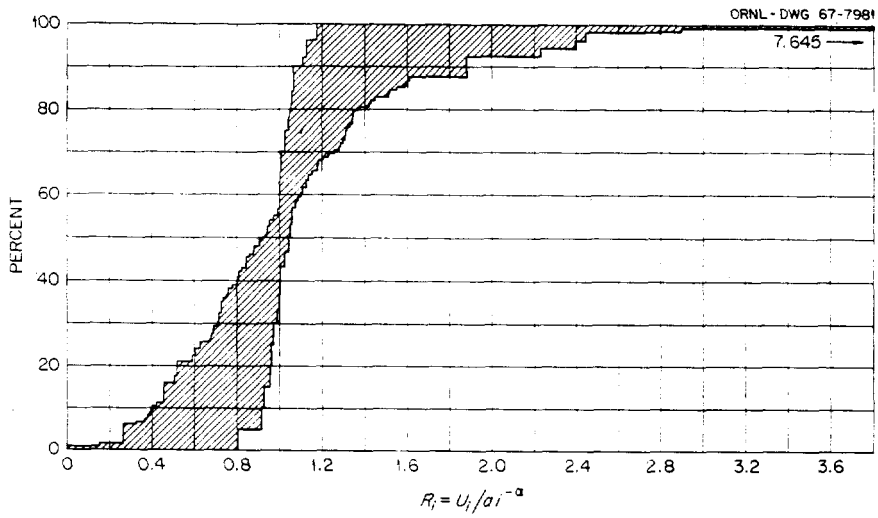

Fig. 25.32. Fluctuations of Daily Urinary Excretion Data of All Patients (Langham, 1950) About Their Own Formula of Best Fit – "Point Fit" Formulas Obtained by Minimizing the Sum of Percent Deviations.

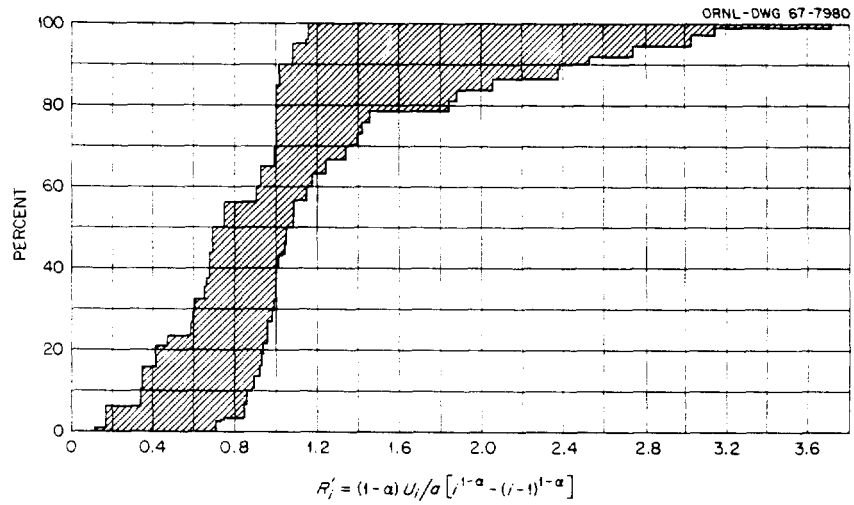

Fig. 25.33. Fluctuations of Daily Urinary Excretion Data of All Patients (Langham, 1950) About Their Own Formula of Best Fit – "Area Fit" Formulas Obtained by Minimizing the Sum of Percent Deviations.

have been described in the literature.[54–56] All these codes are basically of the same general type in that they use the power function $at^{-\alpha}$ describing the trend of urinary excretion following a single intake to blood as a basis for estimating a series of intakes that would be expected to produce the observed excretion pattern as closely as possible. However, these codes have generally used only the trend curve $ai^{-\alpha}$ to estimate the intakes necessary to produce the recorded excretion values and thus took little account of the fact that wide fluctuations of the data are possible and properly should influence the estimates of intake. The present code has been designed to utilize data on the fluctuation of daily excretion levels

[55] J. N. P. Lawrence, *Health Phys.* 8, 61 (1962).

[56] W. S. Snyder, "The Estimation of a Body Burden of Pu from Urinalysis Data," p. 13 in *Proceedings of the Seventh Annual Meeting on Bio-Assay and Analytical Chemistry*, ANL-6637 (1961).

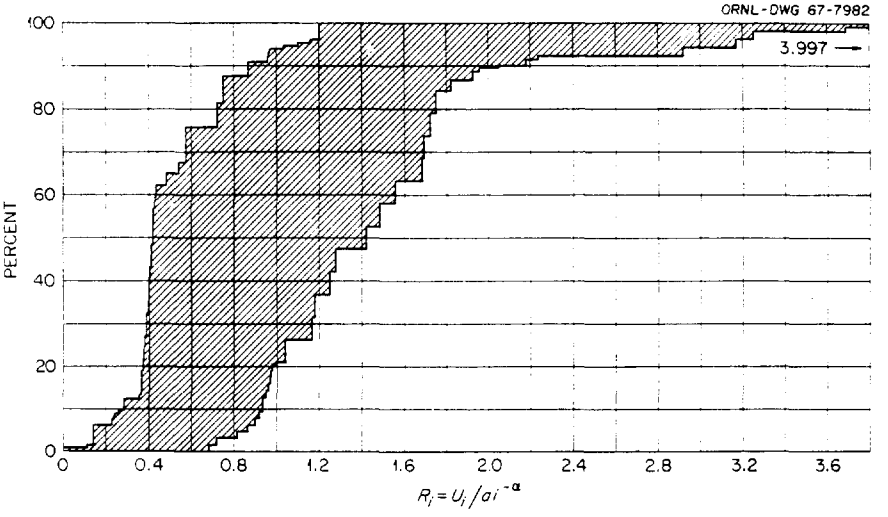

Fig. 25.34. Fluctuations of Daily Urinary Excretion Data of All Patients (Langham, 1950) About the "Typical" Formula of Best Fit – "Point Fit" Formula Obtained by Minimizing the Sum of Percent Deviations.

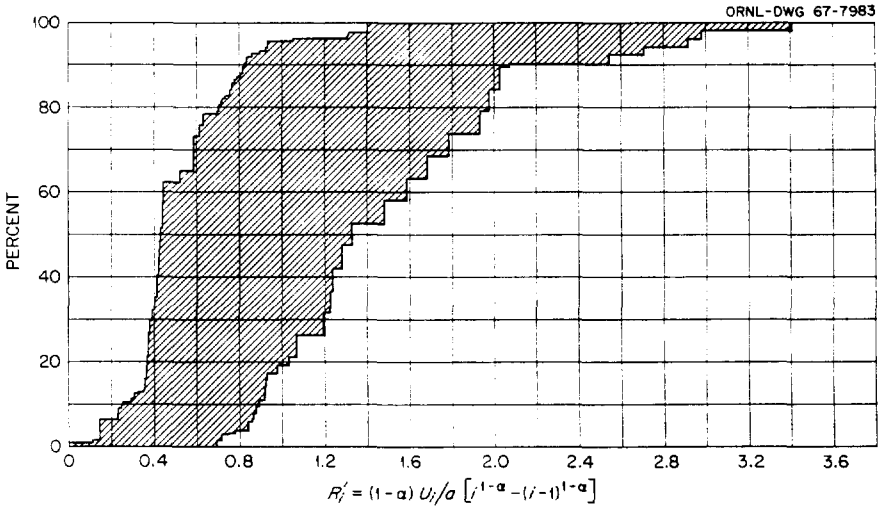

Fig. 25.35. Fluctuations of Daily Urinary Excretion Data of All Patients (Langham, 1950) About the "Typical" Formula of Best Fit – "Area Fit" Formula Obtained by Minimizing the Sum of Percent Deviations.

about the urinary excretion curve $at^{-\alpha}$ and thus reduce somewhat the magnitude and number of intakes that are required.

The code uses as input a value $\Delta \geq 0$, which represents the supposed level of sensitivity of the analytical methods, that is, the minimum detectable level of activity in a daily urine sample. Any sample value which is less than Δ is regarded as being essentially identical to zero, and no intake is considered necessary to account for the reported activity. If the input specifies zero as the value of Δ, no sample will be rejected by this test. Thus use of this feature of the code is at the discretion of the user.

Two percentage values (p, P) also are included as input for the code. These two values specify a certain range of fluctuation, either high or low, which is considered as acceptable, but excretion values lying beyond the range (whether too high or too low) are considered as not acceptable, that

is, as requiring some modification of the intakes previously estimated. The code is designed to modify the estimates of intake in the latter case so as to produce a pattern of intake which is acceptable if that is possible. For example, if U_i is the first sample value and occurs on day t_1, then the computer will estimate an intake I_1 on a day τ_1 by use of either of the formulas given in Eq. (5). There is some arbitrariness here, both in the choice of the day τ_1 and in the use of the formula which only represents a typical value for the excretion. Actually, the excretion on day t_1 might have been higher or lower than would be predicted by the formula. There is no readily apparent way of deciding whether on any given day excretion was higher or lower than is typically the case, but this should not prevent us from recognizing that this arbitrariness, or uncertainty, is there.

The computer code can be designed to make some allowance for the effect of these fluctuations of the day-to-day data. If the first intake is computed as indicated in the preceding paragraph, that is, on the basis of the formula for the typical or average case, and if the next excretion sample, U_2 on day t_2, shows an activity in excess of what would be expected from the intake I_1, it should be recognized that it is not always necessary to postulate that a new intake occurred on some day between the two sample dates. It may be that the first intake I_1 has been overestimated, and this could occur in several ways, either because the day of intake τ_1 has been wrongly assigned or because excretion happened to be unusually high on the day of the first sample. On the basis of Table 25.10, one can assign a confidence level and use the code so that if U_2 exceeds the excretion predicted on the basis of I_1 but not by more than a factor P, then there is a substantial probability that the excess is due only to a chance fluctuation on the high side. On the other hand, if U_2 exceeds the predicted excretion following an intake I_1 by more than the factor P, there is little likelihood that this is a chance excess, and hence it is likely that some new intake, say I_2, occurred between the sample days t_1 and t_2. However, one postulates such an intake only when the excess above the excretion predicted on the basis of I_1 is so great that it is not likely that a chance fluctuation is responsible for the excess. The numerical value of P can be chosen by the user of the code to correspond to various levels of confidence concerning the extent of daily fluctuations he will allow. In fact, the code can be run for a variety of different levels P and the results compared.

In similar fashion, if the excretion U_2 is less than that predicted on the basis of the first intake, one may decide that I_1 should be reduced. Instead of estimating I_1 solely on the basis of U_1 and the trend curve, say ai^{-a}, one may postulate that U_1 is unusually high, say Pai^{-a}, and that U_2 occurred on a day when excretion was low, say as given by pai^{-a}, or he may use a combination of both assumptions.

The above simple illustration involving only two intakes, I_1 and I_2, and two excretion values, U_1 and U_2, applies in principle to any set of intakes and excretion values. If one has estimated intakes $I_1, I_2, \ldots, I_k$ which correspond to and produce given excretion values $U_1, U_2, \ldots, U_k$, then one may estimate the excretion on a later day from the above intakes. If the actual excretion on this later day does not differ too greatly from that predicted, no new intake need be postulated. If the difference is sufficiently great, one seeks to redefine the intakes $I_1, I_2, \ldots, I_k$ and may, in this way, reduce the difference of the actual and predicted values to lie within the expected limits of variability. Only when this adjustment fails to reduce the difference to within the prescribed factor P does one postulate a new intake I_{k+1} to account for the excess. When many intakes have occurred, the number of possible adjustments is enormous, and the best method of arriving at an acceptable set of intakes is still being explored. However, the principle seems well established, and experience to date with the code indicates it is a definite improvement over methods of estimation which neglect the influence of fluctuations of the excretion data.

26. Stable Element Metabolism

W. S. Snyder
Mary Jane Cook
Cyrus Feldman[1]
F. S. Jones[1]
Peggy L. Stewart[2]
Isabel H. Tipton[2]

In many cases information on the metabolism of stable elements in humans has provided a more reliable basis for calculating maximum permissible concentration (MPC) values than small animal data. Therefore, the study has been extended to include analysis of daily intake and excretion of individuals on *ad libitum* diets. These data are also of interest in interpreting excretion data to estimate dose or body burdens.

A large number of the heavy elements are known to localize in the skeleton. However, owing to the large quantity of $Ca_3(PO_4)_2$ the trace element determinations are more difficult on bone than soft tissues. Since different chemical procedures are needed, much attention has been directed to developing a procedure for the determination of trace elements in bone.

The results of this program are presented in the following sections. The data obtained from these studies will be incorporated with other data for estimating internal exposure to radionuclides.

LONG-TERM STUDY OF INTAKE AND EXCRETION OF STABLE ELEMENTS

Isabel H. Tipton Peggy Lou Stewart

Information on the daily elemental intake and excretion of individuals on their usual diets is difficult to obtain for various reasons. In general the published values for ordinary diets have been obtained from a population different from that for which the values for urine were obtained, which in turn are from a different population from that which provided the values for feces. Almost no information is available for the elemental intake and excretion for a set of the same individuals. Of course individual diets differ greatly even in a fairly homogeneous population, and the difference is even greater among different ethnic groups. In spite of these differences, however, it is reasonable to expect that for normal, adequately nourished human beings, the excretion after intake of an element should follow a general pattern which might be observed by studying the intake and excretion of a few individuals.

At the present time daily diets and excreta of three men are being studied. These men have been, and are, collecting duplicates of their daily diets and saving all excreta for a number of years for Dr. R. A. Kehoe's lead studies at Kettering Laboratory, Cincinnati, Ohio. Since September 1963 this material has been sent to the spectrographic laboratory at the University of Tennessee, where it has been stored frozen until methods for analysis were developed. Only two men participate in the study at one time. One of the men discontinued his part in the program in July 1966, and another man entered the program at that time. Data from a continuous period of such a long duration will allow statistical studies on the influence of time after intake, of intake of other elements, and of other factors on the excretion of an element.

So far analyses for two men for the interval between September 9, 1966, and January 7, 1967, have been completed. The data have been treated by two-month periods. This report includes period

[1]Analytical Chemistry Division.
[2]Physics Department, University of Tennessee.

1, September 9 through November 7, 1966, and period 2, November 8, 1966, through January 7, 1967.

Analytical methods appropriate to the element have been developed. That is, calcium, magnesium, potassium, and sodium have been analyzed by flame photometry; phosphorus by a colorimetric method; and aluminum, barium, beryllium, boron, chromium, cobalt, copper, iron, manganese, molybdenum, nickel, silver, strontium, tin, titanium, vanadium, zinc, and zirconium by emission spectroscopy. (Methods are being developed for analyzing zinc, cadmium, cesium, and rubidium by atomic absorption and lead by emission.) A detailed description of these methods is being prepared for publication. Only a summary indicating the range and precision of the method are included here.

Table 26.1 shows the range of concentrations (in micrograms per gram of dry ashed sample) of which the method is capable. In Table 26.2 an indication is given for the repeatability of the method. Column 1 gives the percent standard deviation for 23 elements resulting from 10 analyses of the same ashed sample of urine (the repeatability for food and feces is comparable). Column 2 shows the percent standard deviations of 7 elements in a sample of food carried 12 times through the entire method of ashing and analysis. For chromium, silver, zinc, and zirconium, the high background in the vicinity of the line contributes to the variability. Vanadium is a varying contaminant of the electrodes for which it is difficult to correct. Since the electrodes in which food samples are burned are different from those in which urine and feces are burned, a differential contamination may be found. Although the precision for beryllium is good in all three types of samples, it appears that this element

Table 26.1. Analytical Methods – Range of Concentration

Micrograms per gram of dry ash

Method	Element	Food		Urine		Feces	
		Low	High	Low	High	Low	High
Flame photometry	Ca	7,000	440,000	260	17,000	5,200	340,000
	Mg	2,100	92,000	260	12,000	5,200	230,000
	K	10,000	460,000	10,000	460,000	5,200	230,000
	Na	10,000	460,000	10,000	460,000	1,000	46,000
Colorimetry	P	10,000	200,000	4,200	84,000	25,000	500,000
Arc emission spectroscopy	Al	40	4,300	4	420	90	14,000
	Ba	1	700	1	200	10	1,400
	Be	0.5	10	0.1	10	0.1	10
	B	2	350	2	300	5	100
	Cr	1	120	2	200	8	300
	Co	0.5	60	1	150	5	125
	Cu	2.5	250	2	100	10	1,300
	Fe	50		5	1,100	100	8,000
	Mn	8	1,200	0.5	150	15	2,300
	Mo	0.2	75	0.5	50	0.5	90
	Ni	1	250	1	85	3	450
	Ag	0.3	100	0.1	20	0.5	125
	Sr	1	450	0.3	15	30	3,000
	Sn	3	1,800	2	85	15	4,000
	Ti	1	350	3	220	15	1,100
	V	1	50	0.5	75	3	120
	Zn	65	3,500	90	2,400	150	16,000
	Zr	1	450	5	800	0.5	525

Table 26.2. Repeatability of Methods

Percent standard deviation

Element	Analytical Method[a]	Total Method (Including Ashing)[b]
Ca	0.93	1.3
Mg	1.4	2.1
K	1.5	
Na	0.66	
P	2.3	
Al	4.3	9.4
Ba	3.1	7.2
Be	1.5	
B	8.4	
Cr	25	
Co	4.2	7.7
Cu	7.6	
Fe	3.3	6.9
Mn	3.1	
Mo	6.0	
Ni	6.0	7.5
Ag	13	
Sr	3.3	
Sn	6.8	
Ti	2.8	
V	6.7	
Zn	12	
Zr	11	

[a]Ten replicates of same sample of ash.

[b]Twelve replicates of same sample of wet material.

is sensitive to the gross composition of the material being analyzed, which is different for food, feces, and urine. These analytical difficulties may be a factor in the apparent imbalance of these elements in the diets and excreta of the two subjects.

With a few exceptions the values for the average daily intake and output over two two-month periods compare very well with the values suggested by the Task Group for Standard Man[3] and with the values for the male and female adult subjects reported by us earlier.[4] In general the disagreement occurs for those elements like vanadium and zirconium for which very little information is available (see Table 26.3).

A preliminary study has been made of the relation of the output of an element in urine to the intake of the same element in food for a period of time previous to the day of output for one individual (subject K-H). Urine values were used because it was assumed that any element appearing in the urine must, of necessity, have crossed the intestinal wall (except what had entered the body through absorption from the lung or through abrasions in the skin).

Multiple regressions have been run of the urinary output of all 23 elements with dietary intake of the element on the same day, the previous day, and two, three, four, five, and six days previous. The equation which predicts the urinary output on any day in terms of the intake of the previous week is

$$y = A + a_1x_1 + a_2x_2 + a_3x_3 + a_4x_4 + a_5x_5 + a_6x_6 + a_7x_7 ,$$

where y is the urinary output (μg), x_1, x_2, . . . , x_7 are the daily intake on the same day (x_1), previous day (x_2), two days previous (x_3), etc. (μg), a_1, . . . , a_7 are the partial regression coefficients, A is an added constant (μg) which indicates the amount of an element which would have been excreted if there had been no intake during the previous week.

Table 26.4 gives the values for the coefficients a_1, . . . , a_7 significantly different from zero at the 99% confidence level, the added constant A, the square of the multiple regression coefficient R, and values for the actual and predicted means for boron and nickel. For both elements it appears that the intake on the day previous may be reflected in the urinary excretion on any day. The values for R^2 indicate that about 20% of the variability in urinary output of these elements can be accounted for by the variability in the intake of the previous week.

For the seven-day lag period, very few elements had coefficients significantly different from zero or R^2 above 0.10. A preliminary study on calcium showed an increase in R^2 from 0.08 to 0.22 by increasing the time of lag from 7 to 14 days. It is obvious that longer periods of dietary intake must be investigated.

With the mass of information about the elemental intake and excretion of the same individual over a long period of time that this study provides, it will be possible to make statistical studies on rhythmic

[3]ICRP Task Group for Revision of Standard Man, report in preparation.

[4]I. H. Tipton *et al.*, *Health Phys.* 12, 1683 (1966).

ıtcke and Excretion of Individuals

ıms per day

K-S, ♂				K-H, ♂					
ıys	11-8-66 to 1-7-67, Period 2, 61 Days			9-9-66 to 11-7-66, Period 1, 60 Days			11-8-66 to 1-7-67, Period 2, 61 Days		
:s	Food	Urine	Feces	Food	Urine	Feces	Food	Urine	Feces
)00	13,000	590	14,000	8,700	1,100	8,800	15,000	580	27,000
ı10	520	4.3	590	540	17	590	440	2.8	530
6.8	430[b]	0.24	7.1	110[b]	0.77	10	98[b]	2.8	17
:40	2,000	800	490	1,400	2,300	390	700	990	350
)00	1,900,000	130,000	1,100,000	970,000	180,000	790,000	960,000	130,000	880,000
10	79	46	82	470[b]	86	87	73	53	67
57	580	210	23	220	290	32	360	310	23
)00	1,600	20	1,100	1,100	49	1,300	770	19	1,000
)00	23,000	540	9,000	16,000	1,700	18,000	14,000	1,100	14,000
)00	370,000	110,000	200,000	160,000	130,000	120,000	170,000	130,000	180,000
'00	3,300	23	3,900	2,800	63	3,400	2,200	9.4	4,100
70	1,400	300	210	170	140	140	520	200	220
;80	720	74	430	450	82	230	380	55	290
)00	3,300,000	1,100,000	560,000	1,900,000	1,600,000	560,000	1,700,000	1,200,000	460,000
)00	3,900,000	3,200,000	320,000	1,900,000	2,900,000	290,000	1,600,000	2,700,000	250,000
20	530[b]	11	180	90[b]	8.0	27	350[b]	8.9	59
)00	4,300,000[d]	5,000,000[d]	33,000	3,300,000[d]	5,300,000[d]	42,000	3,200,000[d]	4,700,000[d]	31,000
;90	2,000	58	1,500	1,200	110	1,100	1,500	140	1,200
)00	7,500	68	2,700	11,000	220	8,200	3,700	86	4,400
'70	1,600	370	310	690	410	400	790	250	430
:70	130	34	180	72[b]	32	150	69[b]	26	170
)00	18,000	1,600	17,000	12,000[b]	2,500	18,000	11,000[b]	1,400	15,000
,80	550	190	320	650[b]	160	170	580[b]	100	180

es a spurious negative balance for sodium. Both subjects have corrected this practice and in periods after May 1967 this false

Table 26.3. Mean Values for Intake and E

Micrograms per day

Element	T-P, ♀, 6-12-63 to 7-11-63, 30 Days[a]			T-V, ♂, 6-12-63 to 7-11-63, 30 Days[a]			K-S, ♂			
							9-9-66 to 11-7-66, Period 1, 60 Days			11
	Food	Urine	Feces	Food	Urine	Feces	Food	Urine	Feces	F
Al	18,000	1,000	17,000	22,000	1,000	45,000	11,000	880	12,000	1
Ba	1,800	280	600	1,500	560	1,800	570	11	610	
Be							93[b]	1.2	6.8	
B	420	560	14	350	590	10	1,800	1,100	340	
Ca	760,000	140,000	400,000	1,310,000	200,000	920,000	1,600,000	160,000	890,000	1,90
Cr	330	100	10	400	200	160	740[b]	120	110	
Co	170	190	40	160	140	60	210	330	57	
Cu	1,000	330	710	910	320	1,000	1,500	94	1,600	
Fe				15,000	400	14,000	60,000[c]	1,900	10,000	2
	12,000	2,000	9,000							
Mg	280,000	4,000	150,000	320,000	8,000	190,000	260,000	120,000	140,000	37
Mn	4,400	250	1,200	3,500	320	2,600	3,800	57	2,700	
Mo	99	150	38	100	71	42	490	140	170	
Ni	330	170	110	170	92	140	1,100	140	380	
P	1,200,000	1,000,000	320,000	1,800,000	1,320,000	470,000	2,900,000	1,400,000	600,000	3,3C
K							3,100,000	3,000,000	240,000	3,9C
Ag	44	9	28	35	10	79	340[b]	4.8	120	
Na							4,200,000[d]	5,000,000[d]	28,000	4,3C
Sr	1,400	240	810	1,200	420	970	1,100	110	890	
Sn	1,500	110	2,100	2,500	80	1,600	10,000	100	7,000	
Ti	370	300	340	680	310	890	1,000.	370	770	
V							120[b]	40	270	
Zn							16,000[b]	2,500	23,000	1
Zr							1,200[b]	92	180	

[a] I. H. Tipton *et al.*, *Health Phys.* 12, 1683 (1966).

[b] The apparent imbalance may be due to analytical problems. See text.

[c] Median value was 18,000.

[d] Both subjects, but especially H, were careless about salting the duplicate meal as well as the one consumed. This gives a spurio negative balance should not occur.

Table 26.4. Regression Equations for Predicting Urinary Output from Dietary Intake: Subject K-H

Coefficients significantly different from zero at $p \leq 0.01$ unless indicated otherwise

		Boron		Nickel	
		Period 1	Period 2	Period 1	Period 2
Days previous	Coefficient				
0	a_1				
1	a_2	0.40[a]	0.32	0.79	0.063
2	a_3				
3	a_4			0.53[b]	
4	a_5				
5	a_6				
6	a_7				
Constant A (μg)		1800	870	28	29
R^2		0.24	0.14	0.27	0.14
Actual mean (μg)		2300	990	83	54
Standard deviation		2100	820	75	71
Predicted mean (μg)		2300	980	83	55
Standard error of estimate		1900	810	68	71

[a] $p < 0.001$.
[b] $p < 0.05$.

variations in excretion patterns of elements and to develop mathematical models relating intake and excretion of a number of elements.

TISSUE ANALYSIS LABORATORY

Cyrus Feldman F. S. Jones

Because bone is one of the most difficult tissues to analyze for trace elements, attention has been directed to improving the overall sensitivity for the detection of trace elements by developing a chemical preconcentration procedure.

The Mitchell-Scott procedure (precipitation of trace elements with a mixture of 8-OH quinoline, tannic acid, and thionalide) was selected for investigation. This procedure proved quite effective for collecting several trace elements, but was ineffective with others (e.g., Mn). It was sometimes difficult to prevent the precipitation of substantial amounts of $Ca_3(PO_4)_2$ along with the trace elements, especially under the conditions necessary to precipitate chromium.

Attempts to circumvent the coprecipitation problem by extracting the trace elements from solutions of bone ash were successful for only a few elements. The presence of phosphate again hampered extractions which would otherwise have been successful. It was therefore decided that the development of a general collection procedure would be greatly facilitated by first eliminating phosphate from the sample.

The most straightforward way to do this in this case would be to adsorb all of the cations on a cation exchange column, allowing the phosphate to pass through the column. However, treating a large sample of bone ash by this method would require a large amount of resin. The resulting reagent blanks would probably defeat the purpose

of the procedure, and a great many studies of trace element recovery would be needed.

It was decided instead to try to remove the phosphate by electrodialysis through anion-permeable resin membranes. This approach would permit the handling of large samples without a commensurate increase in contamination. Although other anions besides phosphate would be removed, few of these are of interest in the present case.

A three-compartment cell was prepared, and the sample (a slightly acid solution of natural or synthetic bone ash) was placed in the center compartment. To avoid problems connected with migration of cations through a cation-permeable membrane and deposition of such ions on the cathode, both walls of the center chamber were made of anion-permeable (i.e., cation-impermeable) resin membrane. The acid used to dissolve the bone ash had to be strong enough to accomplish this dissolution, yet weak enough to leave most of the phosphate in the form of an anion (e.g., $H_2PO_4^-$) rather than the neutral H_3PO_4. The anions of this acid also had to have a relatively low affinity for the anionic resin; the acid itself had to be easily purified and easily eliminated from the solution after processing. Formic acid fulfilled these requirements and was chosen as the solvent. A solution of the formic acid was also placed in the cathode chamber, and a solution of NaOH in the anode chamber. Electrodialysis was carried out at ~20 v, 600 to 700 ma. Migration of phosphate ions toward the anode tended to increase their concentration near the anode compartment wall. Since this favored their migration through the membrane, we refrained from stirring the solution in the center compartment.

Tracer experiments showed that the concentration of phosphorus in the center cell decreased almost exponentially with time. Performance of the cell was therefore measured in terms of the "half-life," that is, the time required to reduce the phosphorus concentration in the center cell to one-half its previous value. Typical results are given in Table 26.5. Unless otherwise noted, the sample consisted of 1 g of $Ca_3(PO_4)_2$ dissolved in 5 ml of HCOOH, pH adjusted to 3, with 10% HCOOH in the anode compartment and 1 *N* NaOH in the cathode compartment. Under the last-named conditions in Table 26.5, less than 4% of the original phosphate remained after 6 hr. This degree of removal proved adequate to permit use of the Mitchell-Scott chemical collection procedure and made it possible to improve the procedure's efficiency for the collection of manganese and chromium. This procedure will now be applied to bone ash and tested for the recovery of trace elements.

Table 26.5. Removal of Phosphate from Calcium Phosphate Solution by Electrodialysis Through Anion Exchange Membrane

Voltage (v)	Current (ma)	Time to Reduce PO_4 by Half (min)	Conditions
10	140–70	820	All compartments stirred
10	135–88	500	Center compartment not stirred
23	365–160	320	
23	410–60	270	20% HCOOH in anode compartment
23	650	80	Same as above; center compartment heated to 65–70°

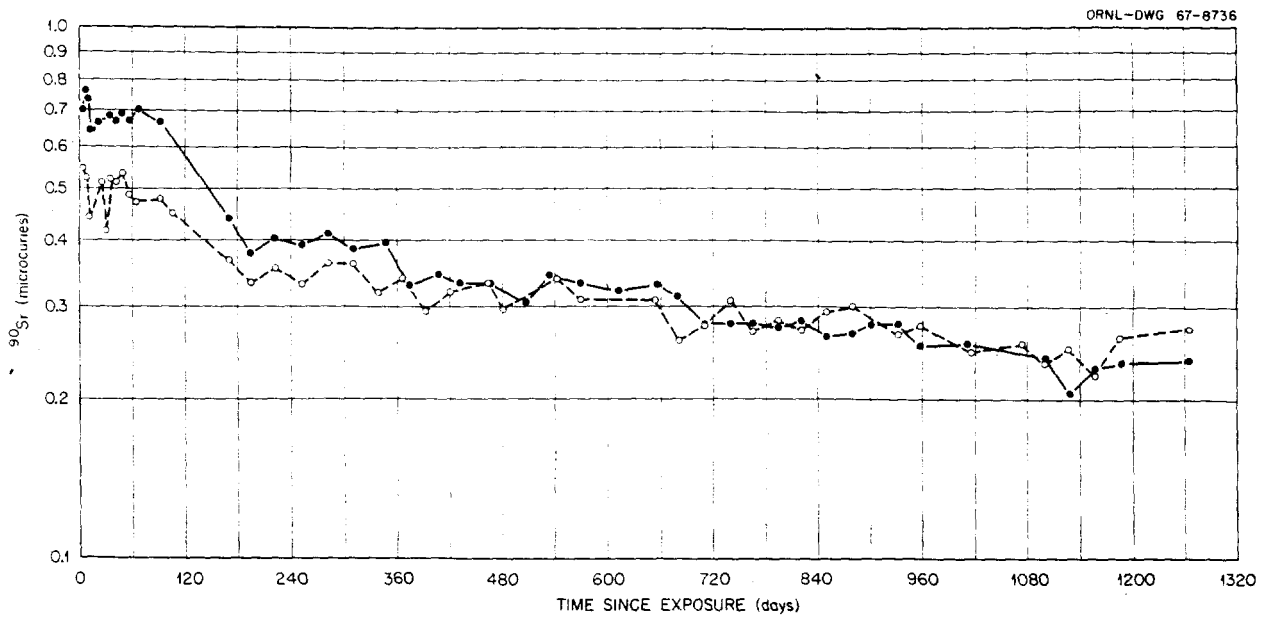

Fig. 28.1. Estimated Lung Burden of Two Subjects Inhaling $^{90}SrTiO_3$.

IN VIVO DETECTION AND MEASUREMENT OF ^{90}Sr-^{90}Y INTERNAL CONTAMINATION

G. R. Patterson, Jr. P. E. Brown

The two employees whose exposure in 1964 to $^{90}SrTiO_3$ by inhalation was reported earlier[5] still are being counted at about one-month intervals using the 8 × 4 in. lead-collimated NaI(Tl) crystal. The estimated chest burdens for these two em-

has the higher whole-body burden, although this is not the case for the chest-burden estimates.

On September 2, 1966, despite procedural changes that were intended to prevent recurrence of such exposures, three more persons were exposed to $^{90}SrTiO_3$ contamination during a similar waste-disposal operation. In this case, the person receiving the highest indicated intake was estimated to have approximately 0.57 μc of ^{90}Sr at the time of his first count, only 1½ hr after the incident.

At that time, an arc count was made using an 8 × 4 in. NaI(Tl) crystal. The face of the crystal was 6 ft from the subject, which is the maximum distance possible in the existing iron room. A scan was made using a 1 × 1 in. NaI(Tl) crystal, collimated with 2 in. of lead (Fig. 28.2). This showed the activity to be located, principally, in the liver-kidney area.

For the next 140 days counting was done using the 6-ft arc position to determine body burden (Fig. 28.3). After that time both arc and scan counts were made. The effective half-life was observed to be 25 days during this time (day 30 to day 190). Based on this, the estimated biological half-life was 54 days. From day 40, liver and kidney counts were made with the 1 × 1 in. collimated counter. Calibrations and correction factors were determined by placing sources in the liver and kidney sections of a water-filled plastic mannikin. Effective half-lives were found to be about 24 days for activity in the liver and about 53 days in the kidney.

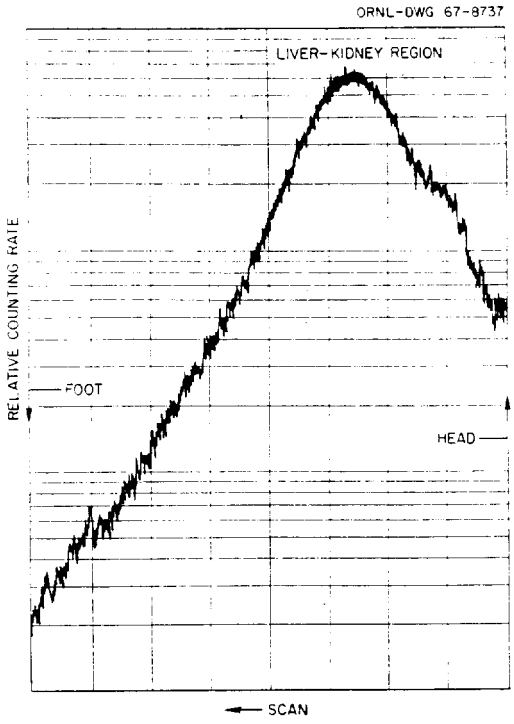

Fig. 28.2. Typical Scan Profile 50 Days After Intravenous Injection of ^{203}Hg.

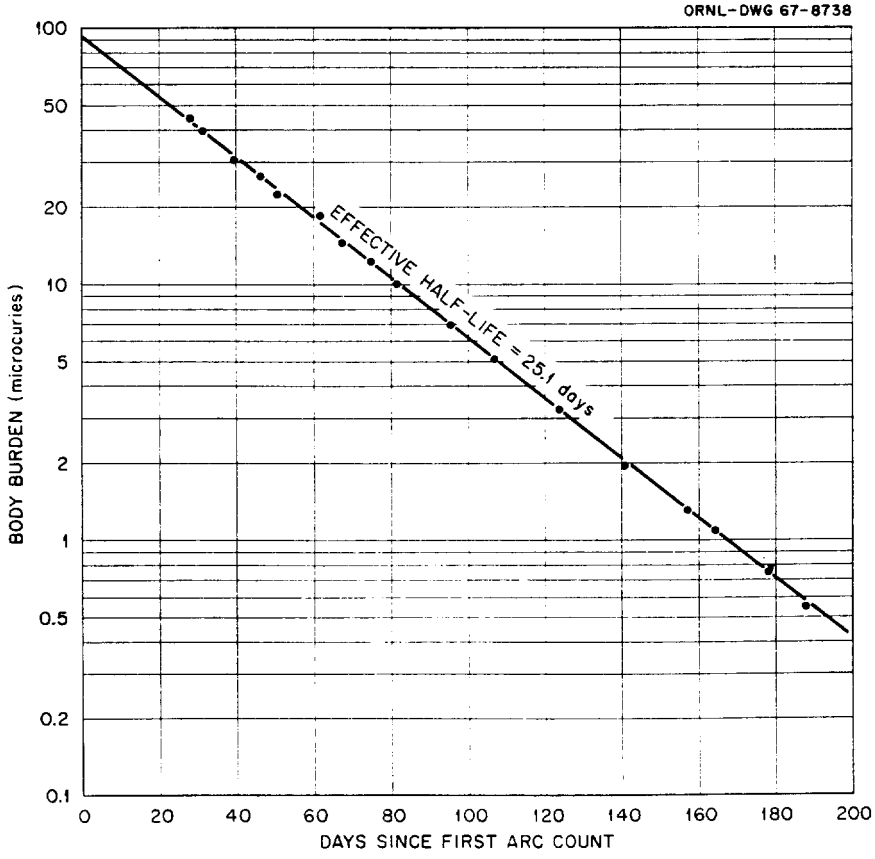

Fig. 28.3. Body Burden of ^{203}Hg Following Intravenous Injection.

Theses, Papers, Publications, and Lectures

Theses

Scott Cram, E. T. Arakawa, G. E. Jones, and R. D. Birkhoff
Transition Radiation and Low-Energy Bremsstrahlung from Silver and Aluminum Foils Bombarded by Grazing Incidence Electrons, ORNL-TM-1571 (September 1966).

Patricia Dalton and J. E. Turner
Mean Excitation Energies Calculated from Stopping Power and Range Data, ORNL-TM-1777 (June 1967).

H. W. Dickson, L. G. Christophorou, and R. N. Compton
Electron Capture by Hydrogen Halides and Their Deuterated Analogues, ORNL-TM-1724 (June 1967).

J. D. Hayes and E. T. Arakawa
The Optical Properties of Vacuum-Evaporated Films of Tellurium and Amorphous Selenium (in preparation).

W. G. Hendrick, L. G. Christophorou, and G. S. Hurst
An Apparatus for Measurement of Electron Capture at High Temperatures, ORNL-TM-1444 (in preparation).

Larry Johnson and H. C. Schweinler
Oscillator Strength in Magnesium Porphin (in preparation).

S. J. Nalley, M. Y. Nakai, F. W. Garber, R. H. Ritchie, and R. D. Birkhoff
Low-Energy Electron Studies in Aluminum (in preparation).

Margaret S. Riedinger and L. C. Emerson
The Determination of the Optical Properties of Palladium Using Ellipsometry (in preparation).

M. U. Shaikh, D. G. Jacobs, and F. L. Parker
A Study of the Movement of Radionuclides Through Saturated Porous Media, ORNL-TM-1681 (January 1967).

J. L. Stanford, E. T. Arakawa, and R. D. Birkhoff
Photoelectric and Optical Properties of Commercial Platinum, Gold, and Palladium Foils and Evaporated Aluminum and Silver Films in the Extreme Ultraviolet, ORNL-TM-1392 (September 1966).

G. F. Stone and J. H. Thorngate
Experimentally Determined Proton-Recoil Spectra in Tissue-Equivalent Material from 3 and 14 Mev Neutrons, ORNL-TM-1927 (in preparation).

J. C. Sutherland, R. N. Hamm, J. R. Stevenson, and E. T. Arakawa
Optical Properties of Sodium in the Vacuum Ultraviolet, ORNL-TM-1776 (June 1967).

W. A. Thomas, S. I. Auerbach, and J. S. Olson
Accumulation and Cycling of Calcium by Flowering Dogwood Trees, ORNL-TM-1910 (in press).

L. H. Toburen, M. Y. Nakai, R. G. Albridge, R. A. Langley, C. F. Barnett, and R. D. Birkhoff
Part I. The Measurement of High-Energy Charge-Transfer Cross Sections for Incident Hydrogen Atoms and Ions in Various Gases. Part II. The K-, L-, and M-Auger, L-Coster-Kronig and the Conversion-Electron Spectra of Platinum in the Decay of ^{195}Au (in preparation).

H. A. Wright and W. S. Snyder
Differentiability of Set Functions (in preparation).

Papers

E. T. Arakawa, J. L. Stanford, and R. D. Birkhoff
Photoemission Studies in Evaporated Aluminum Films in the Vacuum Ultraviolet, Optical Society of America, October 19–21, 1966, San Francisco, California.

E. T. Arakawa and M. W. Williams
Optical Properties of Sapphire in the Vacuum UV, American Physical Society, April 24–27, 1967, Washington, D.C.

J. C. Ashley
Double-Plasmon Excitation by Charged Particles, American Physical Society, August 29–31, 1966, Mexico City, Mexico.

J. A. Auxier
The Present Status of Neutron Monitoring for Personnel Protection, Symposium on Neutron Monitoring for Radiological Protection, August 29–September 2, 1966, Vienna, Austria.

Multilaboratory Intercomparisons of Neutron Dosimetry Systems, Symposium on Neutron Monitoring for Radiological Protection, August 29–September 2, 1966, Vienna, Austria.

J. A. Auxier and M. D. Brown
Neutron Cross Sections and Reaction Products for H, C, N, and O for the Energy Range from Thermal to 15 Mev, First International Congress of the International Radiation Protection Association, September 5–10, 1966, Rome, Italy.

J. A. Auxier, C. N. Wright, and C. M. Unruh
General Considerations in Nuclear Accident Dosimetry and Standardization, Health Physics Society First Topical Symposium on Personnel Radiation Dosimetry, January 30–February 1, 1967, Chicago, Illinois.

J. Baarli, St. Charalambus, J. Dutrannois, K. Goebel, H. H. Hubbell, T. R. Overton, A. Rindi, and A. H. Sullivan
Hazard from Induced Radioactivity near High Energy Accelerators, Conference on Radiological Protection of the Worker by the Design and Control of His Environment, April 18–22, 1966, Bournemouth, England.

R. D. Birkhoff, W. J. McConnell, R. N. Hamm, and R. H. Ritchie
Electron Flux Spectra in Aluminum – Analysis for Linear Energy Transfer Spectra and Excitation and Ionization Yields, AEC Symposium on Biological Interpretation of Dose from Accelerator-Produced Radiation, March 13–16, 1967, Berkeley, California.

R. P. Blaunstein, L. G. Christophorou, and R. N. Compton
Electron Capture by Organic Molecules, Health Physics Society, June 19–21, 1967, Washington, D.C.

B. G. Blaylock
The Effect of Ionizing Radiation on Competition Between Drosophila melanogaster *and* Drosophila simulans, The Genetics Society of America, September 1–3, 1966, Chicago, Illinois.

The Effect of Ionizing Radiation on Interspecific Competition, The Second National Symposium on Radioecology, May 15–17, 1967, Ann Arbor, Michigan.

R. L. Bradshaw
Rheology of Salt in Mine Workings, Symposium on the Geology and Technology of Gulf Coast Salt, May 1–2, 1967, Louisiana State University, Baton Rouge, Louisiana.

R. L. Bradshaw, T. F. Lomenick, W. C. McClain, and F. M. Empson
Model and Underground Studies of the Influence of Stress, Temperature, and Radiation on Flow and Stability in Salt Mines, International Society of Rock Mechanics, First International Congress, September 25–October 1, 1966, Lisbon, Portugal (presented by T. F. Lomenick).

J. G. Carter, L. G. Christophorou, R. D. Birkhoff, and J. W. Pagel
Organic Scintillators with 2-Ethyl Naphthalene as a Solvent, American Physical Society, December 1–3, 1966, Nashville, Tennessee.

L. G. Christophorou
Interaction of Low-Energy Electrons with Polyatomic Molecules, American Physical Society, December 1–3, 1966, Nashville, Tennessee.

L. G. Christophorou, J. G. Carter, and M-E. M. Abu-Zeid
Optical Emission from Organic Liquids Excited by Electron Impact, Radiation Research Society, May 7–11, 1967, San Juan, Puerto Rico.

L. G. Christophorou, G. S. Hurst, and W. G. Hendrick
Swarm Determination of the Cross Section for Momentum Transfer in Ethylene and in Ethylene Mixtures, 19th Annual Gaseous Electronics Conference, October 12–14, 1966, Atlanta, Georgia.

R. N. Compton and L. G. Christophorou
Negative Ion Formation and Electronic Excitation by Electron Impact in H_2O and D_2O, American Physical Society, December 1–3, 1966, Nashville, Tennessee.

R. N. Compton, L. G. Christophorou, G. S. Hurst, and P. W. Reinhardt
Temporary Negative Ion Formation in Complex Molecules, 19th Annual Gaseous Electronics Conference, October 12–14, 1966, Atlanta, Georgia.

R. N. Compton, R. H. Huebner, L. G. Christophorou, and P. W. Reinhardt
Low-Energy Electron Impact Phenomena in Organic Molecules, Radiation Research Society, May 7–11, 1967, San Juan, Puerto Rico.

K. E. Cowser, Jacob Tadmor, D. G. Jacobs, and W. J. Boegly, Jr.
Evaluation of Environmental Hazards from Release of Krypton-85 and Hydrogen-3 in an Expanding Nuclear Fuel Reprocessing Industry, Health Physics Society Meeting, Washington, D.C., June 18–22, 1967.

D. A. Crossley, Jr.
Tracers in Insect Biology and Ecology, Symposium on Application of Radioisotopes and Ionizing Radiation in Entomology, March 27, 1967, Baton Rouge, Louisiana.

Comparative Movement of ^{106}Ru, ^{60}Co, and ^{137}Cs in Arthropod Food Chains, Second National Symposium on Radioecology, May 15–17, 1967, Ann Arbor, Michigan.

J. W. Curlin
Root Dose from Gamma and Fast Neutron Irradiation of Potted Plants, AIBS Annual Meeting, August 14–19, 1966, College Park, Maryland.

Genetic Differences in Growth Response of Eastern Cottonwood to Nitrogen Fertilization, Soil Science Society of America Annual Meeting, August 21–26, 1966, Stillwater, Oklahoma.

The Use of Radioisotopes in Forest Soils Research, Southern Forest Soils Conference, August 30–31, 1966, Greenville, Mississippi.

Mineral Cycling Research at Oak Ridge National Laboratory, Northwest Forest Soils Workshop, September 16, 1966, Seattle, Washington.

R. C. Dahlman
Carbon-14 Cycling in the Root and Soil Components of a Prairie Ecosystem, Second National Symposium on Radioecology, May 15–17, 1967, Ann Arbor, Michigan.

D. R. Davy
Prediction of Biological Damage from Stopping Power Theory, Sixth Annual Meeting of Physics in Medicine and Biology, August 29–September 2, 1966, Melbourne, Australia.

P. B. Dunaway, L. L. Lewis, J. A. Payne, and J. D. Story
Effects of Acute Ionizing Irradiation in Indigenous Rodents and Shrews, Third International Congress of Radiation Research, June 26–July 2, 1966, Cortina, Italy.

P. B. Dunaway, L. L. Lewis, J. D. Story, J. A. Payne, and J. M. Inglis
Radiation Effects in the Soricidae, Cricetidae, and Muridae, Second National Symposium on Radioecology, May 15–17, 1967, Ann Arbor, Michigan.

L. C. Emerson
Vacuum Ultraviolet Studies of Energy Losses in Solids, American Physical Society, December 1–3, 1966, Nashville, Tennessee.

L. B. Farabee
Improved Procedure for Radiostrontium Analysis of Human Urine, The 12th Annual Bio-Assay and Analytical Chemistry Meeting, October 13–14, 1966, Gatlinburg, Tennessee.

B. R. Fish
Electrostatic Forces of Adhesion Between Particles, Symposium on Electrostatic Effects Associated with Dried Powders, April 25–26, 1967, Fort Detrick, Maryland.

Electrostatic Deposition and Adhesion of Particles on Surfaces, American Association for Contamination Control, Sixth Annual Technical Meeting, May 15–18, 1967, Washington, D.C.

H. L. Fisher, Jr.
Distribution of Dose in the Body from a Source of Gamma Rays Distributed Uniformly in an Organ, First International Congress on Radiation Protection, September 5–10, 1966, Rome, Italy.

An Age-Dependent Model for the Bodily Retention of Cesium, 12th Annual Bioassay and Analytical Chemistry Meeting, October 13–14, 1966, Gatlinburg, Tennessee.

Kenneth Fox, J. E. Turner, and V. E. Anderson
Some Ground-State Energy Eigenfunctions for an Electron-Dipole System, American Physical Society, June 21–23, 1967, Toronto, Ontario.

W. R. Garrett
Elastic Scattering of Electrons by $1s^2 2s^2 2p^q$ *Atoms*, 19th Annual Gaseous Electronics Conference, October 12–14, 1966, Atlanta, Georgia.

L. W. Gilley, L. B. Holland, J. W. Poston, and D. R. Ward
Operation Problems with the Health Physics Research Reactor, American Nuclear Society, June 1966, Denver, Colorado (presented by L. B. Holland).

R. N. Hamm, R. H. Ritchie, and J. C. Ashley
Electron Mean Free Paths in a Free Electron Gas, American Physical Society, August 29–31, 1966, Mexico City, Mexico.

H. Hollister and J. E. Turner
On the Relationship of RBE to LET, Health Physics Society, June 19–21, 1967, Washington, D.C.

R. H. Huebner, R. N. Compton, and L. G. Christophorou
Temporary Negative Ion Resonances in Benzene Derivatives, American Physical Society, December 1–3, 1966, Nashville, Tennessee.

T. D. Jones, J. A. Auxier, J. W. Poston, and D. R. Johnson
Dose Distribution Functions for Neutrons and Gamma Rays in Anthropomorphous and Radiological Phantoms, First International Congress of the International Radiation Protection Association, September 5–10, 1966, Rome, Italy.

S. V. Kaye
The Specific Activity Concept and Internal Dosimetry, Bioenvironmental Subcontractors Meeting for Sea-Level Canal Studies, November 15–17, 1966, Columbus, Ohio.

Environmental Pathways and Internal Dosimetry, Bioenvironmental Subcontractors Meeting for Sea-Level Canal Studies, November 15–17, 1966, Columbus, Ohio.

Distribution and Retention of Orally Administered Radiotungsten in the Rat, Health Physics Society, June 18–22, 1967, Washington, D.C.

S. V. Kaye and S. J. Ball
A Coupled Compartment Model for Radionuclide Transfer in a Tropical Environment, Second National Symposium on Radioecology, May 15–17, 1967, Ann Arbor, Michigan.

G. D. Kerr and J. S. Cheka
Developments in Metaphosphate Glass Dosimetry, Health Physics Society First Topical Symposium on Personnel Radiation Dosimetry, January 30–February 1, 1967, Chicago, Illinois.

G. D. Kerr and D. R. Johnson
Comparison of Radiation Dosimeters at the Health Physics Research Reactor, Health Physics Society, June 18–22, 1967, Washington, D.C.

C. E. Klots
The Optical Approximation in Radiation Chemistry, Chemistry Section, National Bureau of Standards, June 23, 1967, Washington, D.C.

C. E. Klots and J. E. Turner
Factors Involved in the Construction of Useful Degradation Spectra, Radiation Research Society, May 7–11, 1967, San Juan, Puerto Rico.

T. F. Lomenick and O. C. Kopp
Thermal Effects and Stratigraphic Relations on the Deformation of Rock Salt, Annual Meeting of the Geological Society of America, November 14–16, 1966, San Francisco, California.

W. C. McClain
The Effect of Nonelastic Behavior of Rocks, Eighth Symposium on Rock Mechanics, September 14–17, 1966, Minneapolis, Minnesota.

Hydraulic Fracturing as a Waste Disposal Method, IAEA Symposium on Disposal of Radioactive Wastes into the Ground, May 29–June 2, 1967, Vienna, Austria.

W. C. McClain, R. L. Bradshaw, and F. M. Empson
Disposal of High Level Solidified Wastes in Salt Mine, IAEA Symposium on Disposal of Radioactive Wastes into the Ground, May 29–June 2, 1967, Vienna, Austria.

K. Z. Morgan
Development of Health Physics as a Profession, First International Congress on Radiation Protection, September 5–10, 1966, Rome, Italy.

A Comparison and Evaluation of Various Radiation Hazards in Metropolitan Areas, Second Symposium on Health Physics, September 26–30, 1966, Pecs, Hungary.

L. D. Mullins and W. R. Garrett
l-Averaged Exchange Term in the Hartree-Fock Equations, American Physical Society, December 1–3, 1966, Nashville, Tennessee.

D. J. Nelson
Ecological Behavior of Radionuclides in Surface Waters, Reservoir Fishery Resources Symposium, April 5–7, 1967, Athens, Georgia.

Cesium, Cesium-137, and Potassium Concentrations in White Crappie and Other Clinch River Fish, Second National Symposium on Radioecology, May 15–17, 1967, Ann Arbor, Michigan.

J. Neufeld, V. E. Anderson, H. A. Wright, and J. E. Turner
Effects of Phantom Geometry on Dose Distribution, First International Congress of the International Radiation Protection Association, September 5–10, 1966, Rome, Italy.

J. S. Olson
Energy Flow into Deciduous Forests, Second National Symposium on Radioecology, May 15–17, 1967, Ann Arbor, Michigan.

B. C. Patten
Kinetics of ^{134}Cs in Carp, Second National Symposium on Radioecology, May 15–17, 1967, Ann Arbor, Michigan.

H. L. Pray, M. Y. Nakai, and R. D. Birkhoff
Low-Energy Electron Studies in Indium and Magnesium, American Physical Society, December 1–3, 1966, Nashville, Tennessee.

J. R. Reed and D. J. Nelson
Radiostrontium Uptake in Blood and Flesh in Bluegills (Lepomis macrochirus), Second National Symposium on Radioecology, May 15–17, 1967, Ann Arbor, Michigan.

D. E. Reichle and D. A. Crossley, Jr.
Investigations on Heterotrophic Productivity in Forest Insect Communities, Working Meeting on the Principles and Methods of Secondary Productivity in Terrestrial Ecosystems, September 1966, Warsaw, Poland.

Trophic Level Concentrations of Cesium-137, Sodium, and Potassium in Forest Arthropods, Working Meeting on the Principles and Methods of Secondary Productivity in Terrestrial Ecosystems, September 1966, Warsaw, Poland.

S. W. Riggs, J. C. Ashley, L. S. Cram, and E. T. Arakawa
Photon Emission from Al Foils Bombarded by Non-Normally Incident Electrons, American Physical Society, December 1–3, 1966, Nashville, Tennessee.

R. H. Ritchie and W. S. Snyder
Estimation of Dose Distribution Within the Body Resulting from the Y-12 and Vinca Criticality Incidents, IAEA Symposium on Neutron Monitoring for Radiological Protection, August 29–September 2, 1966, Vienna, Austria.

L. L. Robinson, L. C. Emerson, J. G. Carter, and R. D. Birkhoff
Optical Properties of Liquid Water in the Vacuum Ultraviolet, American Physical Society, December 1–3, 1966, Nashville, Tennessee.

A. S. Rogowski and Tsuneo Tamura
Runoff and Erosion Losses of Radiocesium on Captina Silt Loam, Meeting of American Society of Agronomy, August 22–26, 1966, Stillwater, Oklahoma.

W. S. Snyder
Health Physics Aspects of Supersonic Transport, First International Congress on Radiation Protection, September 5–10, 1966, Rome, Italy.

The Use of the Lung Model for Estimation of Dose, 12th Annual Bioassay and Analytical Chemistry Meeting, October 13–14, 1966, Gatlinburg, Tennessee.

Estimation of Internal Dose, AEC Health Protection Meeting, February 14–15, 1967, Albuquerque, New Mexico.

Distribution of Dose in the Body from HTO, Symposium on Instrumentation, Experience, and Problems in Health Physics Tritium Control, February 16–17, 1967, Albuquerque, New Mexico.

Dose Estimation in the Context of Health Physics Regulations and Responsibilities, First International Symposium on the Biological Interpretation of Dose from Accelerator Produced Radiation, March 13–16, 1967, Berkeley, California.

The Use of Excretion Data to Predict the Systemic Body Burden of Plutonium, Symposium on Diagnosis and Treatment of Deposited Radionuclides, May 15–17, 1967, Richland, Washington.

W. S. Snyder, J. A. Auxier, M. D. Brown, T. D. Jones, and R. T. Boughner
Distribution of Dose and Dose Equivalent in an Anthropomorphic Phantom Resulting from Broad-Beam Sources of Monoenergetic Neutrons, American Nuclear Society Winter Meeting, October 30–November 3, 1966, Pittsburgh, Pennsylvania.

J. A. Stockdale and L. G. Christophorou
Molecular Scattering of Thermal Electrons, Radiation Research Society, May 7–11, 1967, San Juan, Puerto Rico.

E. G. Struxness

Ultimate Disposal of Radioactive Wastes, 6th Annual Sanitary and Water Resources Engineering Conference, Vanderbilt University, School of Engineering, June 1, 1967, Nashville, Tennessee.

Permanent Disposal of Radioactive Wastes, 2nd National Symposium on Radioecology, May 15–17, 1967, Ann Arbor, Michigan.

J. C. Sutherland and E. T. Arakawa

Extinction Coefficient, k, and Imaginary Part of the Dielectric Constant, ϵ_2, of Sodium in the Vacuum Ultraviolet, American Physical Society, April 24–27, 1967, Washington, D.C.

J. C. Sutherland, R. N. Hamm, and E. T. Arakawa

Computer Calculations of Phase Changes upon Reflection from an Absorbing Layer, American Physical Society, December 1–3, 1966, Nashville, Tennessee.

Jacob Tadmor and K. E. Cowser

Underground Disposal of ^{85}Kr from Nuclear Fuel Reprocessing Plants, American Nuclear Society Thirteenth Annual Meeting, June 11–15, 1967, San Diego, California.

F. G. Taylor, Jr.

Predicted Seasonal Radiosensitivity of Southeastern Tree Species, American Institute of Biological Sciences, August 14–19, 1966, College Park, Maryland.

Factors Which Affect Prediction and Assessment of Radiosensitivity in Higher Plants, Tennessee Academy of Science, November 25–26, 1966, Johnson City, Tennessee.

Nuclear Characteristics of Populus deltoides *Clones*, Association of Southeastern Biologists, April 20–22, 1967, Columbia, South Carolina.

W. A. Thomas

Cycling of ^{45}Ca by Dogwood Trees, Second National Symposium on Radioecology, May 15–17, 1967, Ann Arbor, Michigan.

J. H. Thorngate

Dosimetry, Shielding, and Scattering II, Conference on Principles of Radiation Protection, August 24–26, 1966, Oak Ridge, Tennessee.

Isabel H. Tipton, Judy C. Johns, and Monica Boyd

The Variation with Age of Elemental Concentration in Human Tissue, First International Congress on Radiation Protection, September 5–10, 1966, Rome, Italy.

L. H. Toburen, R. A. Langley, C. F. Barnett, R. D. Birkhoff, and M. Y. Nakai

Charge Exchange Cross Sections for Incident Atomic Hydrogen in Various Gases, American Physical Society, December 1–3, 1966, Nashville, Tennessee.

L. H. Toburen, M. Y. Nakai, and R. A. Langley

Charge Exchange Cross Sections for High Energy Protons and Atomic Hydrogen in Gases, American Physical Society, January 30–February 2, 1967, New York.

J. E. Turner

Penetration of Heavy Charged Particles in Matter, American Physical Society, December 1–3, 1966, Nashville, Tennessee.

J. E. Turner and Kenneth Fox

Minimum Dipole Moment to Bind an Electron to a Finite Dipole, American Physical Society, December 1–3, 1966, Nashville, Tennessee.

Ground-State Energy Eigenvalues and Eigenfunctions for Electron-Dipole System, Radiation Research Society, May 7–11, 1966, San Juan, Puerto Rico.

J. E. Turner, V. E. Anderson, H. A. Wright, W. S. Snyder, and J. Neufeld

Dose from High Energy Radiations in an Interface Between Two Media, AEC Symposium on Biological Interpretation of Dose from Accelerator-Produced Radiation, March 13–16, 1967, Berkeley, California.

R. C. Vehse and E. T. Arakawa
Optical and Photoelectric Properties of Thin Palladium Films in the Far Ultraviolet, American Physical Society, December 1–3, 1966, Nashville, Tennessee.

R. E. Wilems and R. H. Ritchie
Nonlinear Interactions in Bounded Quantum Plasmas, American Physical Society, April 24–27, 1967, Washington, D.C.

The Surface Photoeffect and Surface Secondary Emission from Metal Foils, American Physical Society, December 1–3, 1966, Nashville, Tennessee.

W. H. Wilkie and B. R. Fish
Scintillation Extrapolation Dosimetry of Small Beta-Emitting Sources, Symposium on Solid-State and Chemical Radiation Dosimetry in Medicine and Biology, October 3–7, 1966, Vienna, Austria.

M. W. Williams and E. T. Arakawa
Optical Properties of Single-Crystal MgO, American Physical Society, April 24–27, 1967, Washington, D.C.

M. W. Williams, E. T. Arakawa, and L. C. Emerson
Photon Excitation of Surface Plasmons: Analysis of Data for Al, American Physical Society, December 1–3, 1966, Nashville, Tennessee.

J. P. Witherspoon
Radiosensitivity of Clones of Eastern Cottonwood, American Institute of Biological Sciences, August 14–19, 1966, College Park, Maryland.

Interactions of Fast Neutron Radiation and Growth-Dormancy Cycles in Yellow Poplar Trees, Association of Southeastern Biologists, April 20–22, 1967, Columbia, South Carolina.

Genetic Factors Relating to Radiosensitivity of Populations, Health Physics Society, June 18–22, 1967, Washington, D.C.

Martin Witkamp and M. L. Frank
Cesium-137 Kinetics in Terrestrial Microcosms, Second National Symposium on Radioecology, May 15–17, 1967, Ann Arbor, Michigan.

H. A. Wright, E. E. Branstetter, Jacob Neufeld, J. E. Turner, and W. S. Snyder
Calculation of Radiation Dose Due to High-Energy Protons, First International Congress of the International Radiation Protection Association, September 5–10, 1966, Rome, Italy.

H. A. Wright, J. E. Turner, J. Neufeld, and W. S. Snyder
Calculation of Radiation Dose from High-Energy Nucleons, Health Physics Society, June 19–21, 1967, Washington, D.C.

Edward Yeargers
Ultraviolet Light Effects on Proteins, Symposium on Biologic Effects of Ultraviolet, August 23–26, 1966, Philadelphia, Pennsylvania.

Publications

V. E. Anderson and R. H. Ritchie
Fourier Transform Methods in the Unfolding of Experimental Data, ORNL-TM-1261 (June 1967).

J. C. Ashley
"Transition Radiation from Thin Foils Due to Non-Normally Incident Electrons," *Phys. Rev.* **155**, 208–10 (1967).

J. C. Ashley, L. S. Cram, and E. T. Arakawa
"Photon Emission from Al Foils Bombarded by Non-Normally Incident Electrons," submitted for publication in the *Physical Review*.

Leroy Augenstein, Edward Yeargers, James Carter, and DeVaughn Nelson
"Excitation, Dissipative, and Emissive Mechanisms in Biochemicals," to be published in *Radiation Research*.

J. A. Auxier
"Present Status of Neutron Monitoring for Personnel Protection," pp. 3–14 in *Neutron Monitoring*, IAEA, Vienna, 1967.

"Multilaboratory Intercomparisons of Neutron Dosimetry Systems," pp. 625–29 in *Neutron Monitoring*, IAEA, Vienna, 1967.

"Dosimetry and Exposures in Nuclear Accidents," to be published in *Nuclear Safety*.

"A Discussion of Weapons Effects and Dosimetry," to be published in *Proceedings of First Conference on Long-Range Biomedical and Psychosocial Effects of Nuclear War, Princeton, New Jersey, January 18 Through 21, 1966*.

Report of Trip Abroad by J. A. Auxier During Period August 24, 1966–September 10, 1966, Oct. 12, 1966 (internal memorandum).

"Physical Problems of Dosimetry of Neutrons and Protons," to be published in *Proceedings of Symposium on Accidental Irradiation at Place of Work, Nice, France, April 25 Through 29, 1966*.

J. A. Auxier and M. D. Brown
"Neutron Cross Sections and Reaction Products for H, C, N, and O for the Energy Range from Thermal to 15 Mev," to be published in *Proceedings of First International Congress of the International Radiation Protection Association, Rome, Italy, September 5 Through 10, 1966*.

J. A. Auxier, W. S. Snyder, and T. D. Jones
"Neutron Interactions and Penetration in Tissue," chap. 6 in *Radiation Dosimetry*, vol. 1 (ed. by F. H. Attix and W. C. Roesch), Academic, New York (in press).

J. Baarli, St. Charalambus, J. Dutrannois, K. Goebel, H. H. Hubbell, T. R. Overton, A. Rindi, and A. H. Sullivan
Hazards from Induced Radioactivity near High Energy Accelerators, CERN-DI/HP/84 (April 1966).

R. E. Blanco, J. O. Blomeke, W. J. Boegly, Jr., K. E. Cowser, H. E. Goeller, R. E. Lampton, T. F. Lomenick, and F. L. Parker
Survey of a Site for Nuclear Fuel Processing Plant and Waste Disposal Area at Oak Ridge, ORNL-TM-1748 (Jan. 13, 1967).

B. G. Blaylock
"A Cytogenetic Study of a Natural Population of *Chironomus* Inhabiting an Area Contaminated by Radioactive Waste," pp. 835–46 in *Proceedings of Symposium on Disposal of Radioactive Wastes into Seas, Oceans, and Surface Waters, May 16–20, 1966, Vienna, Austria*, IAEA, Vienna, 1966.

"A Population Cage for Counting Adult *Drosophila* Populations," *Drosophila Inform. Serv.* **42**, 113 (1967).

"Effect of Ionizing Radiation on Interspecific Competition," to be published in *Proceedings of 2nd National Symposium on Radioecology, Ann Arbor, Michigan*.

J. O. Blomeke, R. Salmon, J. T. Roberts, R. L. Bradshaw, and J. J. Perona
"Estimated Costs of High-Level Waste Management," pp. 830–43 in *Proceedings of International Symposium on Solidification and Long-Term Storage of Highly Radioactive Wastes, Richland, Washington, February 15–18, 1966*, CONF-660208 (November 1966).

W. J. Boegly, Jr., R. L. Bradshaw, F. M. Empson, W. C. McClain, F. L. Parker, and W. F. Schaffer, Jr.
"Project Salt Vault: Radioactive Waste Disposal in a Salt Mine," *Proceedings of the 20th Annual Purdue Industrial Waste Conference, Lafayette, Indiana, May 4–6, 1965* (1966).

W. J. Boegly, Jr., and W. L. Griffith
A Survey of Underground Utility Tunnel Practice, ORNL-TM-1714 (February 1967).

R. L. Bradshaw
Current Status, Present Plans, and Future Needs in Project Salt Vault, Jan. 16, 1967 (internal memorandum).

R. L. Bradshaw, T. F. Lomenick, W. C. McClain, W. J. Boegly, Jr., F. M. Empson, and F. L. Parker
"Project Salt Vault: Effects of Temperature and Radiation on Plastic Flow and Mine Stability," pp. 671–84 in *Proceedings of International Symposium on the Solidification and Long-Term Storage of Highly Radioactive Wastes, Richland, Washington, February 15–18, 1966*, CONF-660208 (November 1966).

R. L. Bradshaw, T. F. Lomenick, W. C. McClain, and F. M. Empson
"Model and Underground Studies of the Influence of Stress, Temperature, and Radiation on Flow and Stability in Rock Salt Mines," pp. 429–33 in *Proceedings of the First Congress of the International Society of Rock Mechanics, Lisbon, 25 September to 1 October 1966*, vol. II, 1966.

G. N. Brown and F. G. Taylor, Jr.
"Zinc-65 Distribution and Radiosensitivity of Growth and ^{65}Zn Uptake in Red Oak Seedlings," *Radiation Botany* **6**, 519–24 (1966).

"Interaction of Radiation and Photoperiodism in *Xanthium pensylvanicum:* Effects of Radiation During the Light and Dark Periods of Photoinduction," *Radiation Botany* **7**, 67–72 (1967).

P. H. Carrigan, Jr., and R. J. Pickering
Radioactive Materials in Bottom Sediment of Clinch River: Part B, Inventory and Vertical Distribution of Radionuclides in Undisturbed Cores, suppl. 2B to *Status Report No. 5 on Clinch River Study*, ORNL-3721 (March 1967).

P. H. Carrigan, Jr., R. J. Pickering, T. Tamura, and R. Forbes
Radioactive Materials in Bottom Sediment of Clinch River: Part A, Investigations of Radionuclides in Upper Portion of Sediment, suppl. 2A to *Status Report No. 5 on Clinch River Study*, ORNL-3721 (March 1967).

J. G. Carter and L. G. Christophorou
"Organic Scintillators with 2-Ethyl Naphthalene as a Solvent," *J. Chem. Phys.* **46**, 1883–90 (1967).

J. G. Carter, L. G. Christophorou, and M-E. M. Abu-Zeid
"Emission from Organic Liquids Excited by Electron Impact," submitted for publication in the *Journal of Chemical Physics*.

J. S. Cheka, J. A. Auxier, T. D. Jones, H. H. Hubbell, Jr., and W. S. Snyder
"Estimation of Radiation Dose Received by Survivors of the Hiroshima and Nagasaki Bombings (ORNL-Ichiban)," to be published as *ABCC Research Protocol*.

H. E. Childs, Jr., and G. E. Cosgrove
"A Study of Pathological Conditions in Wild Rodents in Radioactive Areas," *Am. Midland Naturalist* **76**, 309–24 (1966).

L. G. Christophorou and J. G. Carter
"Improved Organic Scintillators in 2-Ethyl Naphthalene: The Role of Excimers," *Nature* **212**, 816–18 (1966).

L. G. Christophorou and R. N. Compton
"Interaction of Low-Energy Electrons with Polyatomic Molecules," to be published in *Health Physics.*

L. G. Christophorou, R. N. Compton, G. S. Hurst, and P. W. Reinhardt
"Dissociative Electron Capture by Benzene Derivatives," *J. Chem. Phys.* **45**, 536–47 (1966).

L. G. Christophorou, G. S. Hurst, and W. G. Hendrick
"Swarm Determination of the Cross Section for Momentum Transfer in Ethylene and in Ethylene Mixtures," *J. Chem. Phys.* **45**, 1081–85 (1966).

R. N. Compton and L. Bouby
"Formation d'ions negatifs dans le glyoxal et le biacetyl," *Comp. Rend.* **264**, 1153–56 (1967).

R. N. Compton and L. G. Christophorou
"Negative Ion Formation in H_2O and D_2O," *Phys. Rev.* **154**, 110–16 (1967).

R. N. Compton, L. G. Christophorou, and R. H. Huebner
"Temporary Negative Ion Resonances in Benzene and Benzene Derivatives," *Phys. Letters* **23**, 656–58 (1966).

K. E. Cowser, L. C. Lasher, L. Gemmell, and S. G. Pearsall
"Operational Experience in the Treatment of Radioactive Waste at the Oak Ridge National Laboratory and Brookhaven National Laboratory," pp. 381–401 in *Proceedings of a Symposium on Practices in the Treatment of Low- and Intermediate-Level Radioactive Wastes, December 6–10, 1965, Vienna, Austria,* IAEA, Vienna, 1966.

K. E. Cowser, W. S. Snyder, C. P. McCammon, C. P. Straub, O. W. Kochtitzky, R. L. Hervin, E. G. Struxness, and R. J. Morton
"Evaluation of Radiation Dose to Man from Radionuclides Released to the Clinch River," pp. 639–71 in *Proceedings of Symposium on Disposal of Radioactive Wastes into Seas, Oceans, and Surface Waters, May 16–20, 1966, Vienna, Austria,* IAEA, Vienna, 1966.

K. E. Cowser, S. V. Kaye, P. S. Rohwer, W. S. Snyder, and E. G. Struxness
Dose-Estimation Studies Related to Proposed Construction of an Atlantic-Pacific Interoceanic Canal with Nuclear Explosives: Phase 1, ORNL-4101 (March 1967).

L. S. Cram and E. T. Arakawa
"Bremsstrahlung and Transition Radiation from Ag Foils Bombarded by Non-Normal Incidence Electrons," *Phys. Rev.* **153**, 455–59 (1967).

D. A. Crossley, Jr.
"Comparative Movement of ^{106}Ru, ^{60}Co, and ^{137}Cs in Arthropod Food Chains," to be published in *Proceedings of 2nd National Symposium on Radioecology, Ann Arbor, Michigan.*

J. Crowell, V. E. Anderson, and R. H. Ritchie
"Ladder Corrections to the Static RPA Dielectric Constant and to Positron Annihilation in Metals," *Phys. Rev.* **150**, 243–48 (1966).

J. W. Curlin
"Clonal Differences in Yield Response of *Populus deltoides* to Nitrogen Fertilization," *Soil Sci. Soc. Am. Proc.* **31**, 276–80 (1967).

J. W. Curlin (with H. C. Jones)
"The Role of Fertilizers in Improving the Hardwoods of the Tennessee Valley," *Proc. TVA Forest Fertilization Symp., Gainesville, Florida* (in press).

J. W. Curlin (with W. M. Ciesla and J. C. Bell, Jr.)
"Color Aerial Photography for Appraisal Surveys of the Southern Pine Beetle," *Photogrammetric Eng.* (in press).

J. W. Curlin and J. P. Witherspoon
"Components and Estimates of Dose to Roots of Potted Plants Exposed to Fast Neutron Radiation," *Health Phys.* (in press).

R. C. Dahlman
"Carbon-14 Cycling in the Root and Soil Components of a Prairie Ecosystem," to be published in the *Proceedings of 2nd National Symposium on Radioecology, Ann Arbor, Mich.*

D. R. Davy
"Personnel Dosimetry for Radiation Accidents" (book review), *Health Phys.* 12, 1508–10 (1966).

"Prediction of Biological Damage from Stopping-Power Theory," *Health Phys.* (in press).

D. R. Davy and L. H. Peshori
"An Absolute Neutron Dosimeter Based on a Generalized Concept for Radiation Dosimetry," *Health Phys.* 13, 783–94 (1967).

D. R. Davy, L. H. Peshori, and J. W. Poston
"Sodium-24 Production in Saline-Filled Phantoms Under Neutron Irradiations," *Health Phys.* 12, 1353–55 (1966).

Wallace de Laguna
Critical Analysis of the Hydrologic Work Carried Out on the Site of the Nuclear Studies Complex at Mol. Report No. 17, C. E. N. Centre d'Etude de l'Energie Nucleaire, Mol, Belgium (1965).

P. B. Dunaway
"Life History and Populational Aspects of the Eastern Harvest Mouse," *Am. Midland Naturalist* (in press).

P. B. Dunaway, J. A. Payne, L. L. Lewis, and J. D. Story
"Incidence and Effects of *Cuterebra* in *Peromyscus*," *J. Mammal.* 48, 38–51 (1967).

P. B. Dunaway, L. L. Lewis, J. D. Story, J. A. Payne, and J. M. Inglis
"Radiation Effects in the Soricidae, Cricetidae, and Muridae," to be published in the *Proceedings of 2nd National Symposium on Radioecology, Ann Arbor, Michigan.*

P. B. Dunaway (with G. E. Cosgrove and T. P. O'Farrell, J. A. Payne, and H. E. Childs)
"Pathology Survey in Small Mammals," *Bull. Wildlife Disease Assoc.* (in press)

F. M. Empson, W. J. Boegly, Jr., R. L. Bradshaw, W. C. McClain, F. L. Parker, and W. F. Schaffer, Jr.
"Demonstration of Disposal of High-Level Radioactive Solids in Salt," pp. 432–43 in *Proceedings of the Second Symposium on Salt*, vol. 1, The Northern Ohio Geological Society, Inc., Cleveland, Ohio, 1966.

F. M. Empson, R. L. Bradshaw, W. J. Boegly, Jr., W. C. McClain, F. L. Parker, and W. F. Schaffer, Jr.
"Project Salt Vault: Design and Operation," pp. 671–84 in *Proceedings of International Symposium on Solidification and Long-Term Storage of Highly Radioactive Wastes, Richland, Washington, February 15–18, 1966*, CONF-660208 (November 1966).

L. B. Farabee
"Improved Procedure for Radiostrontium Analysis of Human Urine," *Proceedings of 12th Bio-Assay and Analytical Chemistry Meeting, Gatlinburg, Tenn., October 13–14, 1966*, CONF-661018 (June 6, 1967).

B. R. Fish (ed.)
Surface Contamination (Proceedings of a Symposium Held in Gatlinburg, Tennessee, June 8–12, 1964), Pergamon, London (1967).

B. R. Fish, R. L. Walker, G. W. Royster, Jr., and J. L. Thompson
"Redispersion of Settled Particulates," p. 75 in *Surface Contamination* (Proceedings of a Symposium Held in Gatlinburg, Tennessee, June 8–12, 1964). Pergamon, London (1967).

H. L. Fisher, Jr.
"A Computer Code for Estimation of Body Burden of ^{90}Sr Based on O.R. and Bone Remodeling Which Are Age Dependent," p. 147 in *Proceedings of 11th Annual Bioassay and Analytical Chemistry Meeting, October 7–8, 1965, Albuquerque, New Mexico*, CONF-651008 (1966).

H. L. Fisher, Jr., and W. S. Snyder
"An Age-Dependent Model for the Bodily Retention of Cesium," p. 174 in *Proceedings of 12th Annual Bioassay and Analytical Chemistry Meeting, October 13–14, 1966, Gatlinburg, Tennessee*, CONF-661018 (1967).

Kenneth Fox
"Bound States of an Electron in a Point Electric-Dipole Field: Quantization of a Classical Solution," submitted for publication in *Physics Letters*.

Kenneth Fox and J. E. Turner
"WKB Treatment of Bound States in an Electron Dipole Potential," *Am. J. Phys.* **34**, 606–10 (1966).

W. R. Garrett and C. P. Bhalla
"Potential Energy Shift for a Screened Coulomb Potential," *Z. Physik* **198**, 453–60 (1967).

W. R. Garrett and H. T. Jackson
"Electron Photodetachment from O^- and Elastic Scattering from Atomic Oxygen," *Phys. Rev.* **153**, 28–35 (1967).

L. W. Gilley, L. B. Holland, J. W. Poston, and D. R. Ward
"Operation Problems with the Health Physics Research Reactor," *Nucl. Safety* **8**(2), 179–82 (Winter 1966–67).

H. Hollister and J. E. Turner
"The Possible Role of Momentum in Radiation Dosimetry. III. Remarks on the 1962 ICRP/ICRU Report," *Health Phys.* **12**, 949–53 (1966).

H. H. Hubbell
Report of Personnel Exchange Between Oak Ridge National Laboratory and the European Organization for Nuclear Research (CERN), Geneva, Switzerland. During Period September 9, 1965, to August 16, 1966, Oct. 13, 1966 (internal memorandum).

G. S. Hurst and J. E. Parks
"Time-of-Flight Determinations of Electron Diffusion Coefficients and Electron Drift Velocities in Ethylene, Water Vapor, and in Hydrogen," *J. Chem. Phys.* **45**, 282–95 (1966).

D. G. Jacobs
"An Interpretation of Cation Exchange by Alumina," *Health Phys.* **12**, 1565–70 (1966).

"Behavior of Radioactive Gases Discharged into the Ground," *Nucl. Safety* **8**(2), 175–78 (Winter 1966–67).

"Negative Sorption by Alumino-Silicates Having a Limited Degree of Lattice Expansion," pp. 319–29 in *Proceedings of the International Clay Conference, 1966, Jerusalem, Israel*, vol. I.

D. R. Johnson
"*Neutron Detectors*," book review, *Health Phys.* **13**, 664 (1967).

D. R. Johnson and W. F. Ohnesorge
"Yield, Energy, and Angular Distributions of Neutrons Produced in Graphite, Copper, and Tantalum Targets Irradiated with 63 Mev Protons," to be published in *Atompraxis*.

D. R. Johnson and J. W. Poston
Radiation Dosimetry Studies at the Health Physics Research Reactor, ORNL-4113 (June 1967).

Edith S. Jones
"Microscopic and Autoradiographic Studies of Distribution of Uranium in the Rat Kidney," *Health Phys.* **12**, 1437 (1966).

G. E. Jones, L. S. Cram, and E. T. Arakawa
"Radiation from Thick Silver Foils Bombarded by Grazing-Incidence Electrons," *Phys. Rev.* **147**, 515–17 (1966).

T. D. Jones

Report of Trip Abroad by T. D. Jones During Period September 3 Through 11, 1966, Oct. 13, 1966 (internal memorandum).

Report of Trip Abroad by T. D. Jones During Period February 2–March 6, 1967, Apr. 26, 1967 (internal memorandum).

T. D. Jones, J. A. Auxier, J. W. Poston, and D. R. Johnson
"Dose Distribution Functions for Neutrons and Gamma Rays in Anthropomorphous and Radiological Phantoms," to be published in *Proceedings of First International Congress of the International Radiation Protection Association, Rome, Italy, September 5 Through 10, 1966.*

K. Katoh and J. E. Turner
"A Study of Elementary Particle Interactions for High-Energy Dosimetry," *Health Phys.* (in press).

S. V. Kaye (with J. L. Roti Roti)
Calibration of ^{90}Sr and ^{90}Y Plaques for Irradiating Insects, ORNL-TM-1921 (submitted).

G. D. Kerr and T. D. Strickler
"The Application of Solid-State Nuclear Track Detectors to the Hurst Threshold Detector System," *Health Phys.* **12**, 1141–42 (1966).

N. R. Kevern
"Feeding Rate of Carp Established by a Radioisotopic Method," *Trans. Am. Fisheries Soc.* **94**, 363–71 (1966).

N. R. Kevern, J. L. Wilhm, and G. M. Van Dyne
"Use of Artificial Substrata to Estimate the Productivity of Periphyte," *Limnol. Oceanog.* **11**, 499–502 (1966).

C. E. Klots
"Energy Deposition Mechanisms," to be published as chap. 1 in *Fundamental Processes of Radiation Chemistry* (ed. by Pierre Ausloos).

"Energy Partition Parameters in Radiation Studies Involving Rare Gases," *J. Chem. Phys.* **46**, 3468–74 (1967).

"Statistical Aspects of Autoionization Lifetimes," *J. Chem. Phys.* **46**, 1197–99 (1967).

C. E. Klots and V. E. Anderson
"Ion Loss by Diffusion in the Radiolysis of Gases," *J. Phys. Chem.* **71**, 265–67 (1967).

R. A. MacRae, E. T. Arakawa, and M. W. Williams
"Optical Properties of Vacuum-Evaporated White Tin," submitted for publication in the *Physical Review.*

L. A. Masironi and B. R. Fish
"Direct Observation of Particle Reentrainment from Surfaces," p. 55 in *Surface Contamination* (Proceedings of a Symposium held in Gatlinburg, Tennessee, June 8–12, 1964), Pergamon, London, 1967.

W. C. McClain
"Surface Subsidence Associated with Longwall Mining," *Trans. AIME* **238**, 231–36 (September 1966).

Research Program on Earth Stress Measurement Using Hydraulic Fracturing, January 1967 (internal memorandum).

W. C. McClain and R. L. Bradshaw
"Stress Redistribution in Room and Pillar Salt Mines," *Intern. J. Rock Mech. Min. Sci.* **4**, 245–55 (April 1967).

W. J. McConnell, R. N. Hamm, R. H. Ritchie, and R. D. Birkhoff
"Electron Flux Spectra in Aluminum; Analysis for LET Spectra and Excitation and Ionization Yields," submitted for publication in *Radiation Research.*

E. F. Menhinick
"^{90}Sr Plaques for Beta Radiation Studies," *Health Phys.* 12, 973–79 (1966).

K. Z. Morgan
"A Comparison and Evaluation of Various Radiation Hazards in Metropolitan Areas," p. 41 in *Proceedings of the II Symposium on Health Physics.* Pecs, Hungary, September 26–30, vol. II, 1966.

M. Y. Nakai, D. A. LaBar, J. A. Harter, and R. D. Birkhoff
"Time-of-Flight Studies of Electrons in the Nanosecond Region," *Rev. Sci. Instr.* 38, 820–26 (1967).

E. C. Neal, B. C. Patten, and C. E. DePoe
"Periphyton Growth on Artificial Substrates in a Radioactively Contaminated Lake," *Ecology* (submitted).

D. J. Nelson
"Ecology and the Industrial Society" (book review), *Health Phys.* 12, 1507–8 (1966).

"Microchemical Constituents in Contemporary and Pre-Columbian Clam Shell," *Quaternary Paleoecology,* Yale University Press, New Haven, Conn. (in press).

"The Prediction of ^{90}Sr Uptake in Fish Using Data on Specific Activities and Biological Half-Lives," pp. 843–51 in *Radioecological Concentration Processes* (ed. by B. Åberg and F. P. Hungate), Pergamon, New York.

"Environmental Biology" (book review), *Environ. Sci. Technol.* (May 1967).

"Ecological Behavior of Radionuclides in Surface Waters," *Proceedings of the Reservoir Fishery Resources Symposium* (in press).

"Cesium, Cesium-137, and Potassium Concentrations in White Crappie and Other Clinch River Fish," to be published in the *Proceedings of 2nd National Symposium on Radioecology, Ann Arbor, Michigan.*

D. R. Nelson, J. G. Carter, R. D. Birkhoff, R. N. Hamm, and L. G. Augenstein
"Yield of Luminescence from X-Irradiated Biochemicals," to be published in *Radiation Research.*

Jacob Neufeld
"Reformulation of the Dielectric Constant and of the Conductivity of an Absorbing Medium," *Intern. J. Electron.* 21, 99–101 (1966).

"Reformulation of the Dielectric Constant and of Ohm's Law in an Absorbing Medium," *Phys. Rev.* 152, 707–17 (1966).

Jacob Neufeld, V. E. Anderson, Harvel Wright, W. S. Snyder, and J. E. Turner
"Effects of Phantom Geometry on Dose Distribution," to be published in *Proceedings of International Congress of International Radiation Protection Association, Rome, Italy, September 5–10, 1966.*

Jacob Neufeld and C. L. Wiginton
"Cyclotron Excitation of Electromagnetic Waves by a Gyrating Electron Beam," *Phys. Rev.* 148, 97–103 (1966).

Jacob Neufeld and Harvel Wright
"Discussion of Paper by John M. Cornwall, 'Cyclotron Instabilities and Electromagnetic Emission in the Ultra Low Frequency and Very Low Frequency Ranges,'" *J. Geophys. Res.* 71, 4200 (1966).

"Excitation of Hydromagnetic Waves by a Helical Proton Stream," *Proceedings of Symposium on Electromagnetic Wave Theory, Delft, September 6–11, 1965* (in press).

T. P. O'Farrell and P. B. Dunaway
"Cell Proliferation as a Function of Metabolism in Three Species of Native Rodents," *Nature* (in press).

"Incorporation and Tissue Distribution of a Thymidine Analog in *Sigmodon hispidus,*" *Comp. Biochem. Physiol.* (in press).

J. S. Olson
"Progress in Radiation Ecology: Radionuclide Movement in Major Environments," *Nucl. Safety* 8, 53–68 (1966).

"Ecology" in *Four Problem Areas in the Recovery from a Large-Scale Nuclear Attack*, National Academy of Sciences, Advisory Committee on Emergency Planning (submitted).

J. S. Olson (ed.)
Systems Ecology and the International Biological Program, National Academy of Sciences, U.S. National Committee for the International Biological Program (submitted).

J. S. Olson (with Victor Obenhaus and Lionel Walford, eds.)
Technology and Man's Relation to His Natural Environment, National Council of the Churches of Christ in the U.S.A. (submitted).

F. L. Parker, M. A. Churchill, R. W. Andrew, B. J. Frederick, P. H. Carrigan, Jr., J. S. Cragwall, Jr., S. L. Jones, E. G. Struxness, and R. J. Morton
"Dilution, Dispersion, and Mass Transport of Radionuclides in the Clinch and Tennessee Rivers," pp. 33–55 in *Proceedings of a Symposium on Disposal of Radioactive Wastes into Seas, Oceans, and Surface Waters, May 16–20, 1966, Vienna, Austria*, IAEA, Vienna, 1966.

B. C. Patten
The Biocoenetic Process in an Estuarine Phytoplankton Community, ORNL-3946 (October 1966).

"Systems Ecology: A Course Sequence in Mathematical Ecology," *BioScience* 16, 593–98 (1966).

B. C. Patten (with J. S. O'Conner)
"Mathematical Models of Plankton Productivity," *Proceedings of Reservoir Fishery Symposium* (in press).

B. C. Patten and B. F. Chabot
"Factorial Productivity Experiments in a Shallow Estuary: Characteristics of Response Surfaces," *Chesapeake Sci.* 7, 117–36 (1966).

B. C. Patten and R. L. Iverson
"Photosynthesis and Uptake of Strontium-85 in Freshwater Plankton," *Nature* 211, 96–97 (1966).

B. C. Patten and G. M. Van Dyne
"Factorial Productivity Experiments in a Shallow Estuary: Energetics of Individual Plankton Species in Mixed Populations," submitted to *Limnology and Oceanography*.

B. C. Patten and M. Witkamp
"Systems Analysis of ^{134}Cs Kinetics in Terrestrial Microcosms," *Ecology* (in press).

J. A. Payne, G. D. Martin, J. D. Story, and G. E. Cosgrove
"Electrophoresis as an Aid in Detecting Pathological Conditions in Wild Mammals," *Bull. Wildlife Disease Assoc.* 3, 21–22 (1967).

P. T. Perdue
"Inexpensive Liquid Nitrogen Level Control for Cold Traps," *Nucl. Instr. Methods* 44, 169–70 (1966).

R. J. Pickering, P. H. Carrigan, Jr., T. Tamura, H. H. Abee, J. W. Beverage, and R. W. Andrew, Jr.
"Radioactivity in Bottom Sediment of the Clinch and Tennessee Rivers," pp. 57–88 in *Symposium on Disposal of Radioactive Wastes into Seas, Oceans, and Surface Waters, May 16–20, 1966, Vienna, Austria*, IAEA, Vienna, 1966.

J. W. Poston
Report of Trip Abroad by J. W. Poston During Period July 23, 1966–July 30, 1966, Aug. 18, 1966 (internal memorandum).

J. R. Reed
"Alarm Substances and Fright Reactions in Some Fishes from the Southeastern United States," submitted to *Animal Behavior*.

J. R. Reed and D. J. Nelson
"Radiostrontium Uptake in Blood and Flesh in Bluegills (*Lepomis macrochirus*)," to be published in the *Proceedings of 2nd National Symposium on Radioecology, Ann Arbor, Michigan.*

D. E. Reichle
"Some Pselaphid Beetles with Boreal Affinities and Their Distribution Along the Postglacial Fringe," *Systematic Zool.* **15**, 330–34 (1966).

"Radiocesium Turnover Rates and Energy Flow in Terrestrial Isopod Populations," *Ecology* **48**(3), 351–66 (1967).

"The Temperature and Humidity Relations of Some Bog Pselaphid Beetles," *Ecology* **48**, 208–15 (1967).

"Relation of Body Size to Food Intake, Oxygen Consumption, and Trace Element Metabolism in Forest Floor Arthropods," submitted to *Ecology.*

D. E. Reichle (with E. C. Williams, Jr.)
"Radioactive Tracers in the Study of Energy Turnover by a Grazing Insect (*Chrysochus auratus* Fab.)," submitted to *Oikos.*

D. E. Reichle and D. A. Crossley, Jr.
"Trophic Level Concentrations of Cesium-137, Sodium, and Potassium in Forest Arthropods," to be published in the *Proceedings of 2nd National Symposium on Radioecology, Ann Arbor, Michigan.*

R. H. Ritchie
"On the Possibility of Observing Characteristic Energy Gain by Fast Electrons in Solids," *Phys. Letters* **22A**, 348–49 (1967).

R. H. Ritchie and V. E. Anderson
"The Use of Fourier Transforms in the Unfolding of Experimental Data," *Nucl. Instr. Methods* **45**, 277–81 (1966).

R. H. Ritchie and J. E. Turner
"Electron Capture and Loss in Electron Swarm Experiments," *Z. Physik* **200**, 259–69 (1967).

R. H. Ritchie, M. Y. Nakai, and R. D. Birkhoff
"Low-Energy Electron Mean Free Paths in Solids," in *Advances in Radiobiology*, vol. 3 (in press).

L. L. Robinson, L. C. Emerson, J. G. Carter, and R. D. Birkhoff
"Optical Reflectivities of Liquid Water in the Vacuum UV," submitted for publication in the *Journal of Chemical Physics.*

A. S. Rogowski, W. D. Shrader, H. P. Johnson, and Don Kirkham
"Tile Drainage Experimentation on Webster Soils: Results of Years 1954–1963," *Iowa State J. Sci.* **41**(1), 25–40 (August 1966).

G. W. Royster, Jr., and B. R. Fish
"Techniques for Assessing 'Removable' Surface Contamination," p. 201 in *Surface Contamination* (Proceedings of a Symposium held in Gatlinburg, Tennessee, June 8–12, 1964), Pergamon, London, 1967.

W. F. Schaffer, Jr., W. J. Boegly, Jr., F. L. Parker, R. L. Bradshaw, F. M. Empson, and W. C. McClain
"Project Salt Vault: Design and Demonstration of Equipment," pp. 685–706 in *Proceedings of International Symposium on Solidification and Long-Term Storage of Highly Radioactive Wastes, Richland, Washington, February 15–18, 1966,* CONF-660208 (November 1966).

H. A. Schroeder, J. J. Balassa, and Isabel H. Tipton
"Essential Trace Metals in Man: Manganese. A Study in Homeostasis," *J. Chronic Diseases* **19**, 545 (1966).

H. A. Schroeder, A. P. Nason, Isabel H. Tipton, and J. J. Balassa
"Essential Trace Metals in Man: Copper," *J. Chronic Diseases* **19**, 1007 (1966).

"Essential Trace Metals in Man: Zinc. Relation to Environmental Cadmium," *J. Chronic Diseases* **20**, 179 (1967).

A. F. Shinn
"Kiln-Firing as a Technique for Studying Nest-Building Behavior of Mud-Dauber Wasps," *Nature* **201**, 112 (1966).

W. S. Snyder
"A Dose Estimate Based on Stable-Isotope Data," p. 161 in *Proceedings of 11th Annual Bioassay and Analytical Chemistry Meeting, October 7–8, 1965, Albuquerque, New Mexico*, CONF-651008 (1966).

"The Standard Man in Relation to Internal Radiation Dose," *Am. Ind. Hygiene Assoc. J.* **27**, 539 (November–December 1966).

"The Use of the Lung Model for Estimation of Dose," p. 74 in *Proceedings of 12th Annual Bioassay and Analytical Chemistry Meeting, October 13–14, 1966, Gatlinburg, Tennessee*, CONF-661018 (1967).

"Distribution of Dose in the Body from HTO," p. 22 in *Abridged Proceedings of the Symposium on Instrumentation, Experience, and Problems in Health Physics Tritium Control, February 16–17, 1967, Albuquerque, New Mexico*, SC-M-67-244 (May 1967).

W. S. Snyder, J. A. Auxier, M. D. Brown, T. D. Jones, and R. T. Boughner
"Distribution of Dose and Dose Equivalent in an Anthropomorphic Phantom Resulting from Broad-Beam Sources of Monoenergetic Neutrons," p. 27 in *Proceedings of the Special Sessions on Radiation Transport and Biological Effects, November 1, 1966, Pittsburgh, Pennsylvania*, ANS-SD-4 (1967); *Trans. Am. Nucl. Soc.* **9**(2), 357 (1967) (abstr).

J. A. Stockdale, L. G. Christophorou, and G. S. Hurst
"Capture of Thermal Electrons by Oxygen," submitted for publication in the *Journal of Chemical Physics*.

E. G. Struxness
"Ultimate Disposal of Radioactive Wastes," to be published in *Proceedings of 6th Annual Sanitary and Water Resources Conference, Vanderbilt University, June 1, 1967*.

"Permanent Disposal of Radioactive Wastes," to be published in *Proceedings of 2nd National Symposium on Radioecology*.

E. G. Struxness, P. H. Carrigan, Jr., M. A. Churchill, K. E. Cowser, R. J. Morton, D. J. Nelson, and F. L. Parker
Comprehensive Report of the Clinch River Study, ORNL-4035 (April 1967).

J. C. Sutherland, E. T. Arakawa, and R. N. Hamm
"Optical Properties of Sodium in the Vacuum Ultraviolet," *J. Opt. Soc. Am.* **57**, 645–50 (May 1967).

Jacob Tadmor and K. E. Cowser
"Underground Disposal of ^{85}Kr from Nuclear Fuel Reprocessing Plants," *Trans. Am. Nucl. Soc.* **10**(1), 159 (1967).

Tsuneo Tamura
"Development and Applications of Minerals in Radioactive Waste Disposal," pp. 425–39 in *Proceedings of the International Clay Conference, 1966, Jerusalem, Israel*, vol. I.

"Selective Removal of Cesium-137 and Strontium-90 in Waste Solutions by Minerals," pp. 91–107 in *Proceedings of Conference on Water, Geology, and the Future*, Indiana University, Bloomington, Indiana, 1967.

J. T. Tanner
"Effects of Population Density on Growth Rates of Animal Populations," *Ecology* **47**, 733–46 (1966).

F. G. Taylor, Jr.
"Predicted Seasonal Radiosensitivity of Southeastern Tree Species," *Radiation Botany* **6**, 307–12 (1966).

"*Spiranthes ovalis* Present in Tennessee," *Castanea* **32**, 99–101 (1967).

"Effects of Acute Gamma Radiation on Bud Production and Stem Elongation of Giant Sequoia Seedlings," submitted to *Radiation Botany*.

J. H. Thorngate
"Dosimetry, Shielding, and Scattering. II," to be published in *Proceedings of Conference on Principles of Radiation Protection, Oak Ridge, Tennessee, August 24 Through 26, 1966.*

An Interval Timer Designed for Use During Irradiations at the Health Physics Research Reactor, ORNL-TM-1559 (August 1966).

J. H. Thorngate, J. A. Auxier, F. F. Haywood, and S. Helf
Energy and Angular Distribution of Neutrons and Gamma Rays – Operation BREN, CEX-62.12 (February 1967).

Isabel H. Tipton and Peggy L. Stewart
"Spectrographic Analysis of Biological Materials," *Devel. Appl. Spectry.* **5** (1966).

J. E. Turner
"Calculation of Stopping Power of a Heavy Charged Particle in Matter," to be published in *Health Physics*.

J. E. Turner and Kenneth Fox
"Minimum Dipole Moment Required to Bind an Electron to a Finite Dipole," *Phys. Letters* **23**, 547–49 (1966).

J. E. Turner and Hal Hollister
"On the Relationship of Collision Theory to the Interpretation of Relative Biological Effectiveness," submitted for publication in the *Journal of Physics in Medicine and Biology*.

G. M. Van Dyne
"Application and Integration of Multiple Linear Regression and Linear Programming in Renewable Resource Analyses," *J. Range Management* **19**, 356–62 (1966).

"Use of a Vacuum-Clipper for Harvesting Herbage," *Ecology* **47**, 624–26 (1966).

G. M. Van Dyne and H. G. Fisser
"Influence of Number and Spacing of Points on Accuracy and Precision of Basal Cover Estimates," *J. Range Management* **19**, 205–11 (1966).

G. M. Van Dyne and W. G. Vogel
"Relation of *Selaginella densa* to Site Grazing and Climate," *Ecology* **48**(3), 438–44 (1967).

G. M. Van Dyne and Ingvi Thorsteinsson
"Intraseasonal Changes in the Height Growth of Plants in Response to Nitrogen and Phosphorus," pp. 924–29 in *Proceedings of Tenth International Grassland Conference, July 7–16, 1966, Helsinki, Finland.*

R. C. Vehse, E. T. Arakawa, and J. L. Stanford
"Photoemission Measurements of Silver and Palladium in the Vacuum Ultraviolet," submitted for publication in *Physical Review Letters*.

"Normal Incidence Reflection of Aluminum Films in the Wavelength Region 800 to 2000 Å," *J. Opt. Soc. Am.* **57**, 551–52 (1967).

E. B. Wagner, F. J. Davis, G. S. Hurst, and J. E. Parks
"Time-of-Flight Investigations of Electron Transport in Some Atomic and Molecular Gases," submitted for publication in the *Journal of Chemical Physics*.

R. L. Walker and B. R. Fish
"Adhesion of Radioactive Glass Particles to Solid Surfaces," in *Surface Contamination* (Proceedings of a Symposium held in Gatlinburg, Tennessee, June 8–12, 1964), Pergamon, London, 1967.

H. D. Waller and J. S. Olson
"Prompt Transfers of ^{137}Cs to the Soils of a Tagged *Liriodendron* Forest," *Ecology* **48**, 15–25 (1967).

W. H. Wilkie
Trip Report: Symposium on Solid State and Chemical Radiation Dosimetry in Medicine and Biology, Vienna, Austria, Oct. 3–7, 1966; Discussions at AERE, Harwell, England, and Karlsruhe Nuclear Research Center, Germany, Nov. 11, 1966 (internal memorandum).

W. H. Wilkie and B. R. Fish
"Scintillation Extrapolation Dosimetry of Small Beta-Emitting Sources," in *Solid State and Chemical Radiation Dosimetry in Medicine and Biology* (Proceedings of a Symposium, Vienna, 3–7 October 1966), IAEA, Vienna, 1967.

M. W. Williams, E. T. Arakawa, and L. C. Emerson
"Photon Excitation of Surface Plasmons – Analysis of Data for Aluminum," *Surface Sci.* **6**, 127–31 (1967).

M. W. Williams, R. A. MacRae, and E. T. Arakawa
"Optical Properties of Magnesium Fluoride in the Vacuum Ultraviolet," *J. Appl. Phys.* **38**, 1701–5 (1967).

J. P. Witherspoon
"Effects of Internal ^{137}Cs Radiation on Seeds of *Liriodendron tulipifera*," *Radiation Botany* (in press).

"Radiosensitivity of Forest Tree Species to Acute Fast Neutron Radiation," to be published in *Proceedings of 2nd National Symposium on Radioecology, Ann Arbor, Michigan.*

Martin Witkamp
"Rates of Carbon Dioxide Evolution from the Forest Floor: Measurement, Environmental Effects, and Relation to CO_2 from Litter," *Ecology* **47**, 492–93 (1966).

"Biological Concentrations of ^{137}Cs and ^{90}Sr in Arctic Food Chains," *Nucl. Safety* **8**, 58–62 (1966).

"Assessment of Microbial Immobilization of Mineral Elements," *Soil Biol.* (in press).

"Aspects of Soil Microflora in Gamma Irradiated Rain Forest," in *The Tropical Rainforest*, ed. by H. T. Odum (submitted).

"Mineral Retention by Epiphyllic Organisms," in *The Tropical Rainforest*, ed. by H. T. Odum (submitted).

"Environmental Influences on Microbial Populations and Activity of the Forest Floor," *Trans. Intern. Congr. Soil Sci., 8th, Bucharest, 1964*, vol. **3**, Soil Biology (in press).

Martin Witkamp, M. L. Frank, and J. L. Shoopman
"Accumulation and Biota in a Pioneer Ecosystem of Kudzu Vine at Copperhill, Tennessee," *J. Appl. Ecol.* **3**, 383–91 (1966).

Martin Witkamp and D. A. Crossley, Jr.
"The Role of Arthropods and Microflora in Breakdown of White Oak Litter," *Pedobiologia* **6**, 293–303 (1966).

Martin Witkamp and M. L. Frank
"Retention of Loss of ^{137}Cs Components of the Groundcover in a Pine (*Pinus virginiana* L.) Stand," *Health Phys.* (in press).

"Cesium-137 Kinetics in Terrestrial Microcosms," to be published in *Proceedings of 2nd National Symposium on Radioecology, Ann Arbor, Michigan.*

Harvel Wright, E. E. Branstetter, Jacob Neufeld, J. E. Turner, and W. S. Snyder
"Calculation of Radiation Dose Due to High-Energy Protons," to be published in *Proceedings of International Congress of International Radiation Protection Association, Rome, Italy, September 5–10, 1966.*

Edward Yeargers
"UV Light Effects on Proteins," to be published in *Proceedings of Symposium on Biological Effects of Ultraviolet, Philadelphia, Pennsylvania, August 23–26, 1966.*

Lectures

S. I. Auerbach

Introduction to Radiation Ecology, Wabash College, July 6, 1966, Crawfordsville, Indiana.

The Importance of Ecology and the Study of Ecosystems, Wabash College, July 6, 1966, Crawfordsville, Indiana.

Current Research in Radioecology, Exhibits Managers' Training Course, Oak Ridge Associated Universities, August 8, 1966, Oak Ridge, Tennessee.

Aspects of Radioecology, Fall Conference of National Association of State Civil Defense Directors, November 15, 1966, Hot Springs, Arkansas.

Ecology and Ecological Research at ORNL, Navy Nuclear Sciences Seminar, Oak Ridge Associated Universities, December 9, 1966, Oak Ridge, Tennessee.

Radiation and Radioisotopes: Their Role in Ecological Research, Department of Ecology and Behavioral Biology, University of Minnesota, May 1, 1967, St. Paul.

J. A. Auxier

The Health Physics Research Reactor and Its Role at the DOSAR Facility, Kernforschungsanlage Julich, August 26, 1966, Julich, Germany.

Selected Aspects of Dosimetry for Human Exposures, Health Physics Society, Lake Mead Chapter, February 14, 1967, Las Vegas, Nevada.

Selected Aspects of Dosimetry for Human Exposures, Health Physics Society, Atlanta Chapter, April 3, 1967, Atlanta, Georgia.

Ichiban: The Dosimetry Program for Nuclear Bomb Survivors of Hiroshima and Nagasaki, Savannah River Laboratory, April 4, 1967, Aiken, South Carolina.

General Problems in Nuclear Accident Dosimetry, Health Physics Society, Savannah River Chapter, April 4, 1967, Augusta, Georgia.

Dosimetry for Human Exposures: Field Experiments and Laboratory Intercomparisons, Health Physics Society, East Tennessee Chapter, July 31, 1967, Oak Ridge, Tennessee.

B. G. Blaylock

Ecological Genetics, Department of Biology, Emory and Henry College, November 14, 1966, Emory, Virginia; Department of Biology, Clinch Valley College, November 15, 1966, Wise, Virginia; Department of Biology, George Peabody College, December 9, 1966, Nashville, Tennessee; Department of Biology, Western Carolina College, December 14, 1966, Cullowhee, North Carolina; Department of Biology, Muskingum College, January 13, 1967, New Concord, Ohio; Seymour Science Club, Catawba College, January 19, 1967, Salisbury, North Carolina; Department of Biology, Virginia Military Institute, February 21, 1967, Lexington, Virginia.

R. L. Bradshaw

Project Salt Vault, Ten-Week Health Physics Course, ORINS Special Training lectures to people responsible for licensing and inspecting of radioisotope users, etc., ORNL, November 7, 1967, Oak Ridge, Tennessee.

L. G. Christophorou

Studies of Electron-Molecule Interactions, Department of Physics, University of Kentucky, April 14, 1967, Lexington.

R. N. Compton

Interactions of Low-Energy Electrons with Complex Molecules, Department of Physics, University of Georgia, October 11, 1966, Athens.

Low-Energy Electron-Molecule Scattering Phenomena, Department of Physics, Tennessee Technological University, February 24, 1967, Cookeville.

Mary Jane Cook

Biological Effects of Radiation, Department of Physics Course on "Special Topics in Health Physics," University of Tennessee, May 4 and 5, 1967, Knoxville.

K. E. Cowser

Movement and Hazards of Radionuclides in Fresh Water, to members of ORINS course in Advanced Isotope Technology, ORNL, August 3, 1966, Oak Ridge, Tennessee.

Clinch River Hazards Analysis, Ten-Week Health Physics Course, ORINS Special Training lectures to people responsible for licensing and inspecting of radioisotope users, etc., ORNL, November 7, 1967, Oak Ridge, Tennessee.

D. A. Crossley, Jr.

Role of Microfauna and Microflora in Breakdown and Transfer of Organic Matter, Seminar on Pesticides, Michigan State University, May 18, 1967, East Lansing.

J. W. Curlin

Soil Activation by Fast Neutrons, Advanced Isotope Technology Course, Oak Ridge Associated Universities, July 13, 1966, Oak Ridge, Tennessee.

Wallace de Laguna

Waste Disposal by Hydrofracturing, Ten-Week Health Physics Course, ORINS Special Training lectures to people responsible for licensing and inspecting of radioisotope users, etc., ORNL, November 7, 1967, Oak Ridge, Tennessee.

B. R. Fish

Radioactivity in Man, ORAU-ORNL Ten-Week Health Physics Course, October 5, 1966, Oak Ridge, Tennessee.

Effects of Air Pollution on the Safety and Well-Being of Society, Reactor Division, ORNL, January 1967, Oak Ridge, Tennessee (2 seminars).

Surface Contamination and Aerosol Physics Research, Atlanta Chapter Health Physics Society, January 9, 1967, Atlanta, Georgia.

In Vivo Detection and Measurement of Transuranic Elements, Transuranium Research Laboratory, ORNL, May 10, 1967, Oak Ridge, Tennessee.

Radiological Health, Radiation Shielding, and Air Pollution, May 5, 1967, University of Texas, Austin (3 seminars).

D. G. Jacobs

Movement of Nuclides Through the Ground, Ten-Week Health Physics Course, ORINS Special Training lectures to people responsible for licensing and inspecting of radioisotope users, etc., ORNL, November 7, 1966, Oak Ridge, Tennessee.

Waste Management, to students at Lenoir Rhyne College, May 12, 1967, Hickory, North Carolina.

Waste Disposal and Environmental Monitoring, Radiation Science Center, March 1, 1967, New Brunswick, New Jersey.

T. F. Lomenick

The Disposal of Radioactive Waste in Terrestrial Environments, Ten-Week Health Physics Course, ORINS Special Training lectures to people responsible for licensing and inspecting of radioisotope users, etc., ORINS, November 8, 1966, Oak Ridge, Tennessee.

K. Z. Morgan

Health Physics Program, U.S. Army Nuclear Science Seminar, Oak Ridge Playhouse, July 19, 1966, Oak Ridge, Tennessee.

Permissible Exposures to Ionizing Radiation, AEC-NSF Basic Institute for Nuclear Science and Engineering, ORNL, August 19, 1966, Oak Ridge, Tennessee.

Establishment of Maximum Permissible Doses and Concentrations, Health Physics Course for PHS Personnel, ORNL, October 6, 1966, Oak Ridge, Tennessee.

Radiation Protection, Past, Present, and Projections, Conference on Principles of Radiation Protection, ORAU, August 24–26, 1966, Oak Ridge, Tennessee.

Health Physics, Sixteenth Naval Nuclear Seminar, ORAU, December 9, 1966, Oak Ridge, Tennessee.

Conflict Between Science and Religion, St. John's Lutheran Church, January 29, 1967, Knoxville, Tennessee.

Health Physics – A New Science and a Challenging Profession, Indiana State University, March 8, 1967, Terre Haute; University of Alabama, June 5, 1967, Birmingham.

D. J. Nelson

Ecological Investigations of Radioactive Waste Releases to the Clinch River, Department of Entomology, Fisheries, and Wildlife, University of Minnesota, January 26, 1967, Minneapolis.

Current Research in Aquatic Ecology, Department of Entomology, Fisheries, and Wildlife, University of Minnesota, January 26, 1967, Minneapolis.

J. S. Olson

Radiocesium Cycling in Deciduous Forests, Advanced Isotope Technology Course, Oak Ridge Associated Universities, July 13, 1966, Oak Ridge, Tennessee.

Tracer Experiments on Forest Ecosystem Relations, Ohio State University Biology Colloquium, November 3, 1966, Columbus.

Systems Ecology, Ohio State University Graduate Ecology Seminar, November 3, 1966, Columbus.

Aims and Methods of Systems Ecology, Notre Dame University, January 9, 1967, Notre Dame, Indiana.

Ecological Models of a Tulip Poplar Forest Tagged with Radiocesium, University of Tennessee Zoology Seminar, February 8, 1967, Knoxville.

Systems Models and Experiments in Forests, Department of Ecology and Behavioral Biology, University of Minnesota, May 1, 1967, St. Paul.

Biological Productivity, Development and Regulation of Ecosystems, University of Minnesota Forest Biology Training Session, June 26, 1967, Minneapolis.

Research Methods and Techniques in Systems Ecology, University of Minnesota Forest Biology Training Session, June 26, 1967, Minneapolis.

F. L. Parker

Radioactive Waste Disposal, ORAU 16th Nuclear Science Seminar (Navy), December 2, 1966, Oak Ridge, Tennessee.

Disposal of Radioactive Wastes, U.S. Army Nuclear Science Seminar, July 20, 1966, Oak Ridge, Tennessee.

Status of Waste Disposal Research, Ten-Week Health Physics Course, ORINS Special Training lectures to people responsible for licensing and inspecting of radioisotope users, etc., ORNL, November 7, 1966, Oak Ridge, Tennessee.

B. C. Patten

Marine Isotopic Studies Off the Coast of Puerto Rico, Advanced Isotope Technology Course, July 13, 1966, Oak Ridge Associated Universities, Oak Ridge, Tennessee.

The Network Variable in Ecology, University of Kentucky, November 2, 1966, Lexington; State University College, February 23–24, 1967, Oneonta, New York; University of Georgia, March 2–3, 1967, Athens; St. Mary's College, March 10–11, 1967, Winona, Minnesota; University of Minnesota, May 12, 1967, Minneapolis; University of Buffalo, June 5, 1967, Buffalo, New York.

D. E. Reichle

Radioactive Tracers in Food Chain Research: Kinetics of Nutrient Cycling and Energy Flow in a Forest Ecosystem, St. Mary's College, Symposium on Ecology, November 1966, Winona, Minnesota.

Food Chain and Energetic Studies in Insects, Advanced Isotope Technology Course, July 13, 1966, Oak Ridge Associated Universities, Oak Ridge, Tennessee.

Bryophyte Succession and the Distribution of Microarthropods in an Illinois Bog, University of Tennessee, Seminar on Bog Ecosystems, April 1967, Knoxville.

Insect Behavior and Its Ecological Significance, University of Tennessee, Graduate Course in Insect Ecology, December 1966, Knoxville.

Pathways of Nutrient Cycling in a Forest Ecosystem, Emory University, March 1967, Atlanta, Georgia.

Radiotracers and the Trophic Dynamics of Forest Arthropods, Northwestern University, March 1967, Evanston, Illinois.

R. H. Ritchie

Radiation Dosimetry, Department of Physics, University of Tennessee, May 25, 1967, Knoxville.

A. S. Rogowski

Inspection of Rainfall Simulator, members of ORINS course in Advanced Isotope Technology, ORNL, August 3, 1966, Oak Ridge, Tennessee.

Soil Plots, Ten-Week Health Physics Course, ORINS Special Training lectures to people responsible for licensing and inspecting of radioisotope users, etc., ORNL, November 7, 1967, Oak Ridge, Tennessee.

Use of Isotopes in Runoff and Erosion Studies, ORINS course in Advanced Isotope Technology, ORNL, August 3, 1966, Oak Ridge, Tennessee.

H. C. Schweinler

The Josephson Effect, Department of Physics, University of Tennessee, April 3, 1967, Knoxville.

W. S. Snyder

Examples of the Variation of Dose Within the Body – Neutrons, Gammas, HTO, Western Pennsylvania Chapter of the Health Physics Society, University of Pittsburgh, November 28, 1966, Pittsburgh.

Monte Carlo Calculations for the Distribution of Dose in the Body from External and Internal Sources of Photons, North Carolina Chapter of the Health Physics Society, Duke University, February 8, 1967, Durham, North Carolina.

Current Activities of the Health Physics Society, Bluegrass Chapter of the Health Physics Society, Holiday Inn, February 11, 1967, Frankfort, Kentucky.

Computer Calculation of Dose, Work Conference on Dosimetry in Total Body Photon Irradiation of Man, ORAU, February 23–24, 1967, Oak Ridge, Tennessee.

Health Physics Society Certification Examination, Baltimore-Washington Chapter of the Health Physics Society, March 21, 1967, Bethesda, Maryland.

The Use of Urinalysis Data to Estimate the Body Burden of Plutonium, Centre d'Etudes Nucléaires, April 20, 1967, Saclay, France; ISPRA, April 24, 1967, Milan, Italy.

Distribution of Dose in an Anthropomorphic Phantom Irradiated by Monoenergetic Neutrons, Centre d'Etudes Nucléaires, April 20, 1967, Saclay, France; Centre de Physique Nucléaire, April 21, 1967, Toulouse, France; ISPRA, April 24, 1967, Milan, Italy.

A Two-Exponential Model for Metabolism of HTO by Man, ISPRA, April 25, 1967, Milan, Italy; Puerto Rico Chapter of the Health Physics Society, May 3, 1967, Mayaguez, Puerto Rico.

Health Physics Aspects of Supersonic Transport, Eastern Idaho Chapter of the Health Physics Society, May 19, 1967, Idaho Falls.

E. G. Struxness

Environmental Monitoring, ORAU, Exhibit Managers, July 29, 1967, Oak Ridge, Tennessee.

Environmental Monitoring, Public Health Agents, State Group, ORNL, October 6, 1966, Oak Ridge, Tennessee; University of Tennessee, March 30–31, 1967, Knoxville; National Science Foundation College Group, Oak Ridge Associated Universities, July 20, 1966, Oak Ridge, Tennessee.

Disposal by Hydraulic Fracturing, Knoxville Science Club, January 20, 1967, Knoxville, Tennessee.

Tsuneo Tamura

Radioactive Waste Disposal, Japan Atomic Forum, October 11, 1966, Tokyo, Japan; Radiation Center of Osaka, October 14, 1966, Kyoto University, Osaka, Japan.

Atomic Wastes: Their Treatment and Disposal, University of Hawaii, October 20, 1966, Honolulu.

Introduction to Waste Disposal Research Program, ORINS course in Advanced Isotope Technology, ORNL, August 3, 1966, Oak Ridge, Tennessee.

Use of Isotopes in Clay Mineralogy Studies, ORINS course in Advanced Isotope Technology, ORNL, August 3, 1966, Oak Ridge, Tennessee.

Clay Mineralogy in Waste Disposal, Ten-Week Health Physics Course, ORINS Special Training lectures to people responsible for licensing and inspecting of radioisotope users, etc., ORNL, November 7, 1967, Oak Ridge, Tennessee.

W. A. Thomas

*Cycling of Calcium in Dogwood (*Cornus florida *L.) Trees*, Department of Ecology and Behavioral Biology, University of Minnesota, May 1, 1967, St. Paul.

J. H. Thomgate

The Research Program at the DOSAR Facility (HPRR), U.S. Army Reserve, 3251st Research and Development Unit, June 6, 1967, Oak Ridge, Tennessee.

Isabel H. Tipton

What Are Little Boys Made of, Kiwanis Club, May 3, 1967, Johnson City, Tennessee.

J. P. Witherspoon

Interactions of Environmental Factors and Ionizing Radiation on Forest Tree Species, Department of Biology, Western Maryland College, October 10, 1966, Westminster; Department of Entomology, Clemson University, November 9, 1966, Clemson, South Carolina; School of Forestry, University of Missouri, December 7, 1966, Columbia; Department of Biology, Woman's College of Georgia, November 2, 1966, Milledgeville; Department of Biology, Winthrop College, January 12, 1967, Rock Hill, South Carolina; Department of Biology, Roanoke College, April 13, 1967, Roanoke, Virginia.

Cycling of Radiocesium in Forest Ecosystems, Department of Entomology, Clemson University, November 9, 1966, Clemson, South Carolina; Department of Biology, Roanoke College, April 13, 1967, Roanoke, Virginia.

Radiation Ecology, AEC Fellows, June 15, 1966, ORNL, Oak Ridge, Tennessee.

HEALTH PHYSICS [

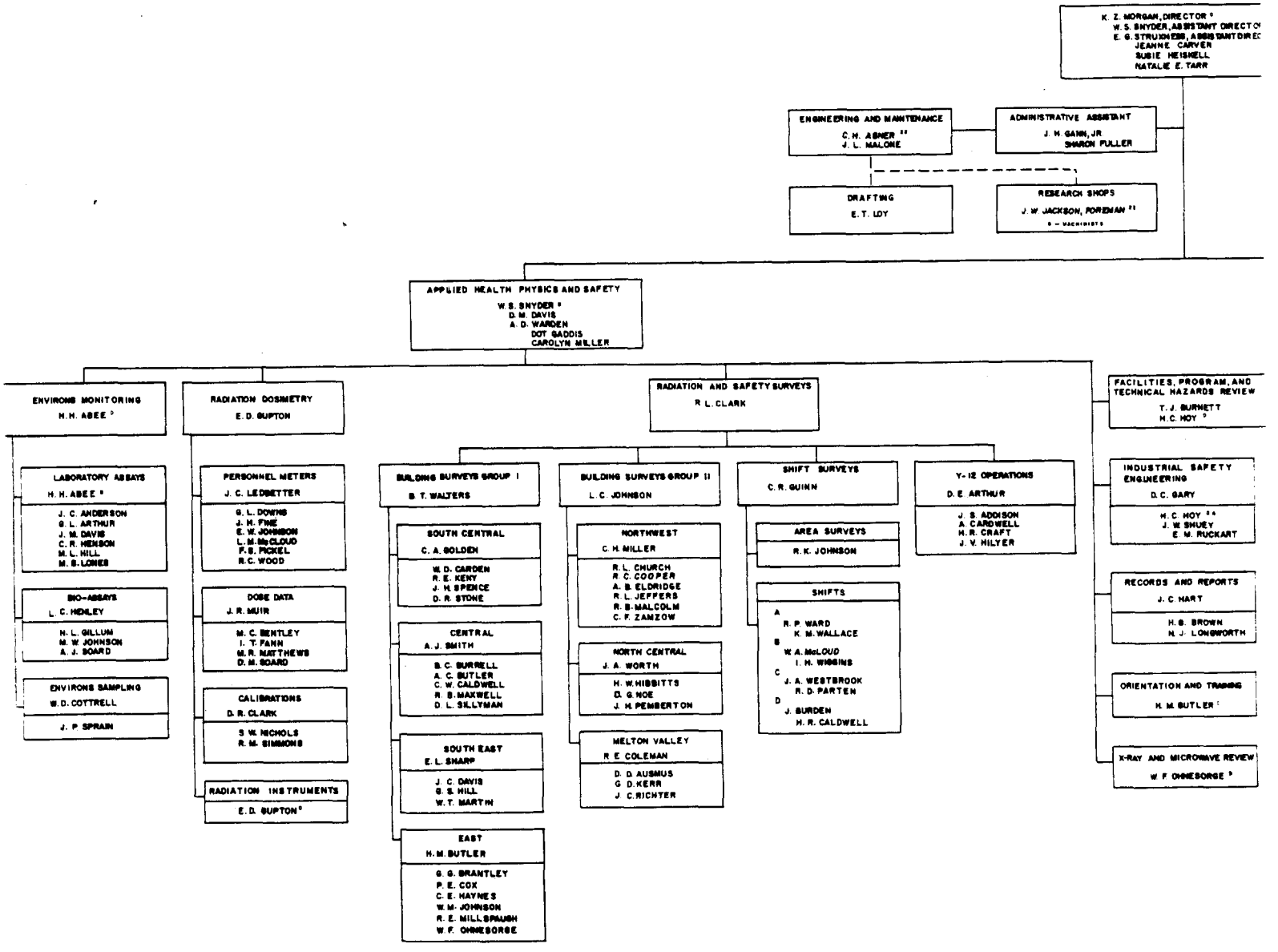

D DUAL CAPACITY
Δ RADIATION CONTROL OFFICER
DIVISION SAFETY OFFICER
Δ LEAVE OF ABSENCE
1 UNIVERSITY OF TENNESSEE
2 MARQUETTE UNIVERSITY
3 U.S. PUBLIC HEALTH SERVICE
4 UNIVERSITY OF PITTSBURG
5 JOHNS HOPKINS UNIVERSITY
6 GEORGIA INSTITUTE OF TECHNOLOGY
7 INDIANA STATE UNIVERSITY
8 NEW YORK UNIVERSITY
9 GEORGE WASHINGTON UNIVERSITY
10 WASHINGTON UNIVERSITY
11 UNIVERSITY OF NEWCASTLE UPON TYNE
12 ALIEN GUEST
13 NEUTRON PHYSICS
14 PART TIME
15 UNIVERSITY OF NORTH CAROLINA
16 I.S.C.
17 JOINT ASSIGNMENT, WASTE DISPOSAL SECTION
18 USDA BEE CULTURE LABORTORY
19 COLORADO STATE UNIVERSITY
20 DALHOUSIE UNIVERSITY
21 ORAU PREDOCTORAL FELLOWS UNIVERSITY OF TENNESSEE
22 P & E DIVISION
23 UNIVERSITY OF MANCHESTER
24 UNIVERSITY OF KENTUCKY
25 JACKSONVILLE STATE TEACHERS COLLEGE
26 UNIVERSITY OF NOTRE DAME
27 PRINCETON UNIVERSITY
28 MEDICAL COLLEGE OF VIRGINIA
29 FLORIDA STATE UNIVERSITY
30 STUDENT
31 CENTRAL DATA PROCESSING FACILITY (ORNDP)
32 TEMPORARY EMPLOYEE
33 JOINT ASSIGNMENT - RADIATION ECOLOGY SECTION
34 U.S. ARMY
35 CLARK COLLEGE
36 LOAN FROM HEALTH PHYSIC TECHNOLOGY

JULY 1, 1967

CS DIVISION